

**PRELIMINARY INDIAN OCEAN YELLOWFIN TUNA STOCK ASSESSMENT
1950-2017 (STOCK SYNTHESIS)**

PREPARED BY: DAN FU¹, ADAM LANGLEY², GORKA MERINO³, AGURTZANE URTIZBEREA IJURCO⁴

02 OCTOBER 2017

DRAFT

¹ IOTC Secretariat, Dan.Fu@fao.org;

² IOTC Consultant, Adam.Langley@gmail.com;

³ AZTI, gmerino@azti.es;

⁴ AZTI, aurtizberea@azti.es;

Contents

1. INTRODUCTION	3
1.1 Biology and stock structure	3
1.2 Fishery overview.....	4
2. OBSERVATIONS AND MODEL INPUTS	7
2.1 Spatial stratification	7
2.2 Temporal stratification.....	8
2.3 Definition of fisheries	8
2.4 Catch history	10
2.5 CPUE indices.....	13
2.5.1 Longline CPUE.....	13
2.5.2 Purse seine CPUE	16
2.6 Length frequency data	17
2.7 Tagging data	21
2.8 Environmental data	26
3. Model structural and assumptions	29
3.1 Population dynamics.....	29
3.1.1 Recruitment.....	29
3.1.2 Growth and Maturation.....	29
3.1.3 Natural mortality.....	31
3.1.4 Movement.....	32
3.2 Fishery dynamics	33
3.3 Dynamics of tagged fish	34
3.3.1 Tag mixing.....	34
3.3.2 Tag reporting.....	35
3.4 Modelling methods, parameters, and likelihood	35
4. ASSESSMENT model runs.....	36
4.1 2016 model updates	36
4.2 Exploratory model runs	36
4.3 Base case and sensitivity.....	38
5. model RESULTS.....	41
5.1 2016 model updates	41
5.2 Exploratory models.....	44
5.3 Base model.....	47
5.3.1 Model fits	48
5.3.2 Selectivity estimates	59
5.3.3 Tag reporting rate.....	61
5.3.4 Recruitment parameters	62
5.3.5 Movement	64
5.3.6 Biomass.....	66
5.3.7 Fishing mortality	68
5.3.8 Fishery impact.....	70
5.4 Sensitivity case	71
6. Stock status.....	77
6.1 Current status and yields	77
6.2 Retrospective analysis.....	81
6.3 Projection	82
7. DISCUSSION	86
8. ACKNOWLEDGMENTS	89
9. REFERENCES.....	89
APPENDIX A: additional plots OF LONGLINE LENGTH COMPOSITION DATA	94
APPENDIX B: ANALYSIS OF TAG recapture data from the RTTP-IO PROGRAM	97
Appendix C: RESULTS FROM THE EXPLORATORY MODELLING	99
Appendix D: RESULTS FROM SELECTED SENSITIVITY MODELS	113

1. INTRODUCTION

This paper presents a preliminary stock assessment of yellowfin tuna (*Thunnus albacares*) in the Indian Ocean (IO) including fishery data up to 2017. The assessment implements an age- and spatially-structured population model using the Stock Synthesis software (Methot 2013, Methot & Wetzel 2013).

Prior to 2008, Indian Ocean yellowfin tuna was assessed using methods such as VPA and production models (Nishida & Shono 2005 & 2007). In 2008, a preliminary stock assessment of IO yellowfin tuna was conducted using MULTIFAN-CL (Kleiber et al 2003, Langley et al. 2008) enabling the integration of the tag release/recovery data collected from the large-scale tagging programme conducted in the Indian Ocean in the preceding years (Langley et al. 2008). The MULTIFAN-CL assessment was revised and updated in the following years (Langley et al. 2009, 2010 and 2011, Langley et al. 2012a, 2012b).

In 2015, the assessment of IO yellowfin tuna was implemented using the Stock Synthesis software (SS3) (Langley 2015). The SS modelling framework is very similar to MFCL conceptually, and the two platforms have yielded similar results. The SS3 assessment had included a comprehensive analysis of the main structural assumptions of the stock assessment model. On basis of that assessment, the yellowfin tuna stock was determined to be **overfished** and **subject to overfishing**. The Indian Ocean Tuna Commission (S20) adopted an Interim Plan for Rebuilding the Indian Ocean Yellowfin Tuna Stock in the IOTC area of competence (Res. 16/01).

The SS3 assessment of IO yellowfin tuna was updated in 2016 (Langley 2016). The 2016 assessment model utilized the new composite longline CPUE indices derived from main distant water longline fleets, replacing the Japanese longline CPUE indices used in the previous assessment. Although the inclusion of the composite CPUE indices resulted in a somewhat more optimistic estimate of current stock status, primarily due to the lower decline in the CPUE indices from the eastern equatorial region (IOTC–WPTT18 2016), the yellowfin tuna stock was determined to remain **overfished** and subject to **overfishing**.

In 2017, the IOTC agreed to amendments to the yellowfin tuna rebuilding plan. However, the impact of the yellowfin measure agreed in 2016 (which only came into effect in January of 2017) has not yet been fully evaluated and so it remains unclear if the amendments made will strengthen the rebuilding of the yellowfin stock. The IOTC Commission has thus tasked the Scientific Committee via its Working Party on Tropical Tunas, to conduct a new assessment of the status of the Yellowfin stock in 2018 using all available data (Res. 17/01). This report documents results of the next iteration of the stock assessment of the Indian Ocean yellowfin tuna stock for consideration at 20th WPTT meeting. This stock assessment is based on the 2016 modelling framework of IO yellowfin tuna incorporating revised and updated fishery data up to 2017.

We note that the models proposed in the assessment (including the base model and sensitivities) are for the purpose of facilitating the discussions of model diagnostics and performance, and are not intended as the final model(s) for providing management advice (which shall be determined by the Working Party on Tropical Tunas after deliberations of all model options explored during the assessment).

1.1 Biology and stock structure

Yellowfin tuna (*Thunnus albacares*) is a cosmopolitan species distributed mainly in the tropical and subtropical oceanic waters of the three major oceans, where it forms large schools. The sizes exploited in the Indian Ocean range from 30 cm to 180 cm fork length. Smaller fish (juveniles) form mixed schools with skipjack and juvenile bigeye tuna and are mainly limited to surface tropical waters, while larger fish are found in surface and sub-surface waters. Intermediate age yellowfin are seldom taken in the industrial fisheries, but are abundant in some artisanal fisheries, mainly in the Arabian Sea.

Longline catch data indicates that yellowfin are distributed continuously throughout the entire tropical Indian Ocean, but some more detailed analysis of fisheries data suggests that the stock structure may be more

complex. Studies of stock structure using DNA techniques have indicated that there may be genetically discrete subpopulations of yellowfin tuna in the north western Indian Ocean (Dammannagoda et al 2008) and within Indian waters (Kunal et al 2013). However, there has been no comprehensive study that encompasses the entire ocean basin. The tag recoveries of the RTTP-IO provide evidence of large movements of yellowfin tuna within the western equatorial region, although there are very few observations of large scale transverse movements of tagged yellowfin. This may indicate that the western and eastern regions of the Indian Ocean support relatively discrete sub-populations of yellowfin tuna.

Spawning occurs mainly from December to March in the equatorial area ($0\text{--}10^{\circ}\text{S}$), with the main spawning grounds west of 75°E . Secondary spawning grounds exist off Sri Lanka and the Mozambique Channel and in the eastern Indian Ocean off Australia. Yellowfin size at first maturity has been estimated at around 60–70 cm (Zudaire et al 2013) and recruitment occurs predominantly in July (as evident in the high catch rates of the Purse seine associated sets in region 1b in the third quarter). Newly recruited fish are primarily caught by the purse seine fishery on floating objects and the pole-and-line fishery in the Maldives. Males are predominant in the catches of larger fish at sizes larger than 150 cm (this is also the case in other oceans).

Medium sized yellowfin concentrate for feeding in the Arabian Sea. Feeding behaviour is largely opportunistic, with a variety of prey species being consumed, including large concentrations of crustacean that have occurred recently in the tropical areas and small mesopelagic fishes which are abundant in the Arabian Sea.

1.2 Fishery overview

Yellowfin tuna, an important component of tuna fisheries throughout the Indian Ocean (Figure 1), are harvested with a diverse variety of gear types, from small-scale artisanal fisheries (in the Arabian Sea, Mozambique Channel and waters around Indonesia, Sri Lanka and the Maldives and Lakshadweep Islands) to large gillnetters (from Oman, Iran and Pakistan operating mostly but not exclusively in the Arabian Sea) and distant-water longliners and purse seiners that operate widely in equatorial and tropical waters (Figure 2). Purse seiners and gillnetters catch a wide size range of yellowfin tuna, whereas the longline fishery takes mostly adult fish.

Prior to 1980, annual catches of yellowfin tuna remained below about 80,000 mt and were dominated by longline catches (Figure 3). Annual catches increased markedly during the 1980s and early 1990s, mainly due to the development of the purse-seine fishery as well as an expansion of the other established fisheries (fresh-tuna longline, gillnet, baitboat, handline and, to a lesser extent, troll). A peak in catches was recorded in 1993, with catches over 400,000 mt, the increase in catch almost fully attributable to longline fleets, particularly longliners flagged in Taiwan, which reported exceptional catches of yellowfin tuna in the Arabian Sea. The Taiwanese longline fishery in the Indian Ocean has been equipped with super-cold storage. Since around 1986, the fleet has fished more frequently with deep sets.

Catches declined in 1994, to about 350,000 mt, remaining at that level for the next decade then increasing sharply to reach a peak of about 520,000 mt in 2004/2005 driven by a large increase in catch by all fisheries, especially the purse-seine (free school) fishery. Total annual catches declined sharply from 2004 to 2007 and remained at about 300,000 mt during 2007–2011. In 2012, total catches increased to about 400,000 mt and were maintained at about that level through 2013 to 2015. Total catches increased slightly in 2016 and 2017 compared to previous four years (Figure 3), despite that IOTC Resolution 17/01 requested major fleets to substantially reduce their yellowfin catches from the 2014 or 2015 catch level.

In recent years (2013–2017), purse seine has been the dominant fishing method harvesting 33% of the total IO yellowfin tuna catch (by weight), with the longline, handline, gillnet fisheries, comprising 14%, 19% and 14% of the catch, respectively. A smaller component of the catch was taken by the regionally important baitboat (5%) and troll (5%) fisheries. The recent increase in the total catch has been attributable to an increase in catch from all the major fisheries.

The purse-seine catch is generally distributed equally between free-school and associated (log and FAD sets) schools, although the large catches in 2003–2005 were dominated by fishing on free-schools. Conversely, during 2013–2017 the purse-seine catch was dominated (65%) by the associated fishery (Figure 3).

Historically, most of the yellowfin catch is taken from the western equatorial region of the IO (47%; region 1b, see Figure 3) and, to a lesser extent, the Arabian Sea (21%), the eastern equatorial region (25%, region 4) and the Mozambique Channel (8%; region 2). The purse-seine and baitboat fisheries operate almost exclusively within the western equatorial region, while catches from the Arabian Sea are principally by handline, gillnet, and longline (Figure 2). Catches from the eastern equatorial region (region 4) were dominated by longline and gillnet (around Sri Lanka and Indonesia). The southern Indian Ocean (region 3) accounts for a small proportion of the total yellowfin catch (1%) taken exclusively by longline (Figure 3).

In recent years (2008–2012), due to the threat of piracy, the bulk of the industrial purse seine and longline fleets moved from the western waters of Region 1b to avoid the coastal and off-shore waters off Somalia, Kenya and Tanzania. The threat of piracy was particularly affected the freezer longline fleet and levels of effort and catch decreased markedly from 2007. The total catch by freezing longliners declined to about 2,000 mt in 2010, a 10-fold decrease in catch from the years before the onset of piracy. Purse seine catches also dropped in 2008–2010 but rapidly recovered to the earlier level. Piracy off the Somali coast was almost eradicated by 2013 although longline catches have not recovered.

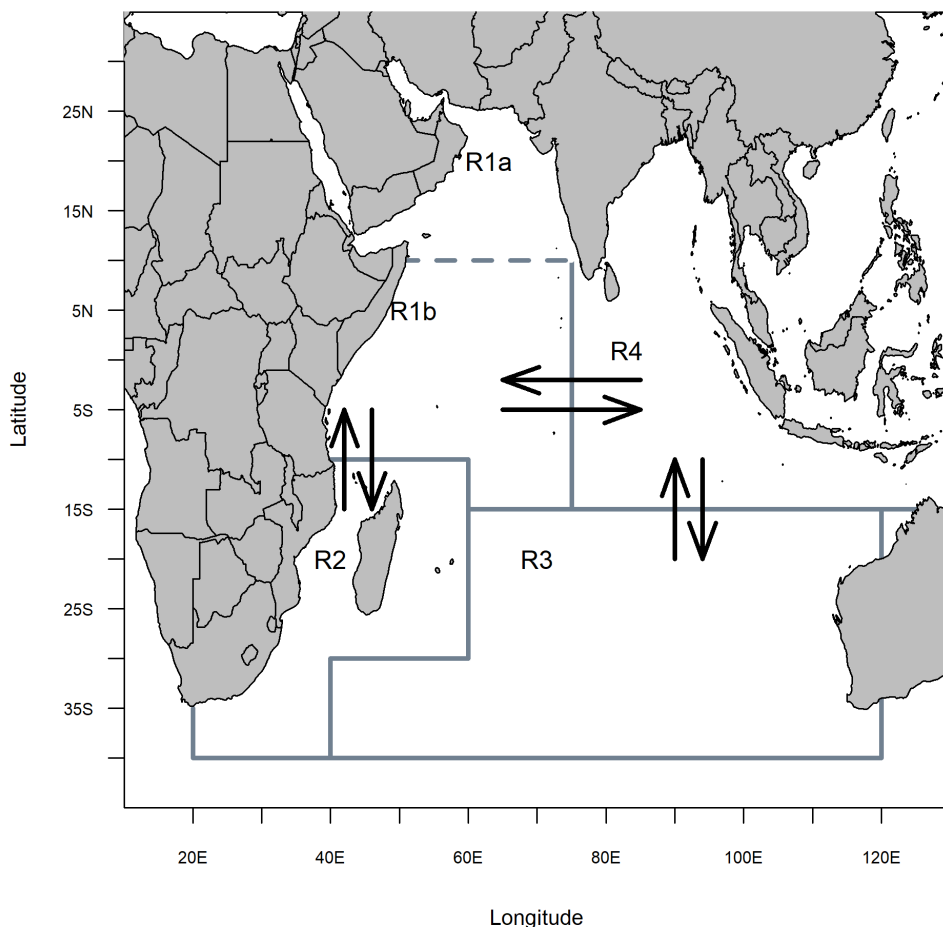


Figure 1: Spatial stratification of the Indian Ocean for the four region assessment model. The black arrows represent the configuration of the movement parameterisation of the base assessment model

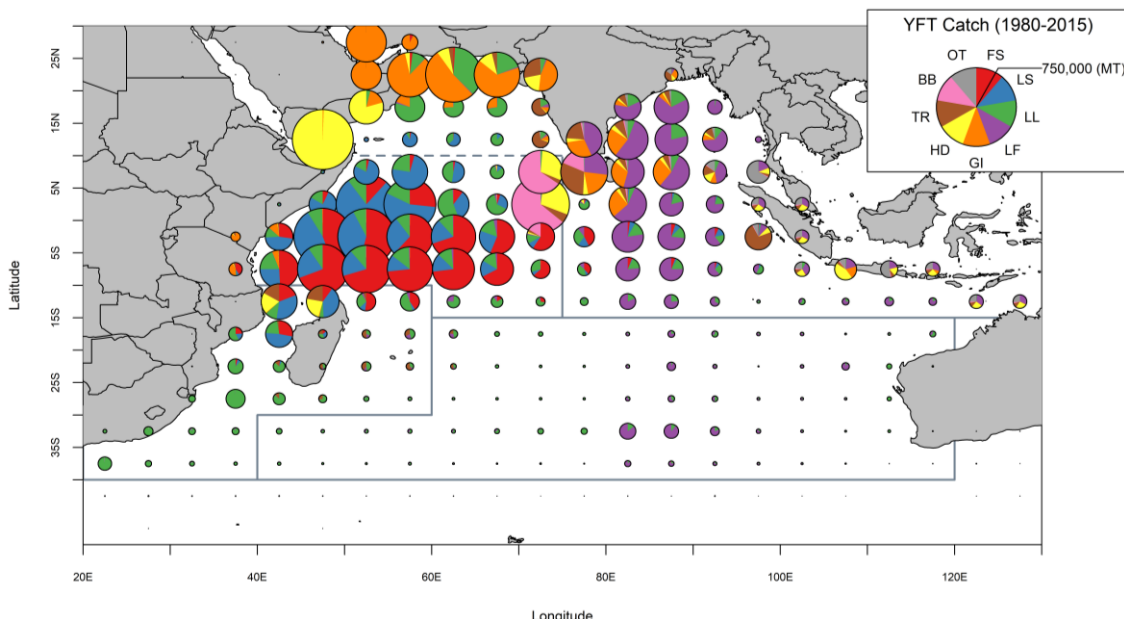


Figure 2: Spatial distribution of Indian Ocean yellowfin catches by main gear types aggregated for 1980–2016. Gear codes are described in Table x.

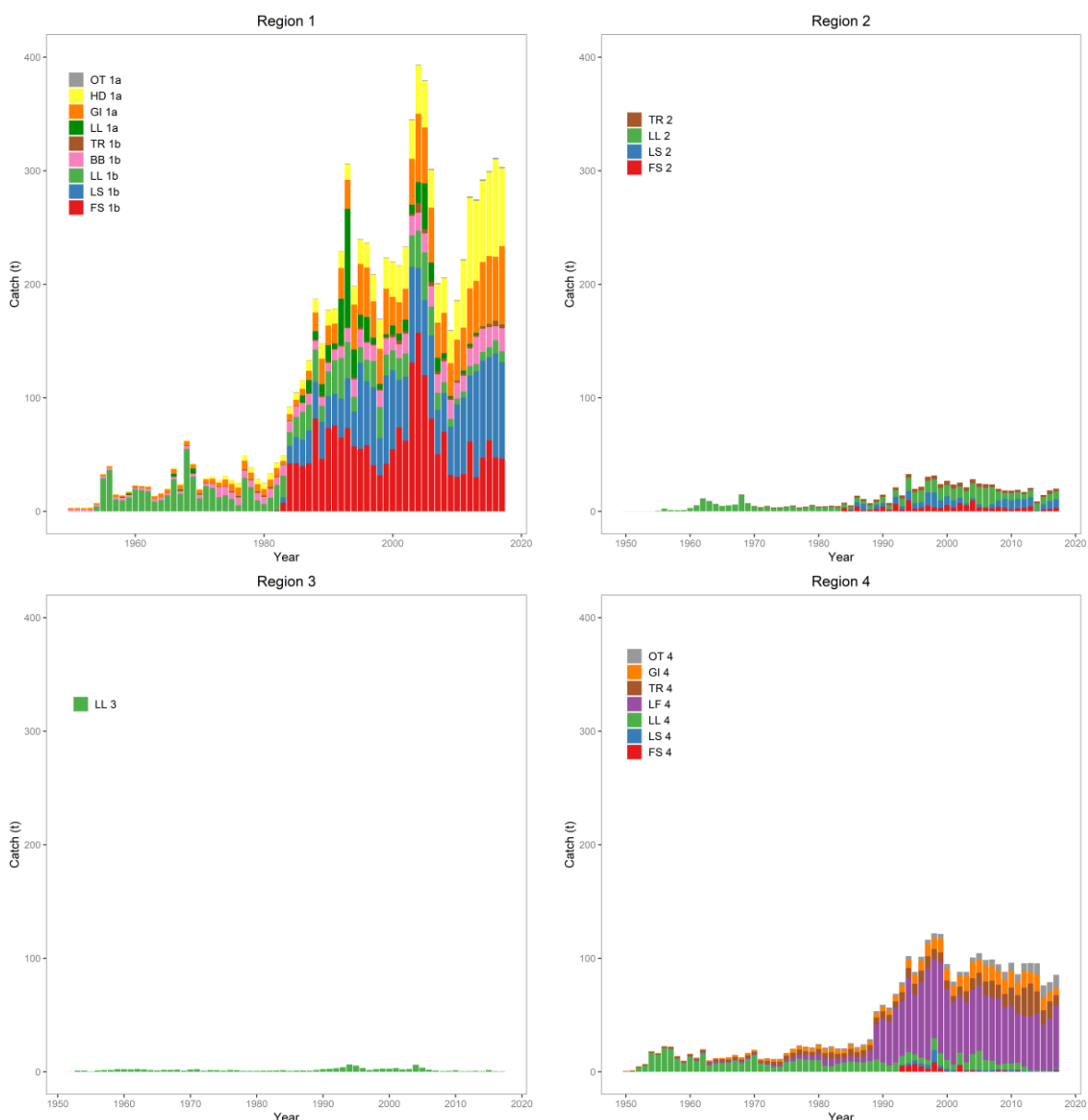


Figure 3: Total annual catch (1000s mt) of yellowfin tuna by fishing method and region (middle and bottom) from 1950 to 2017 (Gear codes are described in Table x).

2. OBSERVATIONS AND MODEL INPUTS

The data used in the yellowfin tuna assessment consist of catch and length composition data for the fisheries defined in the analysis, longline CPUE indices and tag release-recapture data. The details of the configuration of the fishery specific data sets are described below.

2.1 Spatial stratification

The geographic area considered in the assessment is the Indian Ocean, defined by the coordinates 40°S–25°N, 20°E–150°E. Earlier yellowfin stock assessments have adopted a five region spatial structure (see Langley 2012). Preliminary analyses conducted during the 2015 assessment highlighted a number of issues related to the five region model structure (see Langley 2015). There have been no CPUE abundance indices available from the Arabian Sea region (region 1) since 2010 although the area has yielded very high catches from the handline and gillnet fisheries during recent years. The models failed to estimate MSY bench marks seemingly due to the magnitude of the fishing mortality rates in Region I. It was considered that the five region model structure were unlikely to provide a reliable indication of current stock status (Langley 2015).

The base case model of the 2015 assessment thus adopted the four region model structure, combining the Arabian Sea (region 1a) and western equatorial region (region 1b) (Figure 1), although the two sub regions were retained for the definition of spatially distinct fisheries that operate in each area. The spatial structure retains two regions that encompass the main year-round fisheries in the tropical area and two austral, subtropical regions where the longline fisheries occur more seasonally. The four region model structure is used in the current assessment.

Hoyle et.al (2018) proposed a modification to the four regional structure by further subdividing the western equatorial region into a northern (region 1bN) and a southern region (region 1bS) (Figure A1, Appendix A), based on evidence of differential size distributions of yellowfin within the western equatorial region (Hoyle et al. 2017, Satoh 2014). This additional stratification within the western equatorial region is also consistent with the most recent bigeye assessment (Langley 2016). The sensitivity of the stock assessment model to the assumptions regarding spatial structure is further evaluated in the current assessment (see Section 4.2).

2.2 Temporal stratification

The time period covered by the assessment is 1950–2017 representing the period for which catch data are available from the commercial fishing fleets. Langley (2015) suggested that the assessment results were not sensitive to the early catches from the model (pre 1972) and commencing the model in 1950 or 1972 (assuming unexploited equilibrium conditions) yielded very similar results.

Within this model period, the annual data were compiled into quarters (Jan–Mar, Apr–Jun, Jul–Sep, Oct–Dec) (representing a total of 272 time steps). The time steps were used to define model “years” (of 3 month duration) enabling recruitment to be estimated for each quarter to approximate the continuous recruitment of yellowfin in the equatorial regions.

However, the quarterly time step (model “year”) precluded the estimation of seasonal model parameters, particularly the movement parameters. There is a strong indication of seasonal movement of yellowfin to the higher latitudes during the summer period. The assessment thus explored an alternative annual/seasonal model structure which explicitly estimated seasonal movement dynamics (see Section 4.2).

2.3 Definition of fisheries

The assessment adopted the equivalent fisheries definitions used in the previous SS3 stock assessment. These “fisheries” represent relatively homogeneous fishing units, with similar selectivity and catchability characteristics that do not vary greatly over time. Twenty-five fisheries were defined based on location (region), time period, fishing gear, purse seine set type, and type of vessel in the case of longline fleet (Table 1).

The longline fishery was partitioned into two main components:

Freezing longline fisheries, or all those using drifting longlines for which one or more of the following three conditions apply: (i) the vessel hull is made up of steel; (ii) vessel length overall of 30 m or greater; (iii) the majority of the catches of target species are preserved frozen or deep-frozen. A composite longline fishery was defined in each region (LL 1–4) aggregating the longline catch from all freezing longline fleets (principally Japan and Taiwan).

Fresh-tuna longline fisheries, or all those using drifting longlines and made of vessels (i) having fibreglass, FRP, or wooden hull; (ii) having length overall less than 30 m; (iii) preserving the catches of target species fresh or in refrigerated seawater. A composite longline fishery was defined aggregating the longline catch from all fresh-tuna longline fleets (principally Indonesia and Taiwan) in region 4 (LF 4), which is where the majority of the fresh-tuna longliners have traditionally operated. The catches of yellowfin tuna recorded in regions 1 to 3 for fresh-tuna longliners, representing only a 3% of the total catches over the time series, were assigned to area 4.

The purse-seine catch and effort data were apportioned into two separate method fisheries: catches from sets on associated schools of tuna (log and drifting FAD sets; PS LS) and from sets on unassociated schools (free schools; PS FS). Purse-seine fisheries operate within regions 1a, 1b, 2 and 4 and separate purse-seine fisheries were defined in regions 1b, 2 and 4, with the limited catches, effort and length frequency data from region 1a reassigned to region 1b.

The region 1b purse-seine fisheries (log and free-school) were divided into three time periods: pre 2003, 2003–2006 and post 2006. This temporal structure was implemented due to the apparent change in the length composition of the catch from the purse-seine fisheries during the 2000s. The length of fish caught by the FAD fishery was generally smaller from 2007 onwards, while a higher proportion of smaller fish were caught by the free-school fishery prior to 2003.

A single baitboat fishery was defined within region 1b (essentially the Maldives fishery). As with the purse-seine fishery, a small proportion of the total baitboat catch and effort occurs on the periphery of region 1b, within regions 1a and 4. The additional catch was assigned to the region 1b fishery.

Gillnet fisheries were defined in the Arabian Sea (region 1a), including catches by Iran, Pakistan, and Oman, and in region 4 (Sri Lanka and Indonesia). A very small proportion of the total gillnet catch and effort occurs in region 1b, with catches and effort reassigned to area 1a.

Three troll fisheries were defined, representing separate fisheries in regions 1b (Maldives), 2 (Comoros and Madagascar) and 4 (Sri Lanka and Indonesia). Moderate troll catches are also taken in regions 1a and 3, the catch and effort from this component of the fishery reassigned to the fisheries within region 1b and 4, respectively.

A handline fishery was defined within region 1a, principally representing catches by the Yemenese fleet. Moderate handline catches are also taken in regions 1b, 2 and 4, the catch and effort from these components of the fishery were reassigned to the fishery within region 1a.

For regions 1a and 4, a miscellaneous (“Other”) fishery was defined comprising catches from artisanal fisheries other than those specified above (e.g. trawlers, small purse seines or seine nets, sport fishing and a range of small gears).

Table 1: Definition of fisheries for the four-region assessment model for yellowfin tuna

Fishery	Nationality	Gear	Region
1. GI 1a	All	Gillnet	1a
2. HD 1a	All	Handline	1a
3. LL 1a	All	Longline	1a
4. OT 1a	All	Other	1a
5. BB 1b	All	Baitboat	1b
6. PS FS 1b 2003-06	All	Purse seine, school sets	1b
7. LL 1b	All	Longline	1b
8. PS LS 1b 2003-06	All	Purse seine, log/FAD sets	1b
9. TR 1b	All	Troll	1b
10. LL 2	All	Longline	2
11. LL 3	All	Longline	3
12. GI 4	All	Gillnet	4
13. LL 4	All	Longline (distant water)	4
14. OT 4	All	Other	4
15. TR 4	All	Troll	4
16. PS FS 2	All	Purse seine, school sets	2
17. PS LS 2	All	Purse seine, log/FAD sets	2
18. TR 2	All	Troll	2
19. PS FS 4	All	Purse seine, school sets	4
20. PS LS 4	All	Purse seine, log/FAD sets	4
21. PS FS 1b pre 2003	All	Purse seine, school sets	1b
22. PS LS 1b pre 2003	All	Purse seine, log/FAD sets	1b
23. PS FS 1b post 2006	All	Purse seine, school sets	1b
24. PS LS 1b post 2006	All	Purse seine, log/FAD sets	1b
25. LF 4	All	Longline (fresh tuna)	4

2.4 Catch history

Catch data were compiled based on the fisheries definitions. An update of quarterly catches by fishery was provided by the IOTC Secretariat, including catches from 2016 and 2017 (as at 30/9/2018). Two differing nominal catch scenarios were compiled: IOTC-2018-WPTT20-DATA13a_Rev1 and IOTC-2018-WPTT20-DATA13b_Rev1. The former provides a “continuity” estimate using the current estimation procedure, which estimated Indonesian fresh tuna longline catches based on Taiwanese catches. However, given the dramatic changes in fishing operations of the Taiwanese fleet in recent years, using Taiwanese fleets as proxy for estimating Indonesian catches is no longer considered appropriate (Geehan & Braham 2018). The later estimates provided an amendment to the estimation procedure by incorporating recent information on changes within Indonesia’s fresh longline fishery (Geehan & Braham 2018). The current assessment adopted the revised nominal catch estimates (IOTC-2018-WPTT20-DATA13b_Rev1).

For each fishery, the time series of catches were very similar to the catch series included in the 2015 assessment (Figure 4). The main differences in annual catches are in the fresh tuna long catches where the current estimates for 2011-2015 are much lower than the catch included in the previous assessment. The other appreciable differences relate to the Other fisheries in region 4, where the updated estimates for 2012-15 are

considerably higher.

Total annual catches for 2016 and 2017 included in the updated catch history are 409,423mt and 409,151 mt, respectively (Table 2). The total catch in 2017 represents a 3% increase from the 2014 catch level, or a 4.5% increase from 2015.

Table 2: Recent yellowfin tuna catches (mt) by fishery included in the stock assessment model. The annual catches are presented for 2013- 2017.

Fishery	Year				
	2013	2014	2015	2016	2017
1. GI 1a	45,855	56,839	59,973	56,410	69,151
2. HD 1a	70,502	71,419	73,770	85,920	68,567
3. LL 1a	1,668	448	335	459	361
4. OT 1a	1,169	1,293	997	1,228	1,125
5. BB 1b	24,055	20,542	17,642	12,391	20,298
6. PS FS 1b 2003-06	-	-	-	-	-
7. LL 1b	6,446	7,555	8,649	11,694	9,487
8. PS LS 1b 2003-06	-	-	-	-	-
9. TR 1b	1,648	1,516	2,400	4,363	2,860
10. LL 2	6,417	6,330	6,542	6,230	7,126
11. LL 3	779	487	1,466	515	415
12. GI 4	10,310	14,551	11,180	8,313	5,986
13. LL 4	700	789	861	463	552
14. OT 4	7,815	10,110	10,713	8,729	12,021
15. TR 4	29,015	18,967	12,519	14,472	9,309
16. PS FS 2	4,382	205	1,464	1,997	3,060
17. PS LS 2	7,924	461	4,704	7,134	7,482
18. TR 2	1,941	1,772	1,695	3,229	2,392
19. PS FS 4	1	0	60	3	1,248
20. PS LS 4	753	452	278	710	1,917
21. PS FS 1b pre 2003	-	-	-	-	-
22. PS LS 1b pre 2003	-	-	-	-	-
23. PS FS 1b post 2006	30,090	47,222	62,439	47,460	46,392
24. PS LS 1b post 2006	93,207	85,505	73,413	91,423	85,026
25. LF 4	47,271	50,593	40,487	46,279	54,377
Total	391,948	397,054	391,587	409,423	409,151

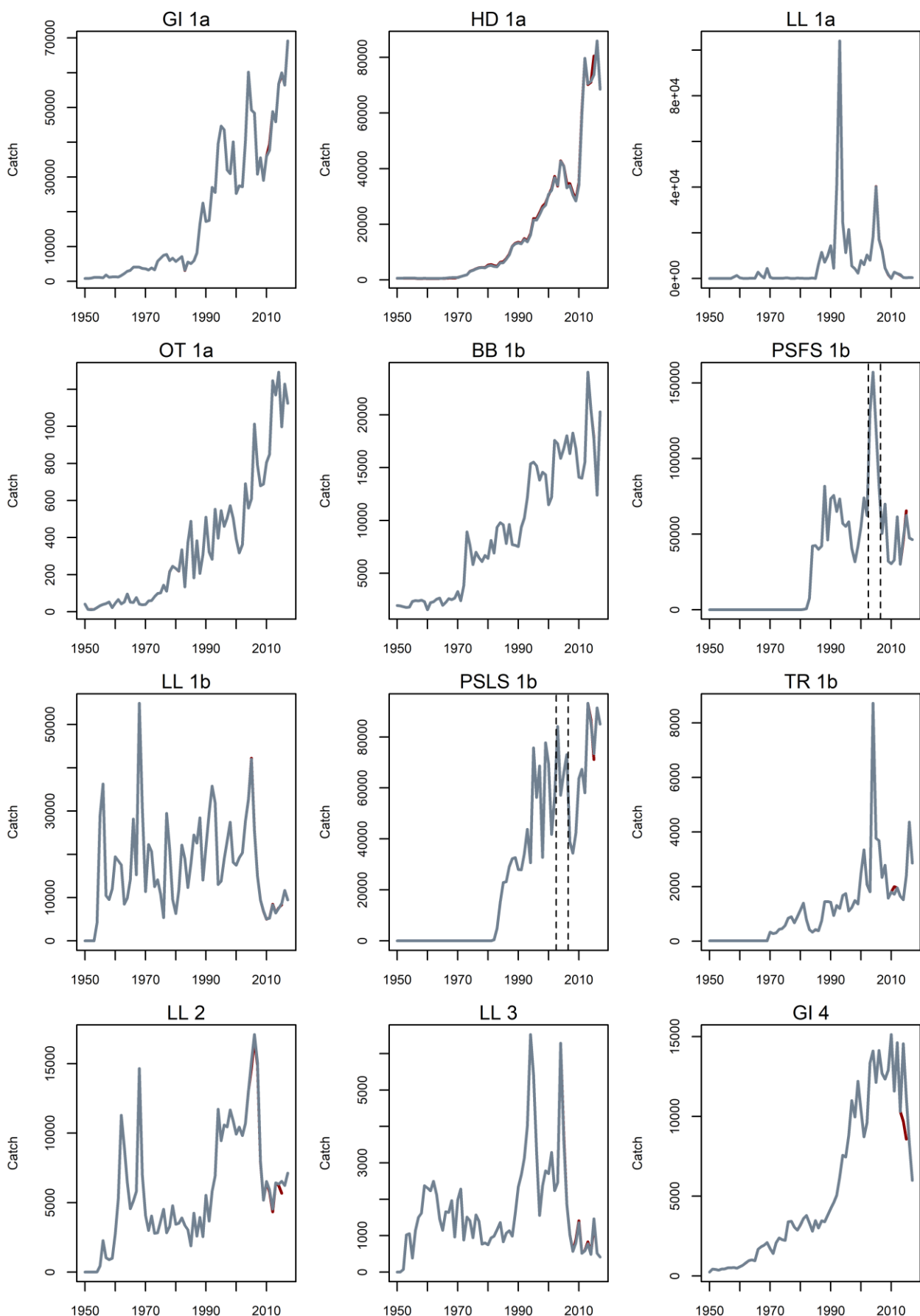
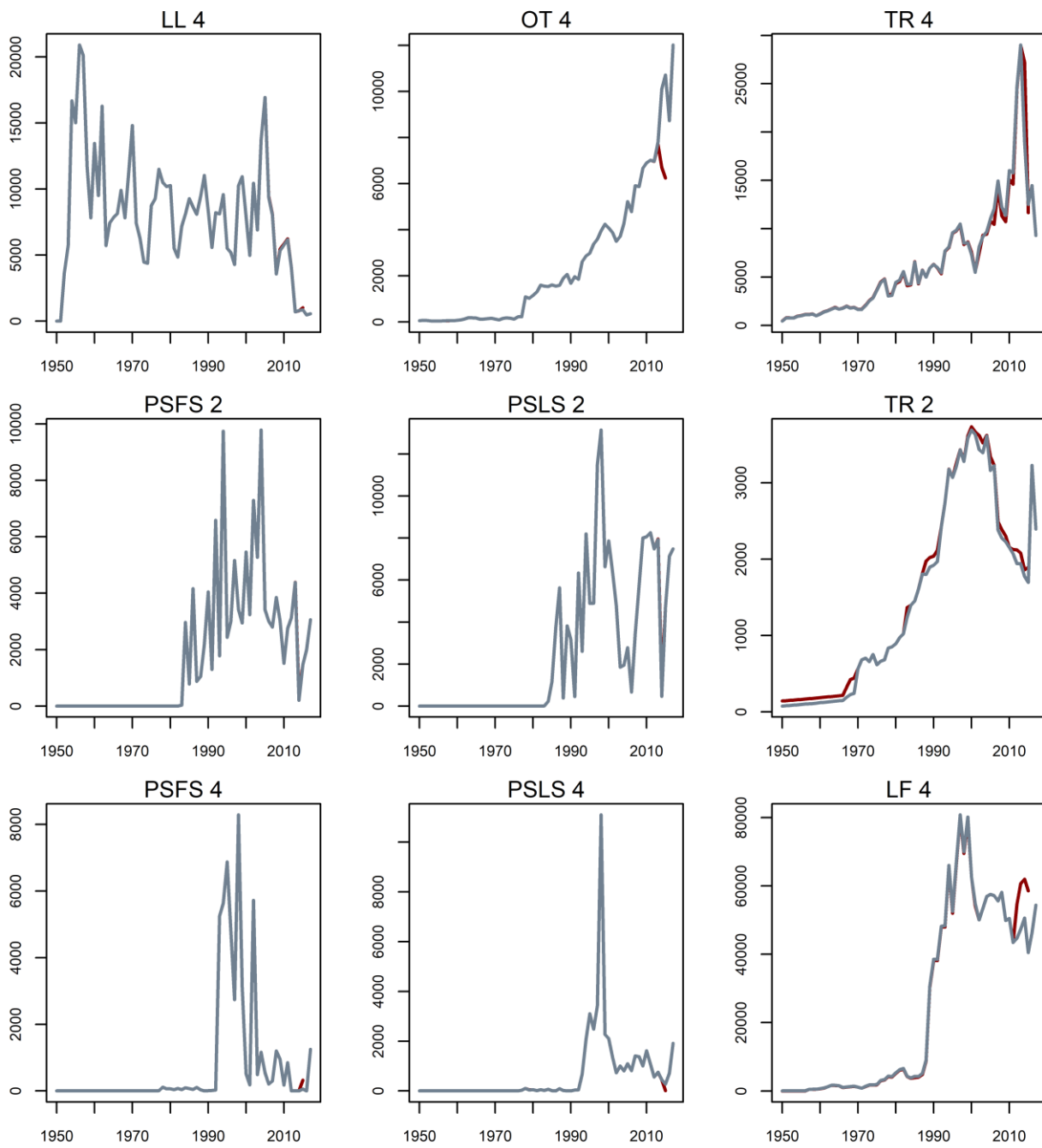


Figure 4: Fishery catches (metric tonnes) aggregated by year. Note the y-axis differs among plots. The dashed lines indicate the separation of PSLS and PSFS fisheries in region 1b into three periods. Red lines are catches used in the 2016 assessment.

Figure 4 continued.

2.5 CPUE indices

2.5.1 Longline CPUE

Standardised CPUE indices were derived using generalized linear models (GLM) from operational longline catch and effort data provided by Japan, Korea, Taiwan, China, and Seychelles (Hoyle *et al* 2018a, b). Cluster analyses of species composition data by vessel-month for each fleet were used to separate datasets into fisheries understood to target different species. Selected clusters were then combined and standardized using generalized linear models. The Seychelles data were made available and were included in the indices that used clustering. Yellowfin catch (numbers of fish) was the dependent variable of the positive catch model (lognormal error structure), while the presence/absence of yellowfin tuna in the catch was the dependent variable in the binomial model. In addition to the year-quarter, models included covariates for vessel identity, 5° square location,

number of hooks, and either cluster (for region 2 and 3) or HBF (for regions 1 and 4). The data from region 1a is not included the standardisations and the indices for region 1b is assumed to index the abundance for region 1

In 2018, three sets of CPUE indices were derived (for each region) based on different treatment of the fishing vessel variable in the CPUE modelling (Hoyle *et al* 2018a). The assessment modelling incorporated the *boat_allyears* set of CPUE indices for the base case (Table 3), on the basis that the indices represented the longest time series (1953–2017) and incorporated vessel effects for the period when individual vessel identifiers were available (1979–2017).

The CPUE indices from the years prior to 1972 were not included in the assessment model (as in the previous assessments in 2015 and 2016). The CPUE indices from the earlier period are considerably higher than for the remainder of the 1970s. The decline in CPUE indices during the late 1960s–early 1970s is inconsistent with the relatively low level of catch taken during this period (Langley 2015). At the 10th WPTT, it was agreed that the decline in the CPUE indices was unlikely to be solely due to changes in stock abundance although the reason for this seemingly excessive initial decline are still poorly understood.

The standardised quarterly CPUE indices included in the assessment are shown in Figure 5. Overall, the updated CPUE indices are similar to those included in the previous assessment in terms of the overall trend, although the updated indices for regions 2 and 3 showed somewhat less decline over 1980–2010. The current indices for region 3 are based on clusters rather than HBF, whereas the HBF-based indices were used previously as there were insufficient data due to a different filtering criteria being applied at the time (Hoyle *et al* 2018a).

Standardised CPUE indices were also provided for the north and south of the western tropical region (region 1bN and 1bS, see Figure A1 in Appendix A). The indices in these two sub-regions followed broadly similar trend although the catch rates were highly variable, possibly due to the paucity of data (these indices were derived separately from the indices for the region 1b, see the details in Hoyle *et al.* 2018b). Both sets of indices were included in the exploratory model configured under the alternative spatial structure (region 1b was split into two sub-regions).

Regional weighting

For the regional longline fisheries, a common catchability coefficient (and selectivity) was estimated in the assessment model, thereby, linking the respective CPUE indices among regions. This significantly increases the power of the model to estimate the relative (and absolute) level of biomass among regions. However, as CPUE indices are essentially density estimates it is necessary to scale the CPUE indices to account for the relative abundance of the stock among regions. For example, a relatively small region with a very high average catch rate may have a lower level of total biomass than a large region with a moderate level of CPUE.

The approach used was to determine regional scaling factors that incorporated both the size of the region and the relative catch rate to estimate the relative level of exploitable longline biomass among regions. This approach is similar to that used in the WCPO regionally disaggregated tuna assessments. During preliminary modelling, the scaling factors used in the previous assessment were considered for continuity. The scaling factors were derived from the Japanese longline CPUE data from 1963–75 by summing the average CPUE in each of the 5°5 latitude/longitude cells within a region.

For each of the principal longline fisheries, the GLM standardised CPUE index was normalised to the mean of the period for which the region scaling factors were derived (i.e. the GLM index from 1963–75). The normalised GLM index was then scaled by the respective regional scaling factor to account for the regional differences in the relative level of exploitable longline biomass among regions

However, these estimates were derived from a period in which the CPUE was considered unreliable (see the previous section). Hoyle & Langley (2018) revised the approach for estimating the regional weighing factors for IO tropical tuna species and proposed a set of alternative estimates for yellowfin based aggregated longline catch effort data. The author recommended the estimates by method ‘8’ for the period 1979–1994 (referred to as ‘7994m8’, see Table 2 of Hoyle (2018)) to be included in the current assessment. The relative scaling factors calculated for regions 1–4 are 1.674, 0.623, 0.455 and 1.000 respectively. The alternative sets of regional scaling factors derived from period 1975–1994 (“7595m8”) and 1980 to 2000 (“8000m8”) were also explored in the assessment.

A number of important trends are evident in the CPUE indices (see Hoyle et al. 2018b for more details).

- The CPUE indices in the tropical areas were characterized by very steep declines prior to 1975. From 1980–1989 the western tropical (region 1b) CPUE increased during the 1980s, then declined until 1995, increased again until 2005, and then decreased again. The low CPUE indices followed the period of exceptionally high catches from the purse seine fishery in region 1b during 2003–2005. The drop in CPUE occurred before the peak in the number of piracy incidents in the western Indian Ocean (2008–2011). After that time, it remained close to the lowest level observed.
- The eastern tropical region 4 followed a similar pattern until 1990 but then declined steadily, and by 2016 was also close to the lowest level in the time series. The recent decline in CPUE in this region is consistent with a decline in the proportion of yellowfin in the combined tuna catch from the Japanese longline fleet in the eastern Indian Ocean (see Figure 44 from Hoyle et al 2015). It is unclear whether the change in species proportion is related to a decline in the abundance of yellowfin in the region (relative to the other species) or a regional change in the targeting of the fishing fleet. However, there is an indication that there has been a differential shift towards deeper longline gear (greater HBF) in the eastern Indian Ocean since 2000 and this may indicate a shift in targeting toward bigeye tuna in this region (Hoyle pers. comm. additional JP LL analyses). Such factors may not be adequately accounted for in the standardisation of the yellowfin CPUE data.
- The CPUE indices in western temperate region 2 followed a similar pattern to the western tropical indices, with a decline until the mid-1970s followed by an increase until the late 1980s, and subsequently a slow decline with significant variability. However, the two sets of CPUE indices diverge somewhat from about 2007 with the CPUE indices from R2 being maintained at a higher level relative to R1.
- The CPUE indices from region 3 are low compared to the other three regions reflecting the low regional scaling factor. However, the overall trend in the CPUE indices is broadly comparable to the other regions. The eastern temperate region 3 the pattern was similar to the western temperate area before 1979. After 1979 catch rates increased until the mid-2000's, but then declined rapidly and reached their lowest observed levels by 2016.
- There is an exceptionally high peak in CPUE indices 1976–78 from region 1. Hoyle et al. (2017) showed this discontinuity exists in Japanese, Taiwanese and Korean data, and in multiple regions in multiple ocean. Hoyle et al (2017) suggested this is unlikely to be explained by changes to the population or catchability but may be associated with catch reporting and data management.
- The spike in the CPUE indices around 2012 in the west equatorial region (region 1) was evident for most fishing fleets. Several hypothesis has been proposed on what could have caused CPUE to have increased, including a return to fishing in areas that were most affected by piracy. However, further investigation is required.

Table 3: the individual sets of CPUE indices used for each model region for the base case model.

Region		Model variables	Indices series name
1		No cluster, HBF	<i>Joint_regY_R2_dellog_boat_allyrs</i>
2		Cluster, no HBF	<i>Joint_regY_R3_dellog_boat_allyrs</i>
3		Cluster, no HBF	<i>Joint_regY_R4_dellog_boat_allyrs</i>
4		No cluster, HBF	<i>Joint_regY_R5_dellog_boat_allyrs</i>

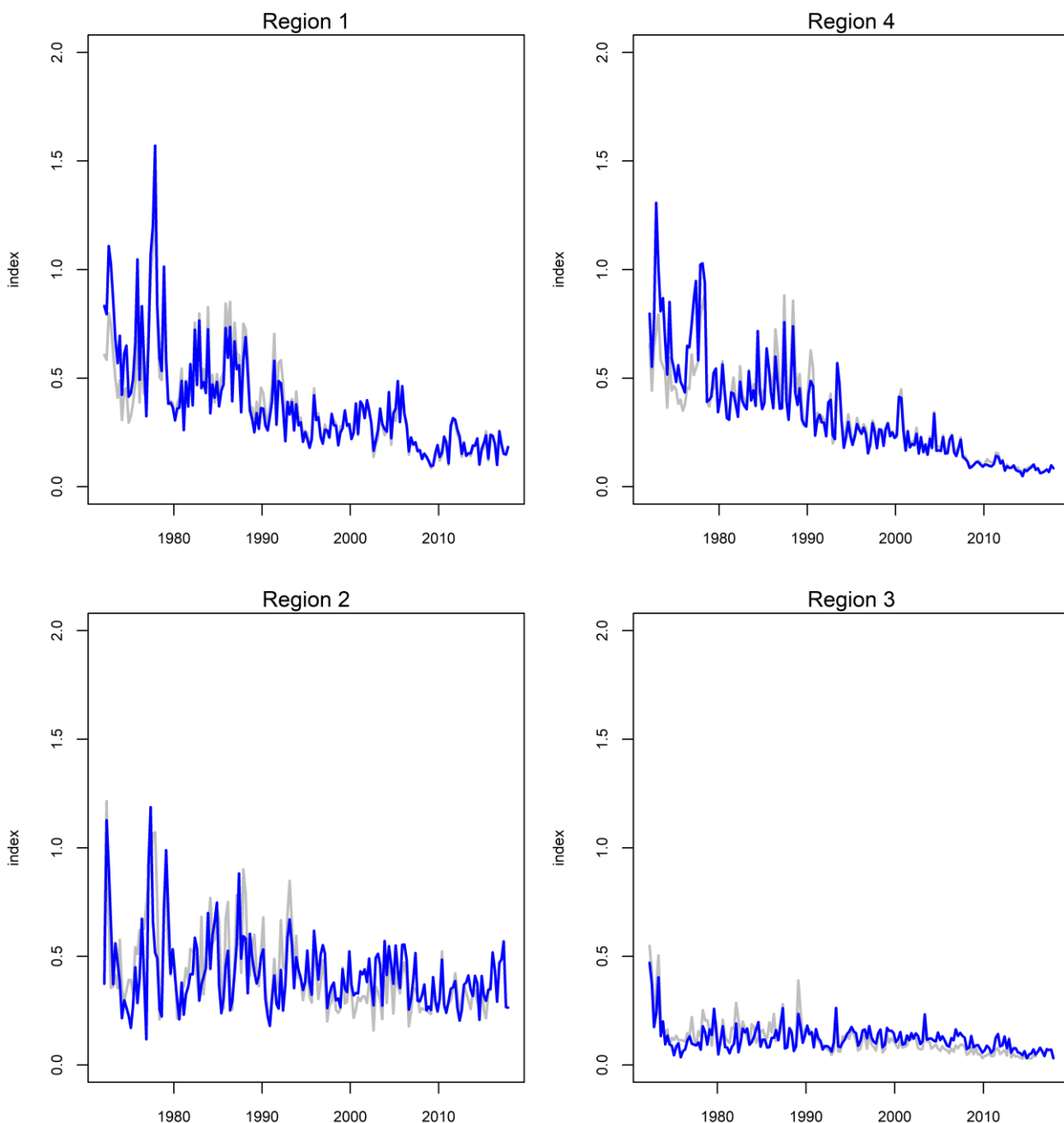


Figure 5: A comparison of the longline CPUE indices included in the 2016 stock assessment (grey line) and the 2018 stock assessment (blue line). The 2016 indices are rescaled to have the same mean of the 2018 indices for each region. The final Indices for region 1 was based on data from region 1b only.

2.5.2 Purse seine CPUE

The European and associated flags purse seine fishing activities in the Indian Ocean during 1981–2016 have been monitored through the collection of logbook and observer sampling. Standardised indices of the biomass of yellowfin caught by the European purse seiners (Spain and France) from sets on associated tuna schools (2007 – 2017) as well as sets on free swimming schools (1986 – 2017) were developed by Katara et al (2018). The standardisation was based on the application of a generalized linear mixed model which considered a comprehensive list of candidate covariates, including non-conventional covariates.

It is well recognised that the relationship between PS CPUE and abundance is unlikely be proportional, as the improvement of catch efficiency due to technology development is difficult to quantify, and the changes in catchability are not fully accounted for in the standardisation process. The WCPO assessments have often estimated substantial changes in PS FAD-associated fisheries (e.g. McKechnie et al 2017). Using a similar

approach, Kolody (2018) estimated a catchability increase of approximately 1.25% per year for the standardised purse seine effort for yellowfin from sets on associated schools. For the current assessment, the purse seine indices are included in sensitivity models.

2.6 Length frequency data

Available length-frequency data for each of the defined fisheries were compiled into 95 2-cm size classes (10–12 cm to 198–200 cm). Each length frequency observation for purse seine fisheries represents the number of fish sampled raised to the sampling units (sets in the fish compartment) while for fisheries other than purse seine each observation consisted of the actual number of yellowfin tuna measured. A graphical representation of the availability of length samples is provided in Figure 6. The length samples are not available for TR 2. The data were collected from a variety of sampling programmes, which can be summarized as follows:

Purse seine: Length-frequency samples from purse seiners have been collected from a variety of port sampling programmes since the mid-1980s. The samples are comprised of very large numbers of individual fish measurements. The length frequency samples are available by set type with associated sets catches typically composed of smaller fish than free school catches (Figure 7). There was a decline in the average length of fish from the FAD schools from 1985 to 2015 (Figure 8). The size composition of the catch from the free-school fishery is bimodal, being comprised of the smaller size range of yellowfin and a broad mode of larger fish (Figure 7). There is a considerable catch of smaller fish taken during free school fishing operation in the Mozambique Channel area in region 2 (Chassot 2014). The free-school fishery in region 4 appears to catch larger fish.

Longline freezing: Length and weight data were collected from sampling aboard Japanese commercial, research and training vessels. Weight frequency data collected from the fleet have been converted to length frequency data via a processed weight-whole weight conversion factor and a weight-length key. Length frequency data from the Taiwanese longline fleet from 1980–2003 are also included in the length frequency data set, although data from the more recent years were excluded due to concerns regarding the reliability of these data (Geehan & Hoyle 2013). Comparisons between size data collected from Taiwanese vessels by observers and logbooks since 2003 revealed that the vessel masters reported considerably larger fish (Simon Hoyle pers. comm.). In recent years, length data are also available from other fleets (e.g. Seychelles).

Overall, the average length of yellowfin caught by the longline fleet is generally comparable among the regions. However, there is considerable temporal variation in the length of fish caught (Figure 8). For all longline fisheries there was a marked decline in the size of fish caught during the 1950s and 1960s, while the size of fish caught stabilised during the 1970s and 1980s. The average length of yellowfin was significantly lower during the 1990s and the early 2000s in most regions, primarily due to the considerably smaller fish being sampled by the Taiwanese fleets (Figure A1, Appendix A). A quick examination of the spatial coverage of the Taiwanese samples did not reveal any apparent anomaly (Figure A2, Appendix A). Hoyle et al. (2017) suggested the substantial changes in the Taiwanese mean sizes are likely due to sampling problems rather than changes in the size composition of the population.

Longline fresh: Length and weight data were collected in port, during unloading of catches, for several landing locations and time periods, especially on fresh-tuna longline vessels flagged in Indonesia and Taiwan/China (IOTC-OFCF sampling). However, the quality of these data is highly variable. Length data from 1998–2008 were included in the previous assessment. But most samples were subsequently found to be biased (F. Fiorellato per. comm., IOTC Secretariat). For the current assessment, only four years of data are included (2002, 2003, 2010 and 2011).

Gillnet: Length data are available from both GN 1 and 4 fisheries. The size of yellowfin taken by the gillnet ranges from 40 to 140 cm.

Baitboat: Size data are available from the fishery from 1983 to 2015.

Troll: No size data are available from the TR 2 fisheries. The size data are available from the TR 1b fisheries in 2015 only. The troll fishery in region 4 was sampled during two periods: 1985–1990 (Indonesian fishery) and 1994–2004 (Sri Lankan fishery). The samples from 1994–2004 were excluded from the current assessment

Handline: Limited sampling of the handline fishery was conducted over the last decade. Samples are available for the Maldivian handline fisheries for this period.

Other: Length samples are available from the “Other” fishery in region 4 (OT 4) fishery and limited data are available from the “Other” fishery in region 1a (OT 1a) (2009–2017).

Length data from each fishery/quarter were simply aggregated assuming that the collection of samples was broadly representative of the operation of the fishery in each quarter.

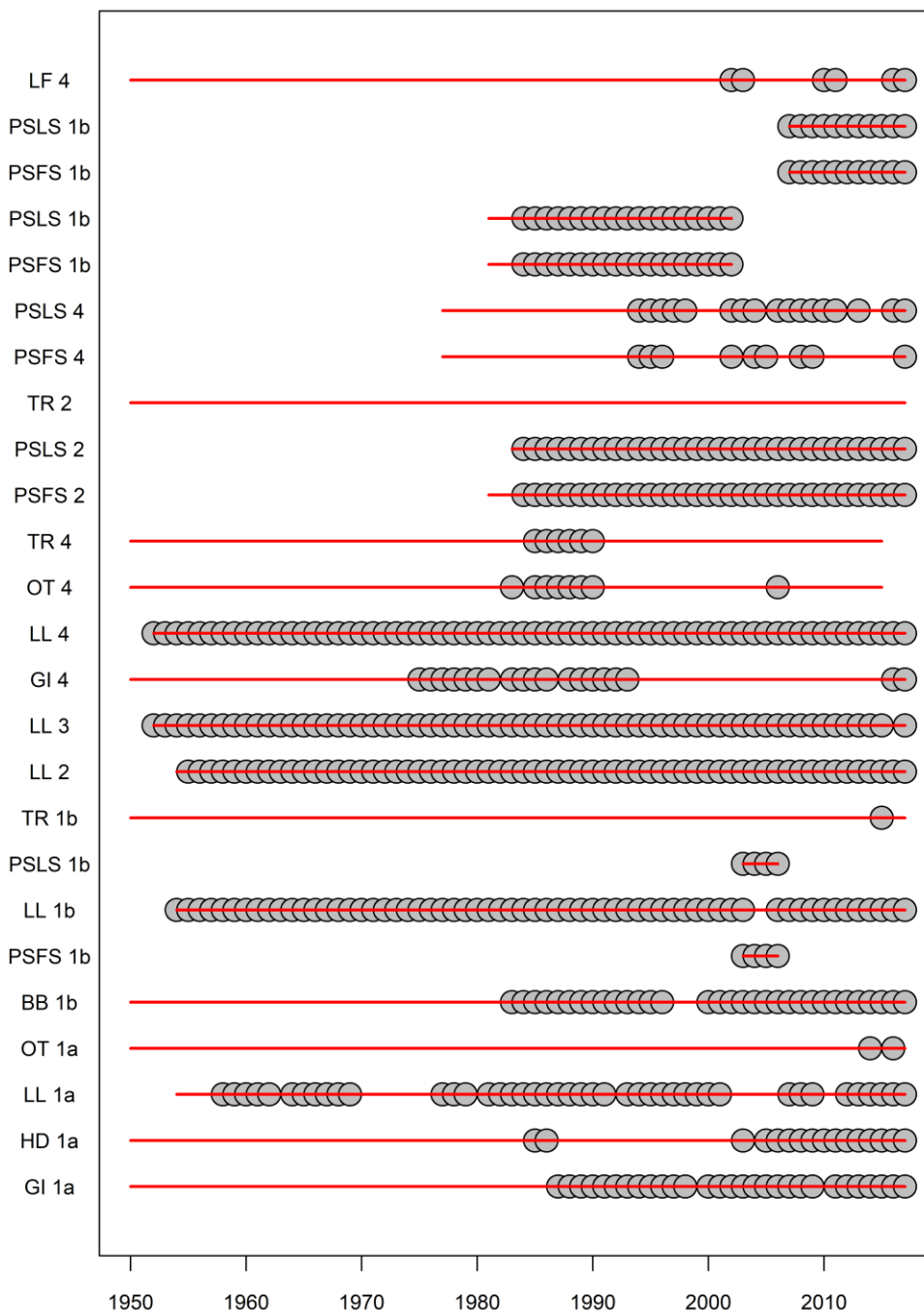


Figure 6: The availability of length sampling data from each fishery by year. The grey circles denote the presence of samples in a specific year. The red horizontal lines indicate the time period over which each fishery operated.

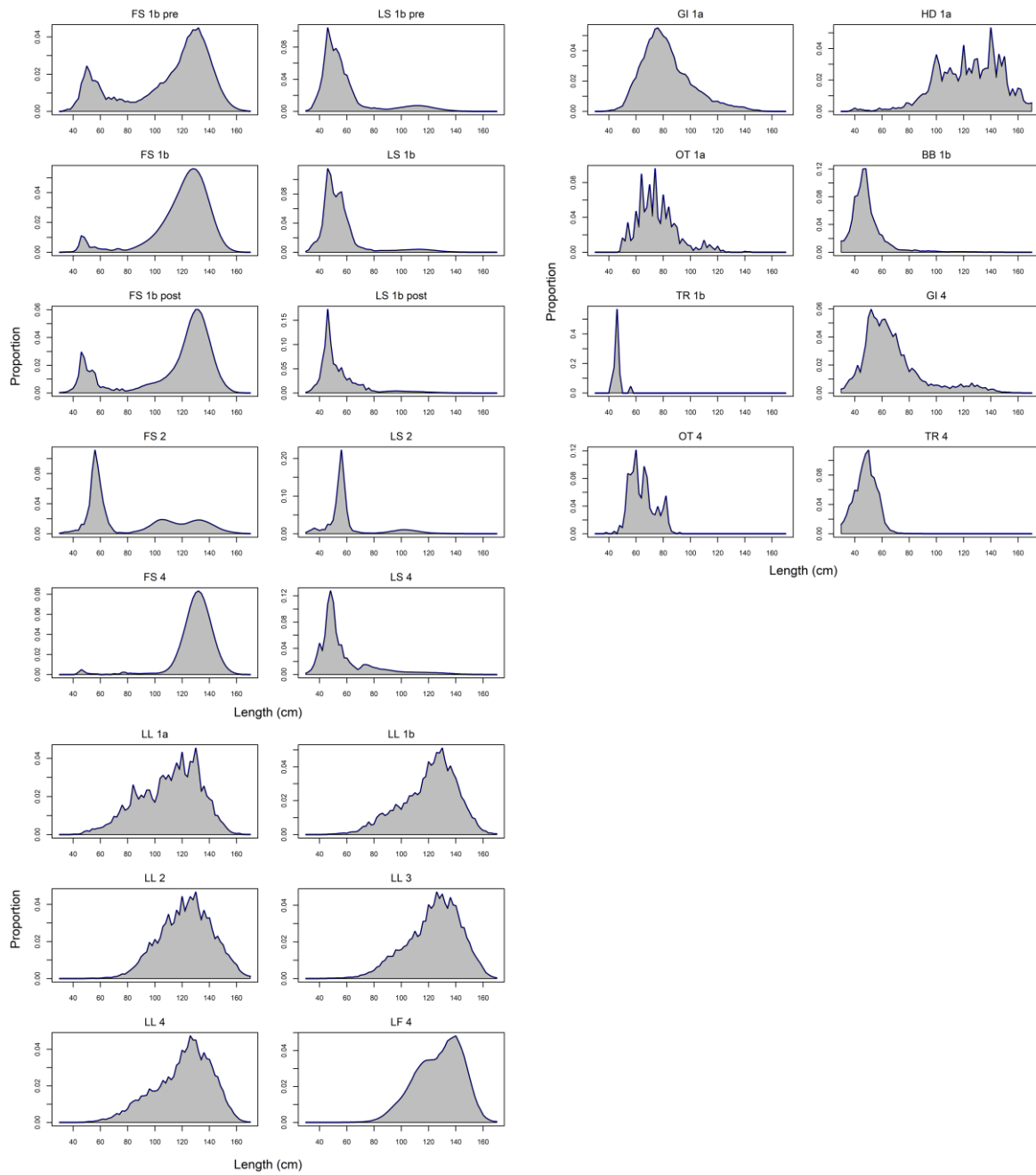


Figure 7: Length compositions of yellowfin tuna samples aggregated by fishery.

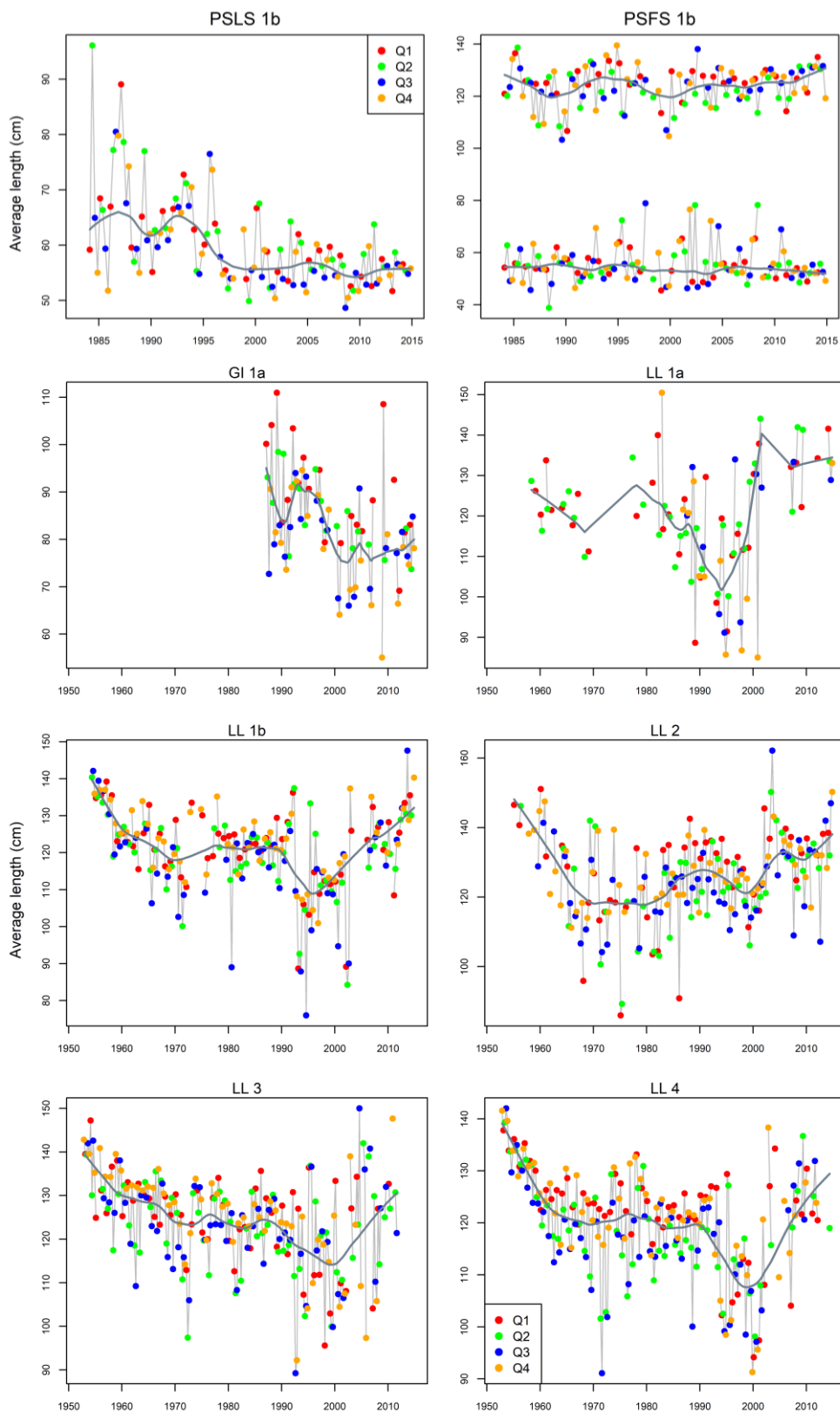


Figure 8: Mean length (fork length, cm) of yellowfin sampled from the principal fisheries (GI 1a, LL 1a-4, PSLS 1b and PSFS 1b) by year quarter. The grey line represents the fit of a lowess smoother to each data set. For PSFS 1b, the mean is calculated for fish ≤ 80 cm and > 80 cm separately.

2.7 Tagging data

A considerable amount of tagging data was available for inclusion in the assessment model. The data used consisted of yellowfin tuna tag releases and returns from the Indian Ocean Tuna Tagging Programme (IOTTP), and mainly from its main phase, the Regional Tuna Tagging Project-Indian Ocean (RTTP-IO) conducted during 2005–2009. The IOTC has continued to compile all the release and recovery data from the RTTP-IO and the complementary small-scale programmes in a single database.

A total of 54,688 yellowfin tuna were released by the RTTP-IO program. Most of the tag releases occurred within the western equatorial region (region 1b) and a high proportion of these releases occurred in the second and third quarters of 2006 (see IOTC 2008a for further details) (Figure 9). Limited tagging also occurred within regions 1a and 2. The model included all tag recoveries up to the end of 2014 and there were no further recoveries since the last assessment. The spatial distributions of tag releases and recoveries are presented in Figure 10 and Figure 11, respectively.

In total, 9916 tag recoveries (removed tags with recovery unknown dates or length) could be assigned to the fisheries included in the model. Almost all of the tags released in region 1 were recovered in the home region, although some recoveries occurred in adjacent regions, particularly region 2. A small number of tags were recovered in region 4 (from tags released in region 1b) and there were no tags recovered from region 3 (Table 4). Most of the tag recoveries occurred between mid-2006 and mid 2008 (Figure 12). The number of tag recoveries started to attenuate in 2009 although small numbers of tags were recovered up to the end of 2014.

Most of the tags were recovered by the purse seine fishery within region 1b (Figure 12). A significant proportion (35%) of the tag returns from purse seiners were not accompanied by information concerning the set type. These tag recoveries were assigned to either the free-school or log fishery based on the expected size of fish at the time of recapture; i.e. fish larger than 80 cm at release were assumed to be recaptured by the free-school fishery; fish smaller than 80 cm at release and recaptured within 18 months at liberty were assumed to be recovered by the floating object fishery; fish smaller than 80 cm at release and recaptured after 18 months at liberty were assumed to be recovered by the free-school fishery.

For incorporation into the assessment model, tag releases were stratified by release region, time period of release (quarter) and age class. The recaptures by fishery for each release group inform the assessment model on fishing mortality and abundance and fish movement. Therefore, factors that might have affected the interpretation of tag returns need to be accounted for to minimise potential bias. Below provides a description of how the tag data are incorporated into the assessment and various options explored.

Age assignment of tag release

The age at release was assumed based on the fish length at release and the average length-at-age from the yellowfin growth function (see Section 3.1.2). Fish aged 15 quarters and older were aggregated in a single age group. Tag releases in regions 1a and 1b were stratified in separate release groups due to the spatial separation of the individual release events. A total of 54,392 releases were classified into 131 tag release groups. Most of the tag releases were in the 5–8 quarter age classes (Figure 9).

Alternatively, the numbers of fish in each age at release were determined by applying an age-length key to the length composition of the tagged fish. The age-length key was derived by assuming an equilibrium population age-length structure based on the age-specific natural mortality, average length-at-age from the yellowfin growth function and the standard deviation of length-at-age (CV 0.1).

Initial tagging mortality

The initial tag retention rate was assumed to be 0.9. (Gaertner and Hallier 2008). In the previous assessment this was accounted for through the SS3 reporting rate parameter. The reporting rate (for the purse seine fisheries) was essentially fixed at a value of 0.81 to account for initial tag retention rates (0.9) as well as the proportion of the total purse-seine catch examined for tags (0.9).

Chronic tag loss

Tag recoveries were also corrected for long-term tag loss (tag shedding) based on an update of the analysis of Gaertner and Hallier (2015). Tag loss for yellowfin was estimated to be approximately 20% at 2000 days at liberty. This was accounted for through the SS3 chronological tag loss parameter (an annual rate of 0.03).

Hoyle (2015) examined the effects of various covariates (e.g. individual tagger effect) on tag failures for the

RTTP program and estimated a combined effect of 20% for all tropical tuna species relative to a base failure rate. No formal estimate was made for the base failure rate but a 10% was suggested based on the assessment of the Western and Central Pacific tuna species. This equates to a total tag failure rate of 30%, which is very close to the initial tagging mortality (10%) plus the chronic tag loss (20%) assumed in the current assessment.

Reporting rate

The returns from tag release group were classified by recapture fishery and recapture time period (quarter). The results of associated tag seeding experiments, conducted during 2005–2008, have revealed considerable temporal variability in tag reporting rates from the IO purse-seine fishery (Hillary *et al.* 2008a). Reporting rates were lower in 2005 (57%) compared to 2006 and 2007 (89% and 94%). Quarter estimates were also available but was similar in magnitude (Hillary *et al.* 2008b). This large increase over time was the result of the development of publicity campaign and tag recovery scheme raising the awareness of the stakeholders, *i.e.* stevedores and crew. SS3 assumes a constant fishery-specific reporting rate. To account for the temporal change in reporting rate, the number of tag returns from the purse-seine fishery in each stratum (tag group, year/quarter, and length class) were corrected using the respective estimate of the annual reporting rate. A reporting rate of 94% was assumed for the correction of the 2008–2014 tag recoveries. (Noting the SS3 reporting rate parameter was fixed at 0.81 to account for the initial tag mortality and the proportion of the total purse-seine catch examined for tags).

Alternatively, the approach by Kolody (2011) and Fu (2017) was used to correct for tag reporting from the Purse seine fishery. This approach is broadly similar to the above procedure, except that for at-sea recoveries, an 100% reporting rate was assumed. Tags recovered from Seychelles landings were corrected for reporting rates based on the quarterly estimates from Hillary *et al* (2008b), and were also corrected for the proportion of the total purse-seine catches examined for tags, based the proportions of EU PS catch landed in the Seychelles relative to the total EU PS catches (Kolody 2011). For example, the adjusted number of observed recaptures for a PSLS fishery as input to the model, R'_L was calculated using the following equation:

$$R'_L = R_L^{sea} + \frac{R_L^{sez}}{P^{sez} r^{sez}}$$

where

R_L^{sea} = the number of observed recaptures recovered at sea for the PSLS fishery.

R_L^{sez} = the number of observed recaptures recovered in Seychelles for the PSLS fishery.

r^{sez} = the reporting rates for PS tags removed from the Seychelles

P^{sez} = the scaling factor to account for the EU PS recaptures not landed in the Seychelles.

The adjusted number of observed recaptures for a PSFS fishery was calculated similarly. For simplicity, the number of tag releases in each release group was reduced by 10% to account for the initial tag mortality, and thus the SS3 reporting parameter was fixed at 1 in the model.

Some of the other (non purse-seine) fisheries also returned a substantial number of tags. There are no direct estimates of fishery specific reporting rates for these fisheries. The reporting rates for these fisheries are estimated within the assessment model.

Small-scale tagging programmes

Additional tag release/recovery data are available from a number of small-scale tagging programmes. The data set included a total of 7,828 tags released during 2002–08, primarily within regions 1b (70%) and 4 (28%). A total of 366 tag recoveries were reported, predominantly from the Bait boat fishery in region 1a. There has been no comprehensive analysis of these data and there is no information available concerning the fishery specific reporting rate of these tags. The tag release/recovery data from the SS tagging programmes were not incorporated in the current range of assessment models. Earlier analysis indicated that the stock assessment results were relatively insensitive to the inclusion of these data (Langley *et al* 2012a).

The options for addressing factors related to tag loss/reporting are summarised in Table 5. The effects of these options on the assessment model are explored in the exploratory modelling.

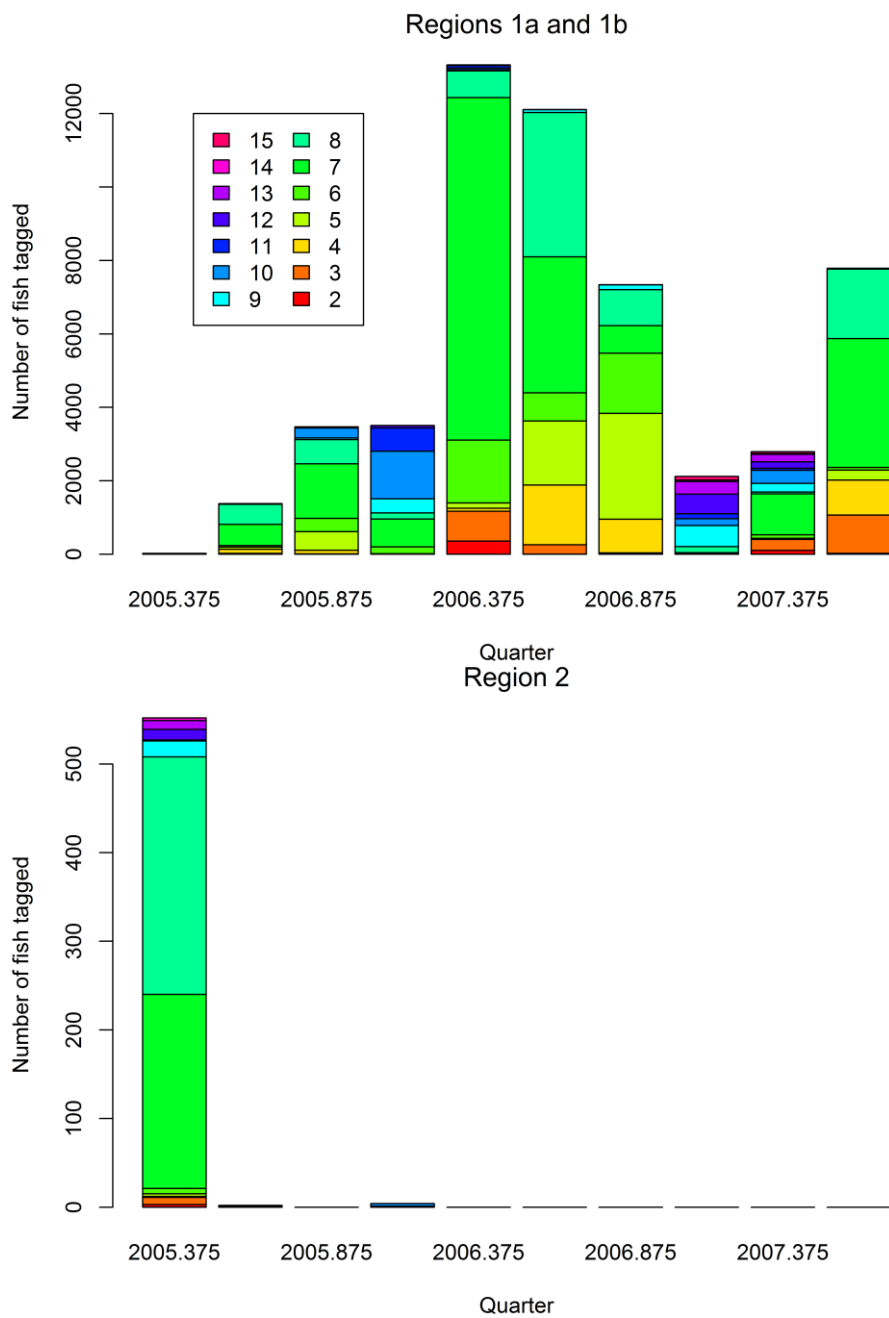


Figure 9: Number of tag releases by region and quarter and age class included in the assessment data set. No tag releases occurred in regions 3 and 4.

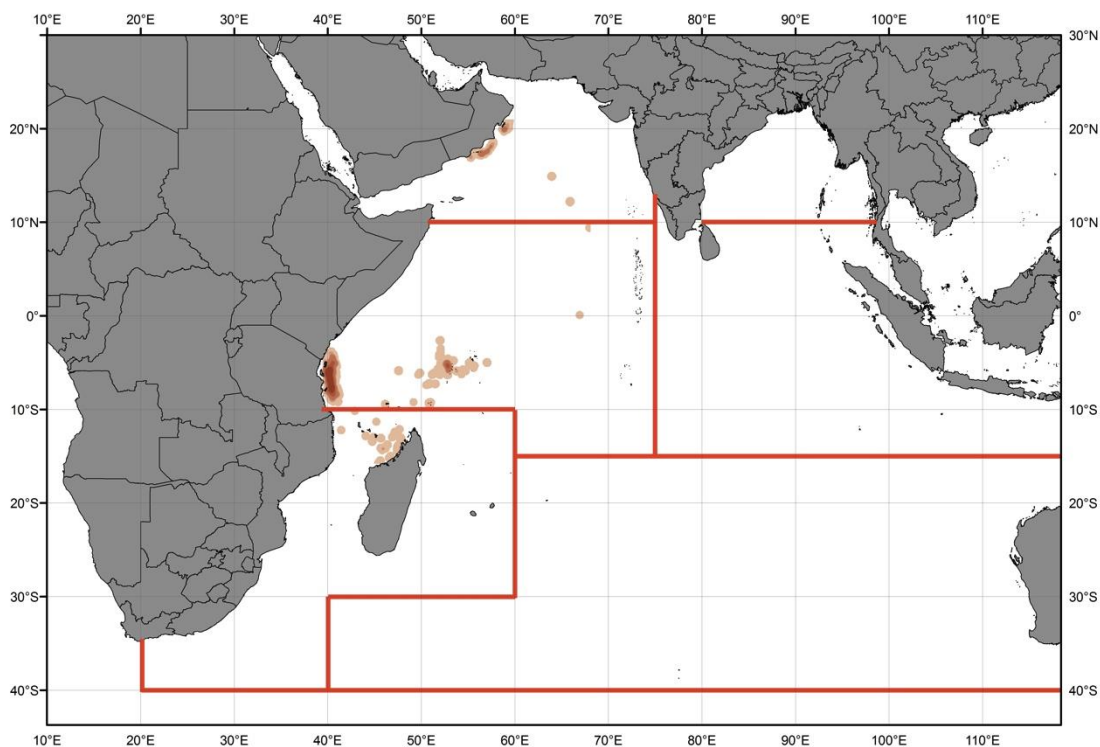


Figure 10. Density of RTTP-IO tag releases.

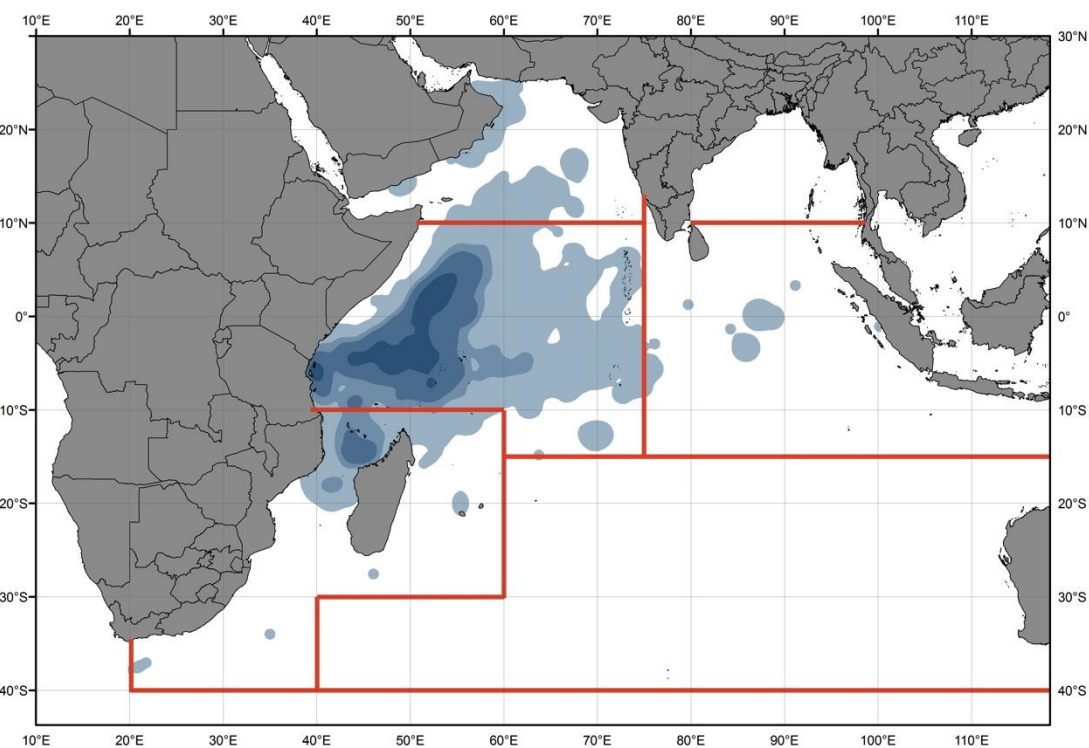


Figure 11: Density of RTTP-IO tag recoveries.

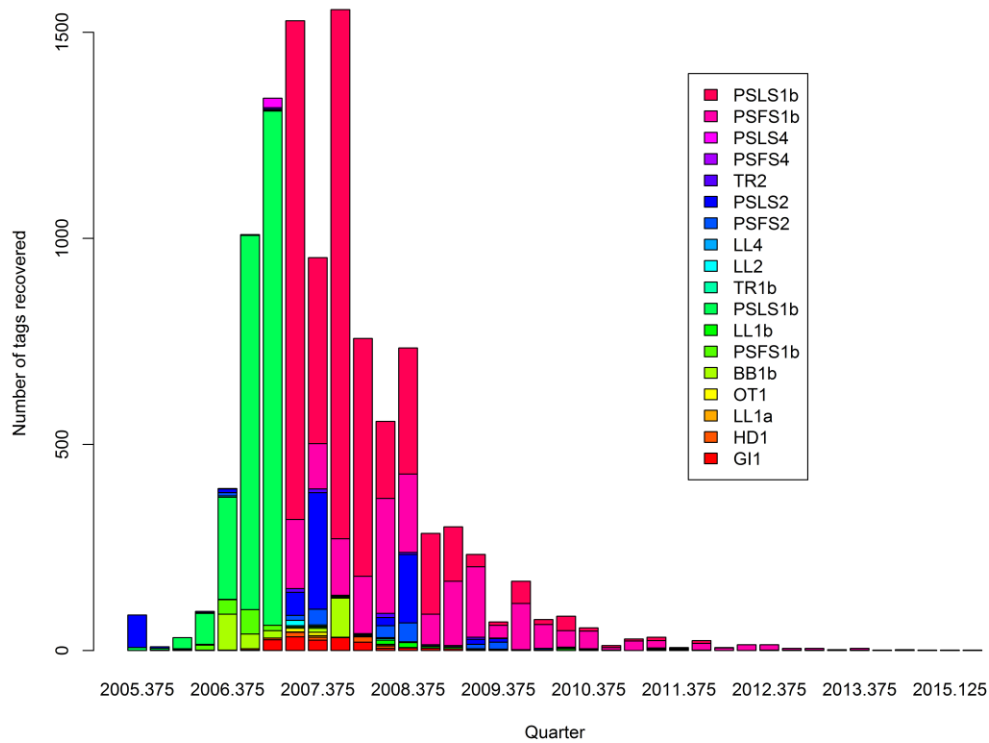


Figure 12: Yellowfin tag recoveries by year/quarter and fishery included in the assessment model. Purse seine tag recoveries have been corrected for reporting rate.

Table 4: Tag recoveries by year of recovery (box), region of release (vertical), and region of recovery. Region of recovery is defined by the definitions of the fisheries included in the model.

Recovery year	Release region	Recovery region		
		1	2	4
2005	1	1	21	-
	2	2	4	47
2006	1	1	2,495	29
	2	2	22	5
2007	1	1	4,127	411
	2	2	13	2
2008	1	1	1,510	277
	2	2	5	-
2009	1	1	464	61
	2	2	3	-
2010	1	1	171	5
	2	2	-	-
2011–2014	1	1	107	12
	2	2	-	-

Table 5: A summary of options of addressing factors relating to tag loss and reporting, for incorporation into the assessment. Alternative options were examined in the exploratory modelling.

Tag data processing	2015 assessment approach	Alternative options	
		<i>eTagNewProc</i>	<i>eTagALK</i>
Assigning age to tag release	mean length at age	mean length at age	Age length Key
Initial tag mortality	10%. SS3 reporting rate parameter fixed at 0.81.	10%. The number of tags in each release group was reduced by 10%. SS3 reporting rate parameter fixed at 1.	as the 2015 assessment
Chronic tag loss	3% annual rate. SS3 chronic tag loss parameter	as in 2015	as the 2015 assessment
Tag reporting (for the PS fisheries)	Tag returns by all PS recoveries were corrected for estimated annual reporting rate	Tag returns by PS recoveries landed in Seychelles were corrected for estimated quarterly reporting rate. At sea recoveries were assumed to have a 100% reporting rate	as the 2015 assessment
PS catches not examined for tags	10%. SS3 reporting rate parameter fixed at 0.81.	Tag returns by PS recoveries were also corrected for catches not examined for tags, based on proportions of EU PS catches landed in Seychelles.	as the 2015 assessment
SS3 reporting rate parameter (PS)	Fixed at 0.81	Fixed at 1	Fixed at 0.81
Number of releases	54392	48956	48956
Number of releases groups	131	131	145
Number of recovers	10428	10919	10897
Number of releases groups	1485	1485	1765

2.8 Environmental data

A range of environmental indices were configured to characterise seasonal and temporal variation in the oceanographic conditions in the Indian Ocean. These indices were primarily defined to investigate the potential for environmental covariates to be incorporated in the estimation of the movement of fish between adjacent model regions.

Regional environmental indices were determined using NOAA NCEP EMC CMB GODAS monthly current (u and v component) and sea temperature data (Behringer & Xue 2004). The model data are resolved by month and a grid of 1 degree longitude and 0.33 degree of latitude and available from January 1980.

Five sets of indices were included in the stock assessment modelling: three sets of SST indices from the Mozambique Channel (SST1), southern Indian Ocean (SST3) and eastern Indian Ocean (SST4) (Figure 13-left) and two sets of current indices from the central Indian Ocean (E/W u vector Current5) and northern Mozambique Channel (N/S v vector Current7) (Figure 13-right). The indices were derived by computing the average of the values within the specified area for each quarter (1980–

2017). Each index was then normalised as deviations from the overall average for the time series.

The SST1 and SST3 indices display a strong seasonal trend with highest values in quarters 1 and 4 corresponding to the austral summer (Figure 14). There are no strong temporal trends in either set of indices. The SST4 index is similar in formulation to the derivation of the Dipole Index. The indices exhibit a weaker seasonal trend and a higher degree of interannual variability compared to the other two sets of SST indices (Figure 14). The Current5 indices exhibit an interannual trend that is generally comparable to the SST4 index derived from an overlapping area in the central Indian Ocean, although the indices indicate that during the 2000s there was been a more persistent eastward flow compared to the preceding decade (Figure 14). This may provide an explanation for the lower longline CPUE in the eastern Indian Ocean (LL4 CPUE index) during the latter period (and the shift to deeper setting of longline gear).

The longer term trend in the Current7 indices is similar to the Current5 index with northward currents tending to prevail from the late 1990s (Figure 14). Langley (2016a) described the corresponding trends in the environmental variables and fishery performance.

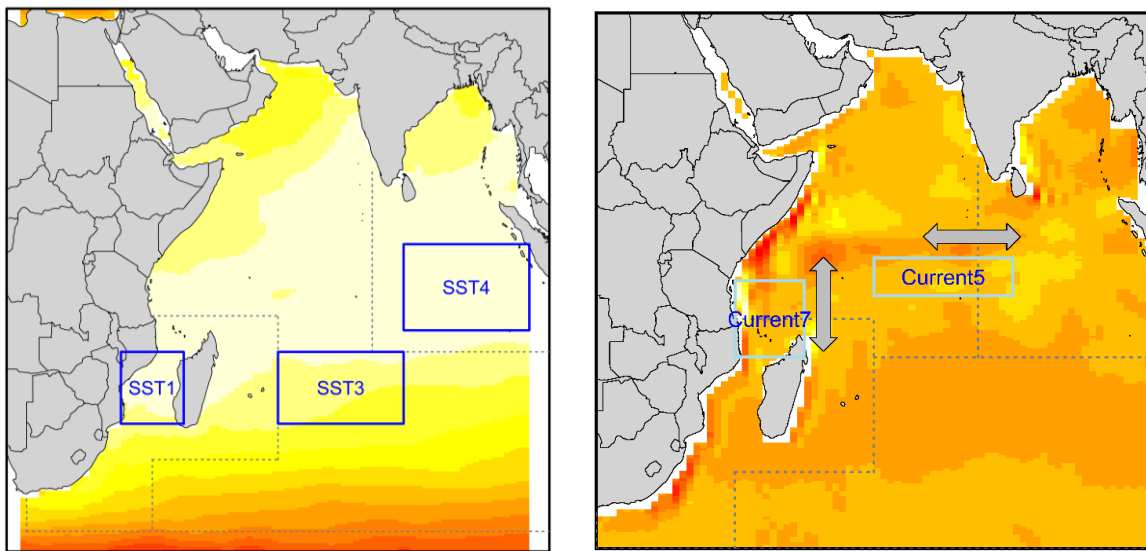


Figure 13: Definition of the areas used to derive the SST environmental indices (left) and the current environmental indices (right).

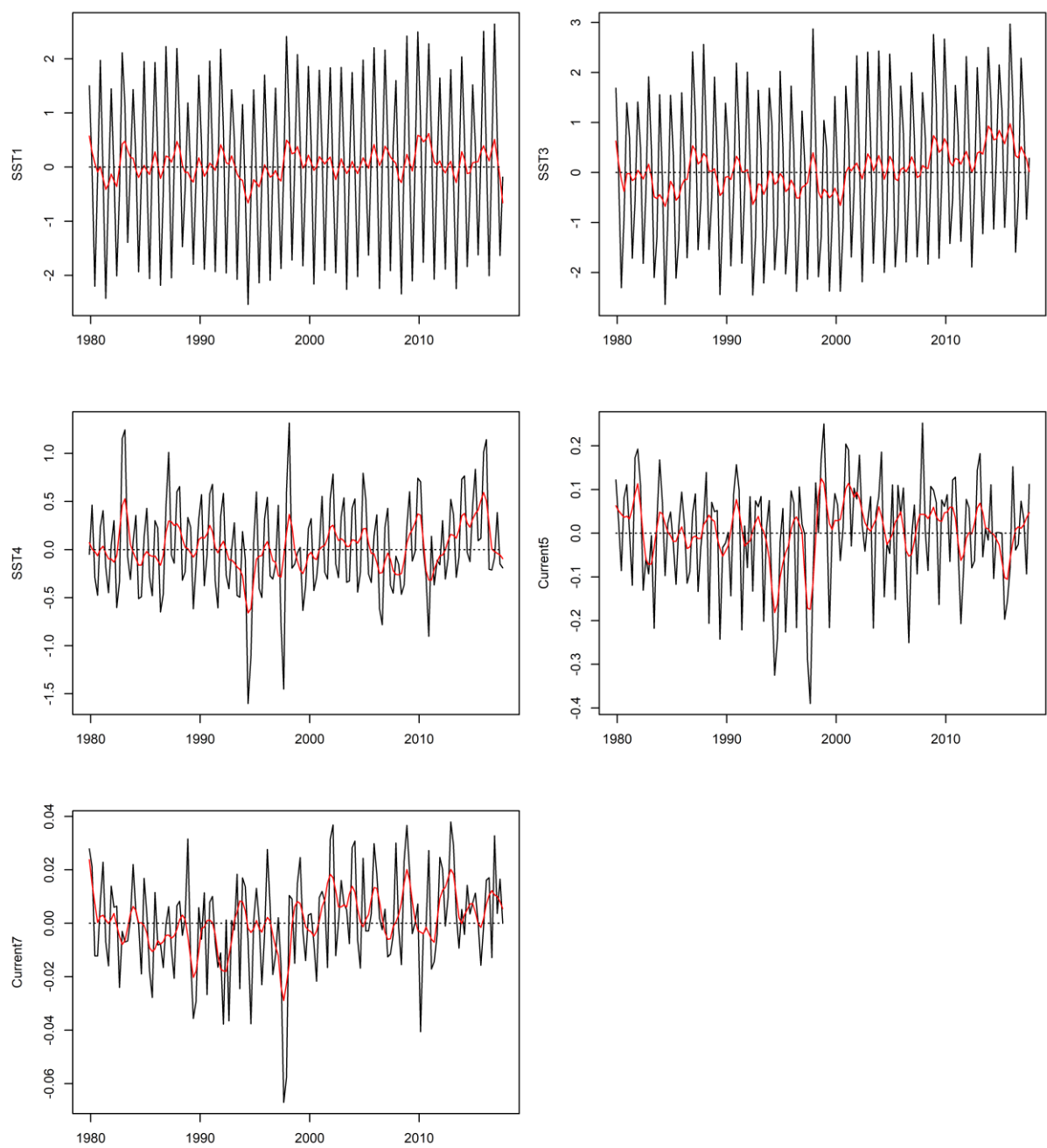


Figure 14: Quarterly indices for each environmental index (black lines) and a lowess smoothed trend for the indices (red line).

3. MODEL STRUCTURAL AND ASSUMPTIONS

3.1 Population dynamics

The spatially disaggregated model partitions the population into four regions. The population in each region is comprised of 28 quarterly age-classes both sexes combined. The first age-class has a mean fork length of around 22 cm and is assumed to be approximately three months of age based on ageing studies of yellowfin tuna (Fonteneau 2008). The last age-class comprises a “plus group” in which mortality and other characteristics are assumed to be constant. Insufficient sex-specific data are available to configure a two sex population model.

The model commences in 1950 at the start of the available catch history. The initial population age structure in each region was assumed to be in an unexploited, equilibrium state.

3.1.1 Recruitment

Recruitment occurs in each quarterly time step of the model. Recruitment was derived from a BH stock recruitment relationship (SRR) and variation in recruitment was estimated as deviates from the SRR. Recruitment deviates were estimated for 1972 to 2016 (180 deviates), representing the period for which longline CPUE indices are available. Recruitment deviates were assumed to have a standard deviation (σ_R) of 0.6. For 1950-1971, recruitment was derived directly from the SRR. The base model assumed a level of steepness (h) of 0.8 for the SRR, an intermediate value within the plausible range of steepness values generally adopted in the tuna assessments by other tuna RFMOs (0.7, 0.8 and 0.9) (Harley 2011).

Recruitment was assumed to occur in the two equatorial regions only (region 1 and 4). This assumption was based on the temperature preference for the spawning of yellowfin tuna and a minimum temperature for larval survival of about 24°C (Suzuki 1993). The constraint precluded large recruitments occurring within the subequatorial regions as evident in previous assessments (see Langley 2012).

The overall proportion of the quarterly recruitment allocated to region 1 and region 4 was estimated (*RecrDist_Area* parameters). The base model estimated 64% and 36% of the recruitment occurred in the respective regions. Variation in the regional distribution of recruitment was included by estimating temporal deviates of the *RecrDist_Area* parameters for 1977 to 2016 (2*160 deviates) (assuming a standard deviation of 1.0 for the deviates).

3.1.2 Growth and Maturation

Previous assessments of IO yellowfin tuna using MFCL have attempted to estimate the growth parameters during the fitting procedure (Langley et al. 2008, 2009). However, the resulting estimates of mean length-at-age were considerably higher than growth parameters estimated externally of the assessment model (Fonteneau 2008, Gaertner et al. 2009). Further examination of the data indicated that the growth parameters in the MFCL were being strongly influenced by the modal progression in the length frequency data from the fisheries in region 1a. This may indicate that growth rates in the Arabian Sea are higher than for the tropical fishery.

For the current assessment, growth parameters were fixed at values that replicated the growth curve derived by Fonteneau (2008) (Figure 15-left), and alternative growth estimates were used in exploratory modelling (Figure 15-right). The non-von Bertalanffy growth of juvenile yellowfin tuna is evident, with slow growth for young age classes and near-linear growth in the 60–110 cm size range. Growth in length is estimated to continue throughout the lifespan of the species, attenuating as the

maximum is approached. The estimated variance in length-at-age was assumed to increase with increasing age (Figure 15). Kolody (2011) cautioned that the artefact effect of the size selectivity may lead to growth estimates to derive from the von Bertalanffy growth.

Dortel et al. (2015) estimated growth integrating otolith readings from mark-recapture data and mode progressions from purse seine length frequency data. These estimates were comparable to the values currently incorporated in the assessment model. However, the estimates of the asymptotic length (L_{∞}) was higher (Figure 15-right)

Estimates by Eveson et al. (2015) using otolith and growth increment from tag data forecasted a mean asymptotic length of about 130 cm FL, which was comparatively low to the maximum lengths historically reported for yellowfin in the Indian Ocean. The sex-specific estimates from a small subset of samples supported the hypothesis that, on average, males grow to a larger size than females, with the mean asymptotic length estimate being 151 cm for males versus 140 cm for females. The sex-specific estimates were included in a two-sex model in the exploratory modelling.

Length based maturity OGIVEs for Indian Ocean yellowfin are available from Zudaire et al (2013). The paper presents two alternative maturity OGIVEs based on either the cortical alveolar or vitellogenetic stages of ovarian development (Figure 16– left). The length-based OGIVEs were converted to age-based OGIVEs assuming an equilibrium population age-length structure (Figure 16– right, derived from age-specific natural mortality, growth function and the assumed variation of length-at-age).

The maturity OGIVE based on cortical alveolar stage development indicates the onset of maturity occurs at about age 5 quarters (about 75 cm) and full maturity is attained at about 12 quarters. The maturity OGIVE based on vitellogenetic stage development is offset by about 3 quarters. The latter (older) estimate was used in a sensitivity in the previous assessment but it did not lead to appreciably different model results. The current assessment included only the OGIVE based on cortical alveolar stage development. The age-based OGIVE was provided to the base model as inputs of proportions mature at age. The length-based ogive was considered in the exploratory modelling.

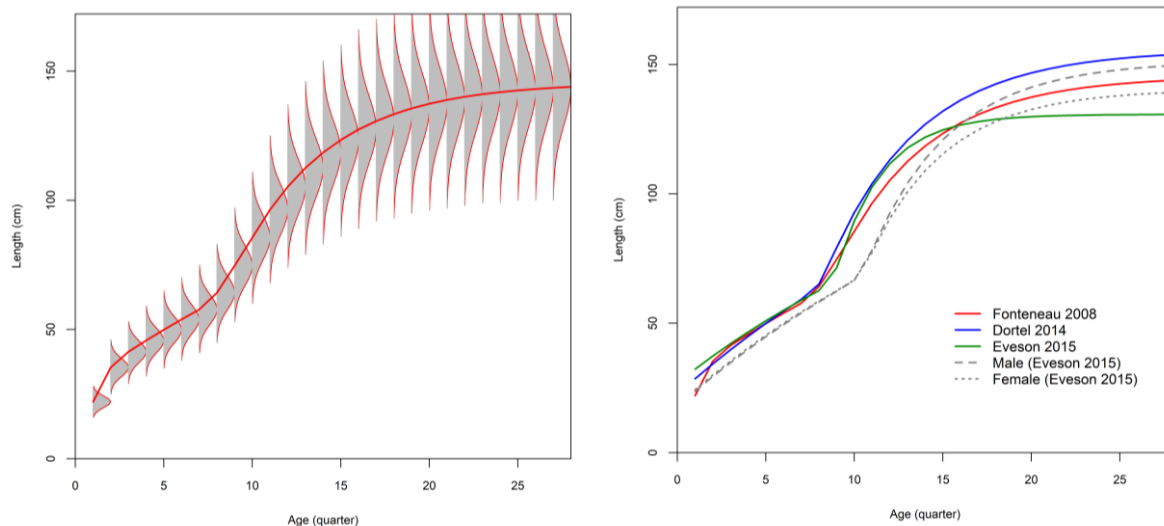


Figure 15: Fixed growth function for yellowfin tuna following Fonteneau 2008 (left – the red line represents the estimated mean length (FL, cm) at age and the grey area represents the assumed distribution of length at age), and alternative growth estimates used in exploratory modelling (right).

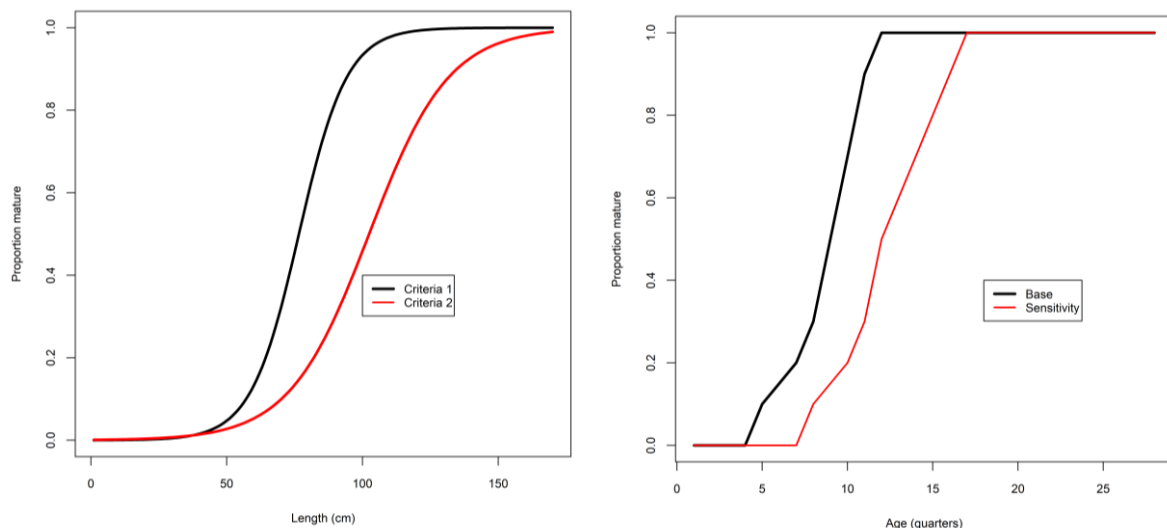


Figure 16: Length-based maturity OGIVES (left – from Zudaire et al 2013) and age-based maturity OGIVES for Indian Ocean yellowfin tuna (right – derived from Zudaire et al 2013). The ‘Sensitivity’ was examined in the previous assessment.

3.1.3 Natural mortality

Natural mortality is variable with age with the relative trend in age-specific natural mortality based on the values applied in the Pacific Ocean (western and central; eastern) yellowfin tuna stock assessments.

For the 2012 stock assessment (Langley 2012), the overall average level of natural mortality was initially fixed at a level comparable to a preliminary estimate of age-specific natural mortality from the tagging data (see IOTC 2008b). However, the overall level of natural mortality is low compared to the level of natural mortality used in the stock assessments of other regional yellowfin stocks (WCPPO, EPO and Atlantic) (Maunder & Aires-da-Silva 2012). The WPTT considered that the IO tag data set was likely to be reasonably informative regarding the overall level of natural mortality and for the final model options the overall (average) level of natural mortality estimated, while maintaining the relative age-specific variation in natural mortality (Langley 2012). The estimated level of natural mortality intermediate between the initial level and the level of natural mortality adopted for the WCPFC and IATTC yellowfin stock assessments (Maunder & Aires-da-Silva 2012).

The resulting age-specific natural mortality has been used as the base level of natural mortality for the 2015 stock assessment and the update in 2016, while the lower level of natural mortality is included in a model sensitivity (M_{low}). (Figure 17). The 2015 assessment also evaluated the utility of the tagging data set for the estimation of natural mortality (Langley 2015).

For the current assessment, the base level M is adopted for the base model and the lower level of natural mortality is included in a model sensitivity (M_{low}). In addition, the Lorenzen type (Lorenzen 1996) of M -at-age function was also explored. The Lorenzen function assumes a monotonically declining relationship between M and the mean weight of fish (W_a) in successively older age classes a , such as $M_a = 3W_a^{-0.288}$. The mean body weight was derived from the growth and the length-weight relationship.

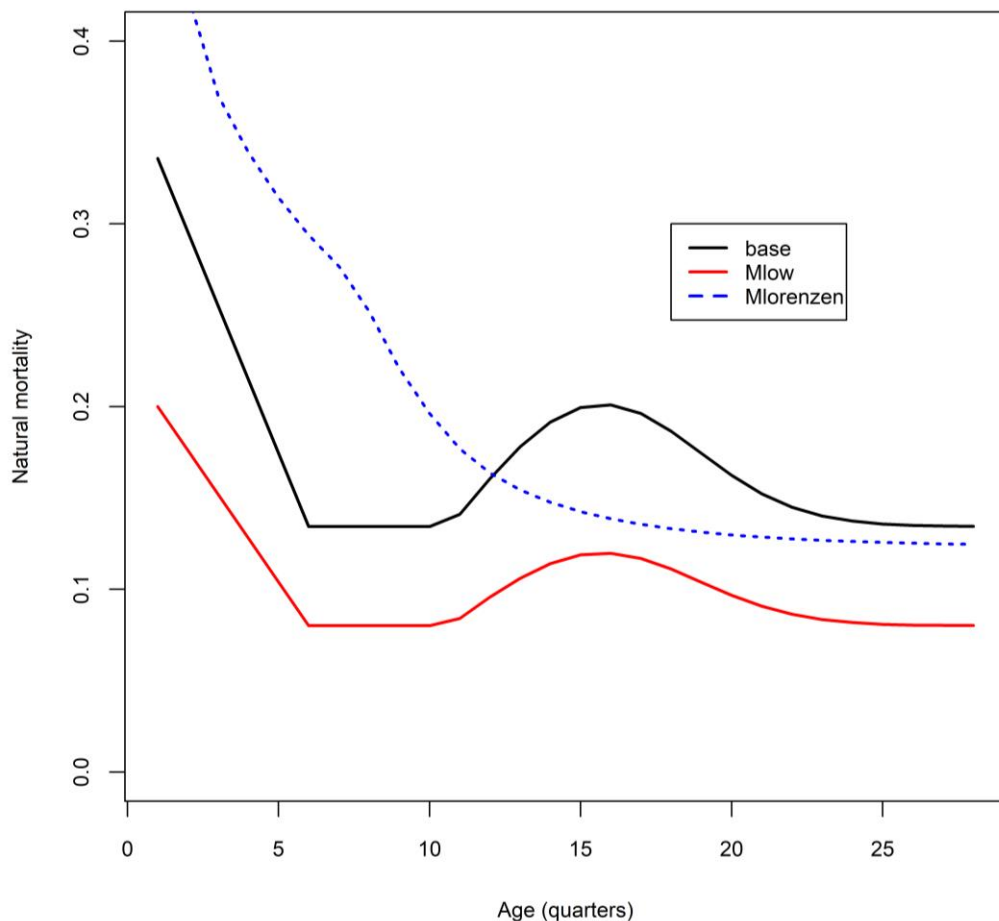


Figure 17: The age-specific natural mortality schedule assumed for the assessment model (*Base*) and other age-specific M schedules from various model options (see text for details).

3.1.4 Movement

For the four region model, reciprocal movement was assumed to occur between adjacent model regions, specifically R1-R2, R1-R4, R3-R4 (3x2) (Figure 1). Movement is parameterised as the proportional redistribution of fish amongst regions, including the proportion remaining in the home region. The redistribution of fish occurs instantaneously at the end of each model time step.

Movement was parameterised to estimate differential movement for young (2–8 quarters) and old (≥ 9 quarters) fish to approximate potential changes in movement dynamics associated with maturation. Thus, for each movement transition two separate movement parameters were estimated. Fish did not commence moving until the end of age 2 quarters.

There is no seasonal structure in the assessment model due to the quarterly time step and consequently it was not possible to directly estimate seasonal movements. The seasonal variation in the longline CPUE indices and the purse-seine catches, particularly in region 2, indicate that there are likely to be significant seasonal changes in the regional abundance of yellowfin.

To incorporate seasonal movement dynamics, a range of environmental covariates were included in the movement parameterisation. These environmental covariates were based on quarterly SST and current flow specific to the transitional areas between regions (defined in Section 2.8). The individual metrics were associated with the specific movement parameters as defined in Table 6. The movements of mature (≥ 9 quarters) fish were linked to SST based metrics, while the movements of

juvenile fish were linked to current based metrics. The environmental covariates were assigned to the preceding quarter to facilitate movement in advance of the fishery (movement is configured to occur at the end of each quarter).

The rationale for linking juvenile movements to current flow was based on an analysis of the IO tag release and recovery location data. The analysis indicated that the location of spatially aggregated tag recoveries could be approximated based on the passive movement of fish from the tag release location.

The movement parameterisation incorporates the environmental covariate by modifying the base movement parameter by adding the product of the link parameter and the environmental index; i.e., $parm'(y) = parm + link * env(y,g)$ where $link$ is the environmental link parameter, $parm$ is the base parameter being adjusted, $parm'$ is the value after adjustment, and $env(y,g)$ is the value of the environmental input g in year. As such the covariates are included as additive effects based on the recommendation of Methot (2013), representing a small revision to the previous assessment in which the covariates were included as multiplicative effects.

Table 6: Estimated movement link parameters from the base case model.

Transition	Life stage	Covariate
R1 to R2	Immature	<i>Current7</i>
R1 to R2	Mature	<i>SST1</i>
R1 to R4	Immature	<i>Current5</i>
R1 to R4	Mature	<i>SST4</i>
R2 to R1	Immature	<i>Current7</i>
R2 to R1	Mature	<i>SST1</i>
R3 to R4	Immature	<i>SST3</i>
R3 to R4	Mature	<i>SST3</i>
R4 to R1	Immature	<i>Current5</i>
R4 to R1	Mature	<i>SST4</i>
R4 to R3	Immature	<i>SST3</i>
R4 to R3	Mature	<i>SST3</i>

3.2 Fishery dynamics

Fishery selectivity is assumed to be age-specific and time-invariant. For the longline fisheries (LL 1a, 1b, 2, 3 and 4) a single selectivity is estimated that is shared among the five fisheries. The selectivity is also shared by the four sets of LL CPUE indices. The longline selectivity was parameterised with a logistic function that constrains the older age classes to be fully selected (“flat top”). The selectivity of the fresh tuna longline fishery (LF4) was estimated using a separate logistic function.

The free-school (FS) and FAD (LS) purse seine fisheries within region 1b were divided into three time periods (pre 2003, 2003–2006 and post 2006) based on the observation that the size of fish caught differed between these periods. Earlier stock assessments had estimated separate selectivities for each time period (and fishery). However, the stock assessment results were relatively insensitive to the temporal changes in selectivity and, these changes in selectivity were associated with the tag data set and, specifically, the apparent recovery of fish at liberty for extended periods (2–3 years) from the purse-seine FAD fishery. For simplicity, a single selectivity was estimated for each method (FS and LS) for the three time periods. The corresponding purse-seine method selectivities were also shared with the purse-seine fisheries in region 2 and region 4.

The two purse seine selectivities (FS and LS) were formulated using a cubic spline interpolation with five nodes. The nodes were specified to approximate the main inflection points of the selectivity function. This formulation was sufficiently flexible to provide a reasonable representation of the modal

structure of the length composition of the catch from the two purse seine methods.

For the other fisheries, selectivity was parameterised using a double-normal function (Methot 2013). No length frequency data are available for the “Other” fishery in region 1a, while limited data are available from the OT 4 fishery. Similarly, size data were available from the troll fishery in region 4, but not from the fisheries in regions 1b and 2. The selectivity of the “Other” fisheries was assumed to be equivalent among the two regions (1a and 4), while a common selectivity was assumed for the troll fisheries in regions 1b and 4.

Fishing mortality was modelled using the hybrid method that the harvest rate using the Pope’s approximation then converts it to an approximation of the corresponding F (Methot & Wetzel 2013).

3.3 Dynamics of tagged fish

3.3.1 Tag mixing

In general, the population dynamics of the tagged and untagged populations are governed by the same model structures and parameters. An obvious exception to this is recruitment, which for the tagged population is simply the release of tagged fish. The probability of recapturing a given tagged fish is the same as the probability of catching any given untagged fish in the same region. For this assumption to be valid, either the distribution of fishing effort must be random with respect to tagged and untagged fish and/or the tagged fish must be randomly mixed with the untagged fish. The former condition is unlikely to be met because fishing effort is almost never randomly distributed in space. The second condition is also unlikely to be met soon after release because of insufficient time for mixing to take place. Depending on the distribution of fishing effort in relation to tag release sites, the probability of capture of tagged fish soon after release may be different to that for the untagged fish. It is therefore desirable to designate one or more time periods after release as “pre-mixed” and compute fishing mortality for the tagged fish based on the actual recaptures, corrected for tag reporting (see below), rather than use fishing mortalities based on the general population parameters. This in effect desensitizes the likelihood function to tag recaptures in the pre-mixed periods while correctly discounting the tagged population for the recaptures that occurred.

An analysis of the tag recovery data was undertaken to determine an appropriate mixing period for the tagging programme (Langley & Million 2012). The analysis revealed that the tag recoveries from the FAD purse-seine fishery were not adequately mixed, at least during the first 6 months following release. Conversely, the free-school tag recoveries indicate a higher degree of mixing within the fished population. Most of the tagged yellowfin were in the length classes that are not immediately selected by the free-school fishery (< 90 cm). A mixing period of about 6–12 months is of sufficient duration for most tagged fish to recruit to free-school fishery (> 90 cm) and no longer be vulnerable to the FAD fishery. However, the maximum displacements of tags reach a plateau within a few weeks of release (Figure B1 Appendix B), suggesting rapid movement of yellowfin within the tag release/recovery areas. On basis of the above, it was considered that a mixing period of three quarters was probably sufficient to allow a reasonable degree of dispersal of tagged fish amongst the yellowfin tuna population within the primary region of release. The distribution of annual RTTP tag returns from the main recovery period (2006–2009) are shown in Figure B2, Appendix B.

The release phase of the tagging programme was essentially restricted to the western equatorial region. The examination of the tag recoveries of bigeye tuna from the PSLS fishery identified considerable differences in the recovery rate (number of tags per tonne of catch) amongst latitudinal zones for tags at liberty for at least 12 months (Langley 2016b). In an attempt to account for the incomplete mixing of tagged fish, the bigeye assessment model further partitioned the western equatorial region into two regions along the equator. A similar analysis was performed to yellowfin tag data, however, the results indicated that the recovery rate of tags after 3 quarters at liberty was similar both in trend and magnitude between latitude band 0 – 10N and 0 – 10S within the western equatorial

region (Figure B3 Appendix B). This suggested a reasonable degree of mixing of tagged fish at the regional scale. Nonetheless, a sensitivity model that further partitions the western equatorial region is still considered in the exploratory modelling.

The distribution of tags throughout the wider IO appears to have been relatively limited as is evident from the low number of tag recoveries from the fisheries beyond region 1b. Tag recoveries from beyond region 1 and 2 are unlikely to significantly inform the model regarding movement rates given the lack of information concerning reporting rates of tags for these fisheries (see below).

3.3.2 Tag reporting

Estimates of tag reporting rates from the purse seine fishery were available from tag seeding trials. These estimates were applied to correct the number of tags included in the recovery dataset for the purse seine fisheries within region 1b and region 2 (see section 2.7 for details)

For the other fisheries, there is very limited information is available to indicate the tag reporting rates and fishery specific reporting rates were estimated based on uninformative priors. All fishery reporting rates were assumed to be temporally invariant

3.4 Modelling methods, parameters, and likelihood

The total likelihood is composed of a number of components, including the fit to the abundance indices (CPUE), tag recovery data, fishery length frequency data and catch data. There are also contributions to the total likelihood from the recruitment deviates and priors on the individual model parameters. The model is configured to fit the catch almost exactly so the catch component of the likelihood is very small. There are two components of the tag likelihood: the multinomial likelihood for the distribution of tag recoveries by fleets over time and the negative binomial distribution of expected total recaptures across all regions. Details of the formulation of the individual components of the likelihood are provided in Methot & Wetzel (2013).

Following the previous assessment, the weighting of the CPUE indices followed the approach of Francis (2011). A series of smoother lines were fitted to the CPUE index and the RMSE of the resulting fit to each set of CPUE indices was determined as a measure of the magnitude of the variation of each set of indices CPUE indices. The resulting RMSEs were relatively high (0.40–0.50). However, a significant proportion of this variation is related to the relatively high seasonal variation in CPUE in most regions. The analysis performed to the annualised CPUE index (Hoyle et al. 2018) resulted in considerable reduction in the RMSEs (0.15–0.2). On that basis, a CV of 0.2 was assigned to each set of CPUE indices in the base model, to ensure the stock biomass trajectories were broadly consistent with the CPUE indices while allowed for a moderate degree of variability in fitting to the indices (a CV of 0.3 was used in the previous assessment).

The relative weighting of the tagging data was controlled by the magnitude of the over-dispersion parameters assigned to the individual tag release groups. In the previous assessment, the over-dispersion parameters for all tag release groups were set at 7.0 - determined iteratively from the residuals of the fit to the tag recovery data (observed – expected number of tags recovered). The same value was used in the current assessment and an alternative value of 70 was used in a sensitivity model.

The reliability of the length composition data is variable across fisheries and over time periods. For that reason, it was considered that the length composition data should not be allowed to dominate the model likelihood and directly influence the trends in stock abundance. Following the previous assessment, an overall effective sample size (ESS) of 5 was assigned to all length composition observations (all fisheries, all time periods) following the Francis (2011) method. This essentially gave the entire length composition data set a relatively low weighting in the overall likelihood. Nonetheless,

due to the magnitude of the length composition data, these data were sufficiently informative to provide reasonable estimates of fishery selectivity and provide some information regarding recruitment trends.

The weightings were applied by the values assigned to components of the likelihood of each observational dataset included in the total model likelihood. A default lambda of 1.0, represented the native weighting of the data. A lower value of Lambda would effectively downweighting the dataset relative to other observations, effectively reducing its influence on the overall model estimates. A lower lambda was applied to the tagging data in a sensitivity model.

The Hessian matrix computed at the mode of the posterior distribution was used to obtain estimates of the covariance matrix, which was used in combination with the Delta method to compute approximate confidence intervals for parameters of interest.

4. ASSESSMENT MODEL RUNS

A series of model runs were conducted for the current assessment, including sequential updates of the base case from the 2016 assessment, exploratory runs to investigate alternative model options, and the final base case and sensitivities to provide estimates of stock status. The assessment was conducted using the 3.24z version of the Stock Synthesis software under the Linux platform. The stock status was reported for the terminal year of the model (2017).

4.1 2016 model updates

The update of the 2016 base case model was to ensure a level of continuity from previous assessment, and to assess the influence of the additional data. The model structure was updated to extend the model period to include the 2016 and 2017 year. The changes were made sequentially to the 2016 assessment during update process, as summarised in Table 7.

Table 7: Description of the sequence of model runs to update the 2016 base model.

Model	Description
Base2016	2016 base case
UpdateCPUE	Revised Longline CPUE indices Model extended to include 2016 and 2017, with catches equivalent to 2015 catches.
UpdateLF	Revised and updated length composition data for 2015 – 2017
UpdateCatch	Revised and updated catches for 2016 and 2017
Update2018	Updated environment covariates for 2016 and 2017; Extend period of estimation for Recruitment deviates (to 2016); Definition of F-age for determination of MSY (2016 – 2017);

4.2 Exploratory model runs

Following further reviews, additional revisions were provided to configuration of the updated model (Table 8). The revised model (*Revised2018*) served as a starting point for the subsequent exploratory analysis. The exploratory phase investigated a range of model options examining assumptions related to the configuration of key data sets, biological parameters and model structure (i.e. spatial and temporal). The analysis extended the exploratory models of the previous assessment. A description of the range of alternative model options considered is presented in Table 8.

These model trials were completed prior to the finalisation of the catch and size data for 2016/2017 and therefore the fishery catches, and size distribution for the last two years were assumed to be equivalent to the 2015 (e.g. *eRevised2018*).

Table 8: Description of the exploratory runs for the 2018 assessment.

Model	Description
<i>Revised2018</i> (<i>eRevised2018</i>)	Revised parameter prior distributions (e.g. relaxing the constraint on some selectivity parameters); environmental linking parameters reparametrized as additive rather than multiplicative effects (see Methot (2013)); Revised length-weight relationship (Chassot et al. 2016); LL CPUE regional weighting factors using the ‘7994m8’ estimates from Hoyle & Langley (2018)
LL CPUE regional weighting	
<i>e7594m8</i>	LL CPUE regional weighting using the ‘7594m8’ estimates from Hoyle & Langley (2018)
<i>e8000m8</i>	LL CPUE regional weighting using the ‘8000m8’ estimates from Hoyle & Langley (2018)
Tag data processing	
<i>eTagNewProc</i>	Tag data processed using the ‘ <i>TagNewProc</i> ’ option as in Table 5
<i>eTagALK</i>	Tag data processed using the ‘ <i>TagALK</i> ’ option as in Table 5
Biological parameters	
<i>eMaturityLogistic</i>	Length-based logistic maturity ogive
<i>eGrowthDortel</i>	Growth estimates by Dortel et al. (2014) approximated by age-varying <i>k</i>
<i>eTwosex</i>	Model was reconfigured to be two sexes with differential <i>Linf</i> growth parameters (150 cm for males and 141 cm for females).
<i>eMlow</i>	Relative age-specific natural mortality equivalent to base model. Overall level of <i>M</i> approximately 60% of the base level.
<i>eMlorenzen</i>	Age-specific natural mortality parameterised using the Lorenzen functional form. Overall level of <i>M</i> approximately 120% of the base level.
Fishing selectivity	
<i>eSelPSRegion</i>	Estimating separate PSLS selectivity by region
<i>eSelTimeVarying</i>	Estimating selectivities by time blocks for GI 1b fishery (2000-2017), and HD 1b fishery (2003-2007); Estimating time-varying selectivities for LL fisheries 1955-1972 (parametrised as annual deviations), and for PSLS fisheries 1983-2015 (parameterised as random walks);
Spatial structure	
<i>eRegion5</i>	A five-region model with the western equatorial region (region 1b) partitioned into two regions – the area south of the equator and the area north of the equator (R1bS and R1bN). Region 1bN and Region 1a were treated as one model region; Separate LL CPUE indices for R1bN and R1bS (Hoyle et al. 2018); Partitioning the longline and purse seine fisheries in region 1b in accordance with the new regional structure (but no temporal split of the purse seine fisheries); size data in region 1b was simply assigned to the northern fisheries with shared selectivity with the southern fisheries. Partitioning the tag data according to the new regional structure; Recruitment assumed to occur in R1a and R1bN (as one region), R1bS, and R4; constant movement not linked to environment variables; (estimated for R1bN-R1bS, R1bN-R4, R1bS-R4; R1bS-R2, R3-R4)
Table 8. continued.	

Temporal structure	
<i>eYearSeason</i>	<p>Model configured using the SS3 internal year-season structure in which an annual cycle consists of 4 seasons (3 month each);</p> <p>Spawning biomass is calculated once a year, and is apportioned among seasons with temporal variations estimated for 1970 to 2016;</p> <p>Constant movement rates are estimated for juvenile (2 year and under) and adults (3 year and over), separately for each season (no environmental data);</p> <p>The tag ages are assigned to annual increment; Fishery selectivities are modelled using a length-based process rather than age based;</p> <p>Age (annual)-specific natural mortality (base M averaged over quarterly ages); age (annual)-varying growth k to approximate the growth estimates by Fonteneau (2008)</p>

4.3 Base case and sensitivity

Based on results of the exploratory modelling, the configuration for a base model was identified (Table 9). Further sensitivity models were conducted to address assumptions related steepness, tag mixing, and the utility of purse seine CPUE indices (Table 10)

Table 9: Main structural assumptions of the yellowfin tuna base analysis and details of estimated parameters. Changes to the 2016 base case are highlighted in red.

Category	Assumptions	Parameters
Recruitment	Occurs at the start of each quarter as 0 age fish. Recruitment is a function of Beverton-Holt stock-recruitment relationship (SRR). Regional apportionment of recruitment to R1 and R4 only. Temporal recruitment deviates from SRR, 1972–2016. Temporal deviates on proportion of recruitment allocated to R1 and R4, 1977–2016.	R_0 Norm(10,2); $h = 0.80$ $PropR1$ Norm(1.5,0.25); $Prop R4$ Norm(0.5,0.25) $SigmaR = 0.6$. 180 deviates. Deviates Norm(0,1), 320 deviates.
Initial population	A function of the equilibrium recruitment in each region assuming population in an unexploited state prior to 1950. Initial fishing mortality fixed at zero for all fisheries.	
Age and growth	28 quarterly age-classes, with the last representing a plus group. Growth based on VonBert growth model with age-specific k to approximate the mean length at age determined by Fonteneau (2008). SD of length-at-age based on a constant coefficient of variation of average length-at-age. Mean weights (W_j) from the weight-length relationship $W = aL^b$ (source IOTC-2016-WPDCS12-INF05).	$L_{infinity} = 145\text{cm}$, k (base) = 0.455, k deviates for ages 2–13. CV = 0.10 $a = 2.459 \text{ e-05}$, $b = 2.9667$
Natural mortality	Age-specific. Relative variation amongst ages based on WCPO yellowfin assessment and overall scale of natural mortality estimated in 2012 IO yellowfin assessment (see Figure Figure 17). Constant over time and among regions.	
Maturity	Age-dependent, specified. Derived from length based maturity OGIVE in Zudaire et al (2013). Mature population includes both male and female fish (single sex model).	age-class 0-4: 0; 5: 0.1; 6: 0.15; 7: 0.2; 8: 0.5; 9: 0.5; 10: 0.7; 11: 0.9; 12-28: 1.0
Movement	Age-dependent with two blocks; age classes 2-8 and 9-28. Constant among quarters. Correlated with oceanographic covariates.	10 movements * 2 age blocks. Norm(0,4). 12 parameters Norm(0,1).
Selectivity	Age specific, constant over time. Principal longline fisheries share logistic selectivity parameters. Common selectivity for all PSLS fisheries. Common selectivity for all PSLS fisheries. LF4 fishery logistic selectivity. All other fisheries: double normal selectivity. OT 1a & 4 and TR 1b & 4 share selectivity parameters. GI 1a estimated selectivity for time blocks before and after 2000; HD 1a	Logistic $p1$ Norm(14,1), $p2$ Norm(4,1) Five node cubic spline Five node cubic spline

	estimated selectivity for time blocks before and after 2005	
Catchability	Constant over years and among regions for LL CPUE indices. CPUE indices are scaled to reflect different region sizes. Scaling factors were revised using the '7994m8' estimates from Hoyle & Langley (2018). No seasonal variation in catchability for LL CPUE. LL CPUE indices have CV of 0.2 for all regions.	Unconstrained (nuisance) parameter <i>LLq</i>
Fishing mortality	Hybrid approach (method 3, see Methot & Wetzel 2013).	
Tag mixing	Tags assumed to be randomly mixed at the model region level three quarters following the quarter of release. Accumulation after 16 quarters	
Tag loss	Chronic tag loss represents tag shedding of 20% over 2000 days (Gaertner & Hallier). Applied to all tag release groups.	Parameter -3.5
Tag reporting	All (corrected) reporting rates constant over time. Common tag reporting rate fixed for all PS fisheries. Non PS tag reporting rates uninformative priors.	Tag observations corrected for reporting rate/tag loss following the 'NewTagProc' option in Table 5
Tag variation	Over dispersion parameter of 7.0. Applied to all tag release groups.	Tag OD 7.0
Length composition	Multinomial error structure, all length samples assigned ESS of 5.0.	

Table 10: Description of the sensitivity runs for the 2018 assessment.

Model option	Description
<i>base</i>	base model
<i>reference</i>	Excluded size composition data 2015 – 2017
<i>h70</i>	Stock-recruitment steepness parameter 0.7
<i>h90</i>	Stock-recruitment steepness parameter 0.9
<i>Mlow</i>	Relative age-specific natural mortality equivalent to base model. Overall level of <i>M</i> approximately 60% of the base level.
<i>NoEnviroMove</i>	Excluding the environmental data and movement rates are assumed to be constant
<i>TagMix4Q</i>	- increase tag mix period to 4Q from 3Q
<i>TagMix8Q</i>	- increase tag mix period to 8Q from 3Q.
<i>TagOD70</i>	- increase tag over-dispersion parameter from 7 to 70
<i>TagDwt01</i>	- Tag dwt lambda = 0.1 for both components of tag likelihood. Represents an arbitrary level of weighting applied to the tag data set that is 10% of the weight associated with the actual number of tag recoveries.
<i>CPUETWR1</i>	- incorporate region 1 Taiwanese LL CPUE indices 1998–2016, CV 0.2 - exclude region 1 (Joint) LL CPUE indices 1998–2016
<i>PS_CPUE</i>	- incorporate region 1 PS FAD CPUE indices, high weighting CV 0.1 - incorporate region 1 PS SCH CPUE indices, high weighting CV 0.1 - selectivity of PS FAD CPUE linked to PSLS fishery 24. - selectivity of PS SCH CPUE linked to Fishery 23. - Dwt LL region 1 CPUE indices = CV 1.0
<i>PS_CPUE_Q125</i>	- incorporate region 1 PS FAD CPUE indices, high weighting CV 0.1 - incorporate region 1 PS SCH CPUE indices, high weighting CV 0.1 - assuming a catchability increase of approximately 1.25% per year (both) - Dwt LL region 1 CPUE indices = CV 1.0
<i>PS_CPUE_estQ</i>	- incorporate region 1 PS FAD CPUE indices - incorporate region 1 PS SCH CPUE indices - lambda = 0 both series and estimate analytic catchability This model is to estimate the annual catchability change from the trend in the residuals from the fit to the PS CPUE indices (see Kolody 2018 for details)
<i>LLFAD</i>	- incorporate region 1 PS FAD CPUE indices, high weighting CV 0.1

5. MODEL RESULTS

5.1 2016 model updates

The step-wise models showed broadly consistent biomass trend as the 2016 base model. However, updating the CPUE indices reduced the estimates of the spawning biomass prior to the 1990s (Figure 18), as the new indices suggested less decline in abundance compared to the indices included in the previous assessment, particularly in region 2 and 3 (see Figure 5). The update of size composition data (mostly with the addition of data for 2014 – 2017) increased the spawning biomass estimates, particularly after the 2011 and the initial biomass (Figure 18). Further model updates (updated and revised catches, and extending the period of estimation of recruitment deviates and the period for defining the F-at-age matrix) had very little effect on model estimates (Figure 18).

The simple update (*Update2018*) of the model did not change the estimate of the terminal stock status in relation to the reference point (the stock is estimated be overfished and subjected to overfishing in 2017). But the updated/revised size composition data appeared to have an appreciable impact on recent biomass estimates (e.g. the ratio of SB2015/SBMSY estimated to be greater than 1), which was

corroborated by the retrospective analysis conducted for the final models (see Section 6.2). We note that the 2016 assessment was conducted as a simple update and therefore used the same size data as the 2015 assessment (up to 2013). The current assessment thus added four years of additional size data (2014 – 2017) compared to the previous assessment, with further revisions made to the size data in the early years for some fisheries (e.g. LF 4 and HD 1a).

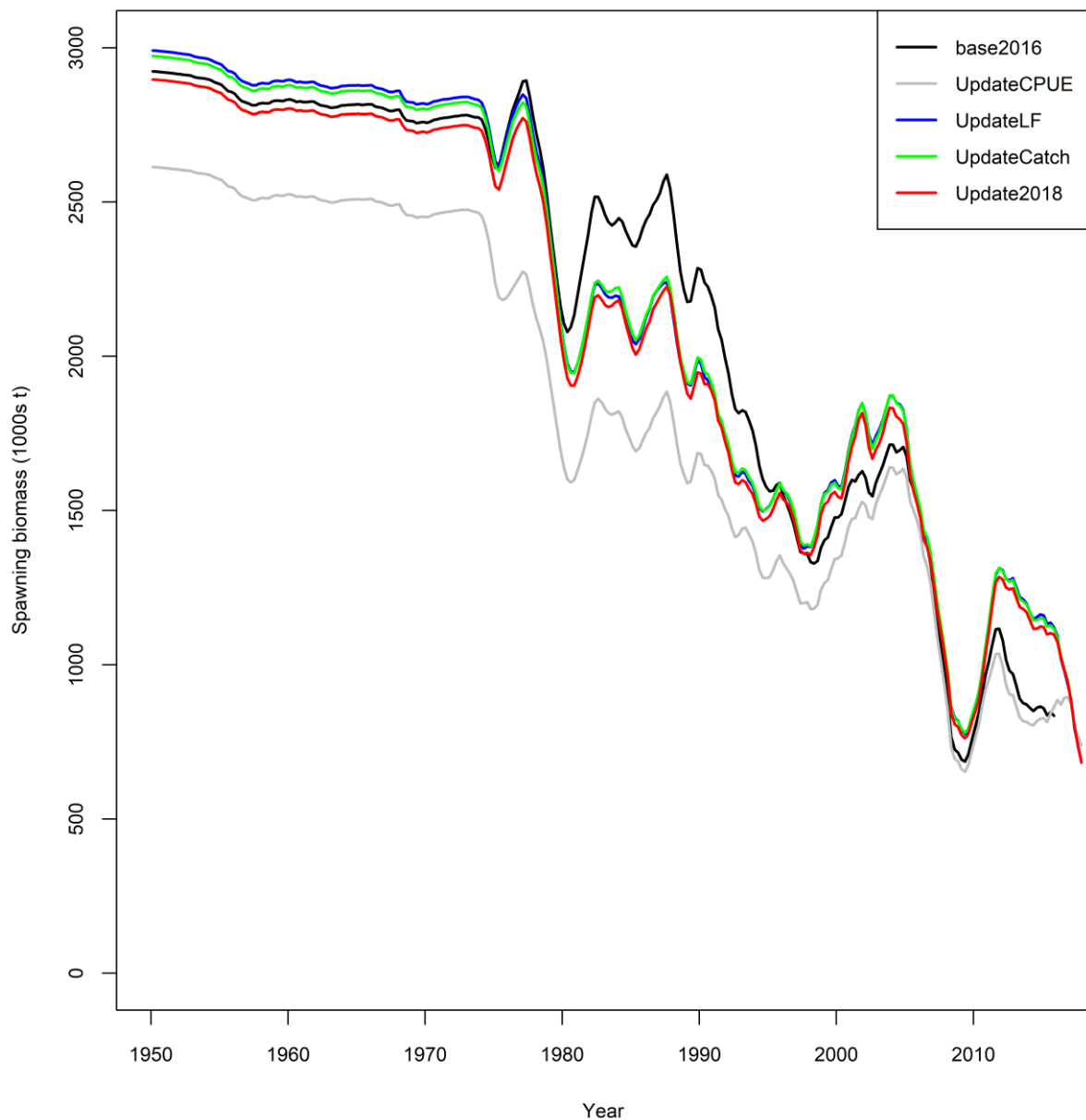


Figure 18: Spawning biomass trajectories for IO yellowfin tuna from the step-wise model updates for 2018 (from Base 2016).

Table 11: Estimates of management quantities for the step-wise updates of the 2016 stock assessment model.

Option	SB_0	SB_{MSY}	MSY	SB_{2015}	SB_{2017}	SB_{2015}/SB_{MSY}	SB_{2017}/SB_{MSY}	F_{2015}/F_{MSY}	F_{2017}/F_{MSY}
<i>Base2016</i>	2,923,680	947,250	421,840	844,042	-	0.89	-	1.11	-
<i>UpdateCPUE</i>	2,613,720	857,451	392,611	836,713	794,718	0.98	0.93	1.23	1.13
<i>UpdateLF</i>	2,991,360	988,627	377,173	1,137,483	775,888	1.15	0.78	1.03	1.01
<i>UpdateCatch</i>	2,973,250	954,942	369,273	1,129,263	775,418	1.18	0.81	1.03	1.15
<i>Update2018</i>	2,897,440	939,231	378,937	1,105,255	774,066	1.18	0.82	1.08	1.13

5.2 Exploratory models

The exploratory runs aim to explore model options relating parameter and structural assumptions and to identify potential revisions to the updated model. These models further extended the exploratory analysis conducted in the previous assessment (Langley 2015). The results of the exploratory runs are given in Appendix C and are also summarised below.

Rewvisions to the updated model

On basis of the simple model updates (*Update2018*), several minor revisions were made to model configurations (*Revised2018*), including the adoption of more uninformative (wider) prior distributions for some parameters (e.g. selectivity parameters), the revised length-weight relationship (IOTC 2016), and reparameterization of the environmental effects. The revised model estimated a lower stock biomass than the updated model (Figure 19), and further investigation suggested that this is primarily related to the relaxation of one of the selectivity parameters for the handline fishery in region 1a (it was bounded incorrectly).

Revised2018 also adopted the new regional weighting factors for the LL CPUE, as discussed below.

Regional weighting factors for LL CPUE.

Update2018 estimated a very large proportion of biomass resides in region 2 (more than region 1 in recent years), which represents a significant change to the 2016 base model (Figure C3). Despite the adoption of the same regional weighting (based on the Japanese longline CPUE data from 1963–75), the LL CPUE index in region 2 relative to region 1b changed considerably compared to the previous assessment (for the 2016 base model, the R2 indices are much lower than R1 index; but for the updated model, the R2 indices are much closer to the R1 index up to the late 1990s, and are much higher in more recent years, see Figure C2). Some of these changes are related to changes in the data cleaning method in the standardisations (S. Hoyle pers. comm). The very large biomass in region 2 was considered implausible given the relatively small contribution of catches in the region (Langley 2015).

On basis of above, *Revised2018* adopted the revised regional weighting factors, estimated using the ‘7994m8’ method as recommended by Hoyle & Langley (2018). The revised model estimated a much smaller proportion of biomass in region 2, with its initial biomass being about a third of region 1 (Figure C3). The revised regional weighting factors changed the relative distribution of biomass among regions, but they have very little impact on the overall biomass estimates.

Further model runs were conducted using alternative scaling factor estimates derived from different time periods, namely 1975 – 1994 (e7594m8) and 1980 – 2000 (e8000m8) (see Hoyle & Langley 2018). These models produced very similar regional and overall biomass estimates (Figures C3 and C4).

Options of processing Tag data:

eTagNewProc incorporated a number changes in correcting the tag observations for reporting rates by the Purse seine fleet (see Table 5). This model resulted in a small reduction in overall biomass estimates (Figure C5).

eTagALK appeared to have a bigger impact on the biomass estimates (Figure C5). The age-length-key approach of assigning tag release ages tend to produce a wider age distribution for tag releases, which may impact the estimates of fishing mortality, giving the difference of selectivity and natural mortality amongst age classes. The model didn’t improve or deteriorate the overall fit to the time series of tag recoveries (Figure C6).

Overall the effects of these alternative options in dealing with tag data were not considered to be significant. They did not change the conclusion of stock status. (Table C1)

Biological parameters

A number of model were conducted to investigated uncertainty in biological parameters including natural mortality, growth, and maturity.

Langley (2016) suggested that the *eMlow* natural mortality schedule could be considered to represent the lower bound for the range of credible values of natural mortality. Similar to the previous assessment, The *eMlow* option yielded a considerably more pessimistic stock status than the base level natural mortality (Table C1, Figure C7). The *Mlow* option had better fit to overall tag recoveries up to age 23 quarters but appeared to over-estimate the tag returns for the older age classes (Figure C8).

The *eMlorenzen* assumed higher values of natural mortality up to age 12 quarter than the base level, and lower values for older age classes, with an average about 20% higher than the base level. The model estimated a slightly lower biomass level but similar stock status. Further investigations indicated that estimates of stock productivity depend more on the overall level of natural mortality than the schedule of its functional form. However, the high values of natural mortality for the juveniles is not supported by some of early analysis of the IO tag release/recovery data which suggested natural mortality of fish younger than about 12 quarters may be lower (Langley 2016a).

A two-sex model was initially implemented in the 2015 assessment to account for differential sex ratio of the larger fish in the population. However, that model was not able to derive *MSY* based reference points, which appeared to be related to the high values of differential *M* assigned to female fish. That model is revised here by assuming same natural mortality for both sexes, but the males has a higher *Linf*(150) than females (140.3), based on estimates of Eveson (2015). *eTwoSex* estimated substantially lower spawning biomass than the other model options because it represents female biomass only (Figure C9). However, the estimated total biomass is almost the same as the one sex model (Figure C10). *eTwoSex* appeared to be able to produce the expected trend in sex ratio for the larger length classes (shifting towards male fish above 110 cm), commonly observed for yellowfin worldwide (Figure C11).

eGrowthDortel yielded much lower biomass estimates and a more pessimistic stock status (Figure C9). As the change in mean size of a fished population relative to the unfished state was usually interpreted by the stock assessment model as fishery-induced depletion, the lack of large fish in the catch, relative to the higher asymptotic length in the model would imply a higher level of fishing mortality and, hence a large fishery depletion effect (McKechnie et al 2017). *eGrowthDortel* resulted a poorer fit the overall length composition (Figure C12). However, it is important to note that the fit to the size distribution is also influenced by the assumed natural mortality.

The use of length-based OGIVES (*eMaturityLogistic*) had almost no effect on estimates of spawning stock biomass.

Selectivity

In the 2015 assessment, the model estimated a high proportion of juvenile fish resides in R2 creating a “refuge” for juvenile fish. One of the concern was that this may be an artefact of the model relating to the constraint imposed by the shared selectivity for the purse seine FAD schools, which might ‘distort’ the movement dynamics as the model was trying to fit the tag recovery data. The movement dynamics estimated in the current assessment changed considerably due to the adoption of the revised regional weighting on the LL CPUE. However, we still explored a model that relaxed the assumption shared PSLS selectivity amongst regions. *eSelPSRegion* estimated that in region 2 there were less fish being selected after approximately 8 quarters by the PSLS fishery than region 1b. This is consistent with that tags were rarely recovered by the FAD fishery after 8 quarters at liberty in region 2, whereas they are vulnerable to FAD fishery for an extended period in region 1b (see Figure B4). Relaxing the

selectivity constraint did not change the movement dynamics nor stock status (Figure C13).

There are several fisheries that exhibit considerable shifts in the length composition of the catch. Notable examples include the recent decrease in the length of fish caught from the Gillnet fishery in region 1a (GI 1a), the marked increase in the length of fish sampled from the Handline fishery in the same region (HD 1a) in the last few years. The size of fish caught by the longline fisheries declined considerably during the 1950s and 1960s, and there is also long-term decline in average length in the PSLS. These observations may indicate significant changes in the overall selectivity of these fisheries. *eSelTimeVarying* estimated a decrease in selectivity after around 2000 for GI 1a fishery, and an increase of selectivity after around 2005 for HD 1a fishery. The model estimated a general shift in the LL selectivity function during 1955–1972 with the age of 50% selectivity shifting from 14 to 12 quarters over the period. The model also estimated some shift in selectivity for the PSLS. The model show improvement in the fits to the length composition from these fisheries in terms of better capturing the trend in the data (Figure C14). The model yielded slightly more optimistic estimates of biomass (Figure C13). This is because the decline in mean size in these fisheries (i.e. LL and PSLS) was interpreted by the model as due to the change in selectivity rather than fishing pressure.

Regional structure

The further partition of the western equatorial region (region 1b) did not fundamentally change the model conclusion. The model (*eRegion5*) estimated the initial spawning biomass in the southern area of region 1b (R1bS) is about 30% higher than the area encompassing the northern area of region 1b (R1bN) and region 1a (R1a). The abundance in both regions followed a similar trend as the LL CPUE indices are broadly similar between the two regions. Overall the five-region model yielded a slightly higher biomass estimate than the four-region model (Figure C15, Table C1). The model did not fundamentally change the relative distribution of biomass among the IO regions (Figure C16). There appeared to be some improvement in the fit to the time series of tag recoveries in region 1 (R1a, R1bN, and R1bS) (Figure C17), as the further split of tag groups and fisheries permits refinement of tag recovery dynamics (and tag mixing assumption is less likely to be violated at smaller spatial scale). However, the improvement appeared to be very marginal (possibly because the model has similar constraints such as the assumption of shared fishery selectivity).

Temporal structure

The model configured as the annual/season temporal structure (*eYearSeason*) was implemented to investigate the model's ability to capture seasonal migration pattern. Setting-up the annual/season model involved considerable modification of the temporal structure (see Table 8). Although the aim was not to establish a 'equivalent' model, the changes to the model configurations were not expected to fundamentally alter the population processes and fishery dynamics (some of the biological parameters in the annual/season model cannot completely mirror that of the quarterly model, e.g. age-specific M and K). A more detailed comparison between the two model structures (SS3 internal year-season vs. calendar season as model year) in terms of their differences in approximating finite population process (recruitment, growth, selectivity, etc) are described in Fu (2017).

In general, *eYearSeason* yielded broadly similar results to the quarterly model. The model provided reasonable fits to most observational datasets. But the fit to the time series of tag recoveries was worse for tag covered in later years, i.e. after the 2nd quarter of 2009 (Figure C18). The model estimated lower biomass but similar current stock status relative to the reference points (Figure C15, Table C1).

The movement rates estimated by *eYearSeason* were broadly consistent with the quarterly model overall (where the movement coefficients are linked to environmental covariates), but also show some considerable differences (Figure C19). However, despite the model estimated significant seasonal difference in movement rates in some regions (i.e. Juvenile in region 1, 2 and Adult in region 2), the model was not able to capture seasonal variability as exhibited in the LL CPUE indices (Figure C20).

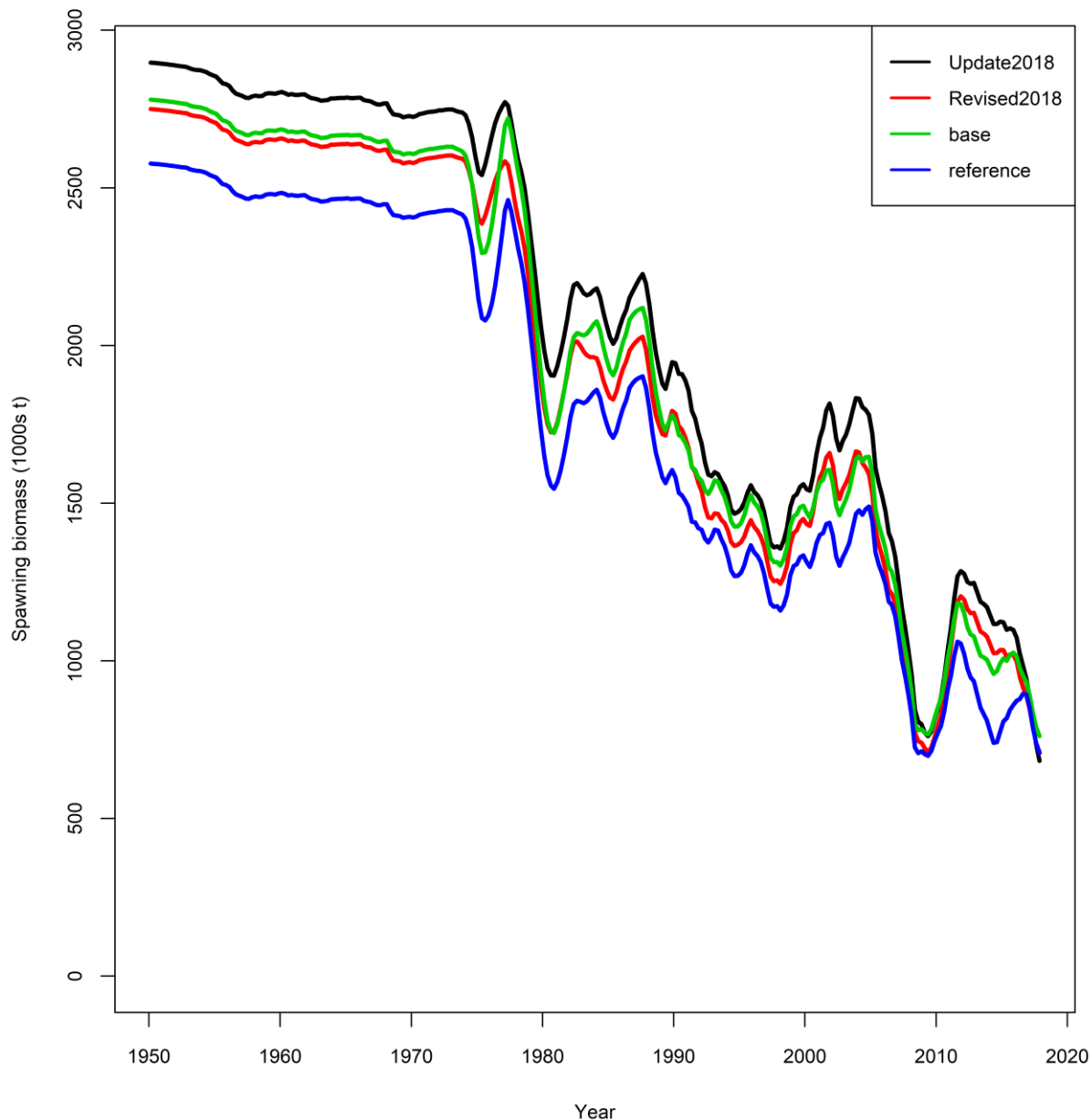


Figure 19: Spawning biomass trajectories for IO yellowfin tuna for the *Update2018* model, the *Revised2018* model, the 2018 based model and reference model (see later Sections).

5.3 Base model

Following the exploratory modelling, a base model was configured (Table 9). The base model adopted the configuration of the *Revised2018* model which incorporated several revisions and updates to the base case form the previous assessment (see Table 8). In addition, the base model also (1) estimated the selectivity for the gillnet and handline fisheries in region 1a using time blocks (see Table 9), (2) adopted the revised procedure to process tag data using option ‘TagNewProc’ (see Table 5), (3) reduced the CV for the LL CPUE from 0.3 to 0.2 (the updated size data appeared to have deteriorated

the fit to the CPUE in recent years). The base model retains the four-region spatial structure and included the environmental covariates in the movement parameterisation. Overall these changes to the model configurations were minor.

We note that the base model proposed here is for the purpose of facilitating the discussions of model diagnostics and performance and is not intended as the final model for providing management advice (which shall be determined by the Working Party on Tropical Tunas after deliberations of all model options explored during the assessment).

5.3.1 Model fits

The performance of the model was evaluated by examining the fit to the three predicted data classes – the CPUE indices, the length composition data, and the tag recovery data.

- The model provides a reasonable fit to the overall trend in the CPUE indices for each region (Figure 20). The CPUE indices exhibit a high degree of seasonal variability that is not estimated by the model. There are appreciable temporal trends in the residuals from the fit to the CPUE indices for region 1 and region 2. For region 1, the residuals tended to be positive before 1990s, and negative after during 2005–2017 (primarily relating to the poor fit to the higher seasonal CPUE indices during 1972–1980), while there is an opposite trend (increasing) in the LL2 residuals over the data period (Figure 21). The model estimated a high degree of mixing between region 1 and 2 (see Section 5.35), implying the population trends between the two regions are similar. However, the larger decline in the CPUE index for region 1b over the data period appeared to indicate a higher level of deletion in the region. The model also significantly under-estimates the higher CPUE indices from region 2 from 2016–2017.
- For most fisheries, there is a reasonable overall fit to the length composition data (Figure 22). However, the model tends to underestimate the proportion of fish in the smaller length mode from purse-seine FAD fisheries, while over estimating the proportion of fish in the 70–100 cm length range. Conversely, the model tends to underestimate the proportion of fish in the larger length classes sampled from purse-seine free-school fisheries in region 1b in 2003–06 and 2006–2017. There is a reasonable fit to the five longline fisheries which are constrained to share a common selectivity among regions. There are appreciable improvement in the fits to the length data from the handline fisheries in region 1a as a result of allowing the selectivity to change for different time periods.
- For the main longline fisheries (LL1a, 1b, 2–4), the model does not fit the observed decline in fish size during the 1950s and 1960s, and does not capture well the increase in fish size during more recent years (Figure 23).
- The other main sets of length frequency data included in the model are from the purse seine fisheries in region 1a and region 2. The average size of fish sampled from the PSFS fishery is variable amongst quarters, probably due to size related schooling behaviour of adult yellowfin tuna (Figure 24). However, the recent trends in the predicted average fish size for the PSFS1b and PSFS2 fisheries are broadly consistent with the sampling data with larger fish caught during the mid-2000s and smaller fish from 2010 onwards. There is a marked decline in the average size of fish sampled from the purse seine FAD fisheries in both region 1b and region 2 (Figure 24), particularly during the mid-1990s. This trend is not evident in the predicted average fish size derived from the model. The decline in fish size in the mid-1990s coincided with a sharp increase in the catch from the fishery, indicating a significant change in the operation of the fishery at that time. This change appears to have resulted in a decline in the relative proportion of fish in the secondary mode of the length composition (90–130 cm).
- The decline in fish size for the LL fishery in the 1950s and 1960s, and for the purse fisheries on associated schools in the 1990s can be better captured by allowing for time-varying selectivity

(*eSelTimeVarying*). This option was not adopted in the base model, as the long term trend in the size may have reflected the changes in the population.

- A comparison of the observed and predicted numbers of tags recovered from each fishery (excluding recoveries during the three quarter mixing period) by quarterly time period for each release group are presented in Figures 25–Figure 28. Overall, the model provides a reasonable fit to the tag recoveries during the main recovery period (2007–2009). Most of the tag returns were from the purse-seine fishery in region 1b, to a lesser extent, region 2. In region 1b., there are a number of quarters when the model substantially underestimates the number of tag recoveries from both regional purse seine fisheries. These were the first three quarters of 2007 and the second quarter of 2008. These quarters correspond to the first quarter following the three quarter mixing period for the large releases of tags in 2006 (quarters 2, 3 and 4) and 2007 quarter 3 (see Figure 25). The lack of fit to the recoveries in those quarters suggests that the three quarter mixing period may not be sufficient to allow for adequate dispersal of tagged fish in the population. The tag returns in region 2 are highly variable, reflecting the small volume and the high seasonality of the catch in the region (Figures 27 and 28). In some cases, the lack of fit to the observed recoveries occur near the boundary between region 1 and 2 and is possibly influenced by where the boundary is drawn. The fits were also presented for age at recovery and for time at liberty from the main fisheries (**Error! Reference source not found.**). There appears to be some lack of fit for the older age groups (e.g. >24 quarters) for the main PSFS fishery, probably suggesting that the assumed natural mortality vector is not entirely consistent with the tagging data. The maximum tag returns occurred around three to four quarters following release for the purse seine sets on associated schools and around six to eight quarters for the free schools (Figure 29), reflecting the differences in the age of recruitment into these fisheries. In region 1b, the tags remained vulnerable to purse seine associated sets for an extended period.
- Tag recoveries from the non purse-seine fisheries are not considered to be very informative and the model has the flexibility to freely estimate reporting rates for these fisheries. Of these fisheries, only the LL fisheries in region 1b and region 2 recovered moderate numbers of tags during the period following the three quarter mixing phase. The numbers of tags recovered from these fisheries was low relative to the purse-seine fishery and the fishery specific tag reporting rates were estimated to be very low. The model provided a reasonable approximation of the temporal trend in the number of tags recovered from the two longline fisheries (Figure 29).

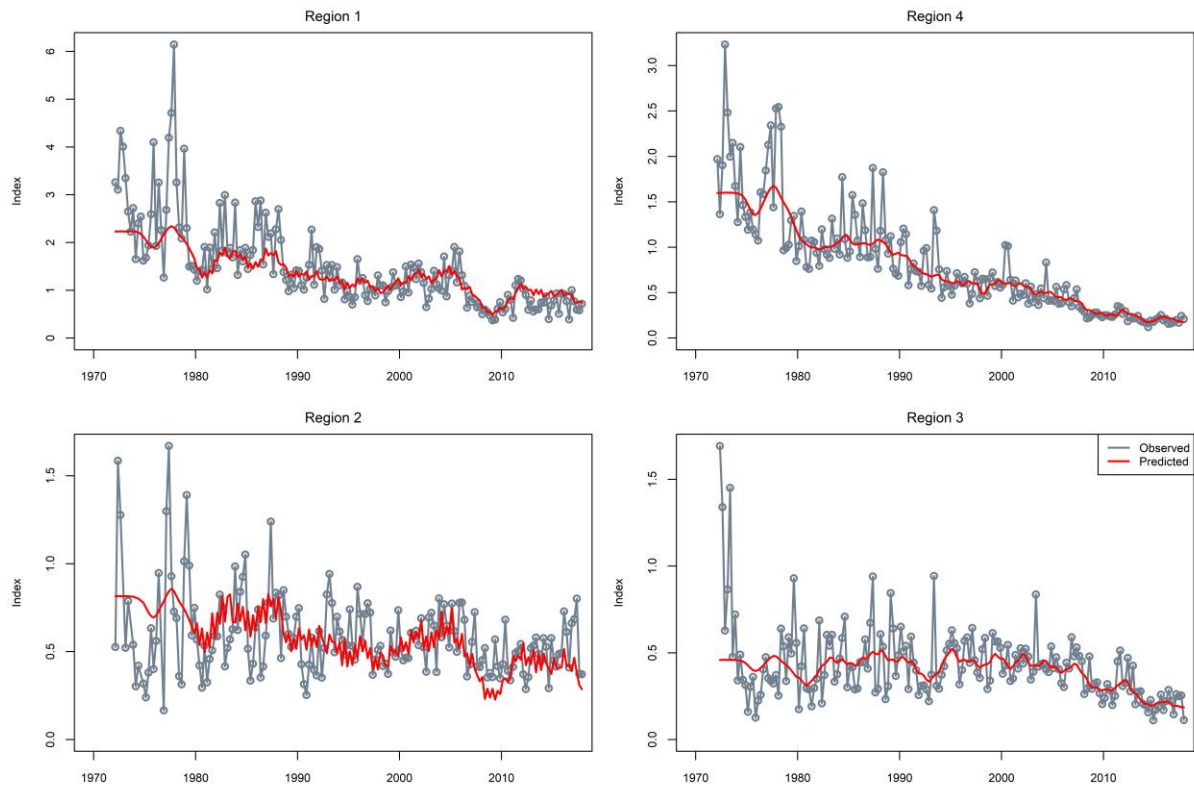


Figure 20: Fit to the regional longline CPUE indices, 1972–2017.

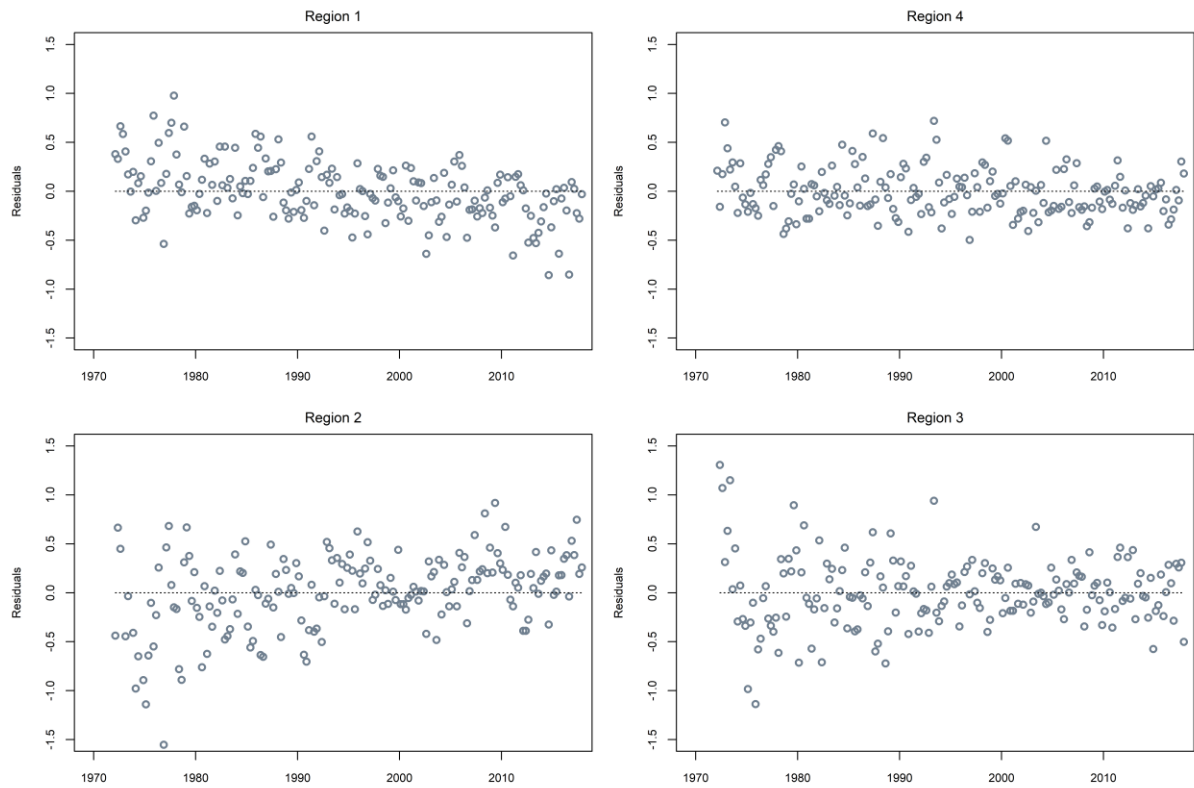


Figure 21: Residuals (observed – expected) from the fit to the CPUE indices in each region.

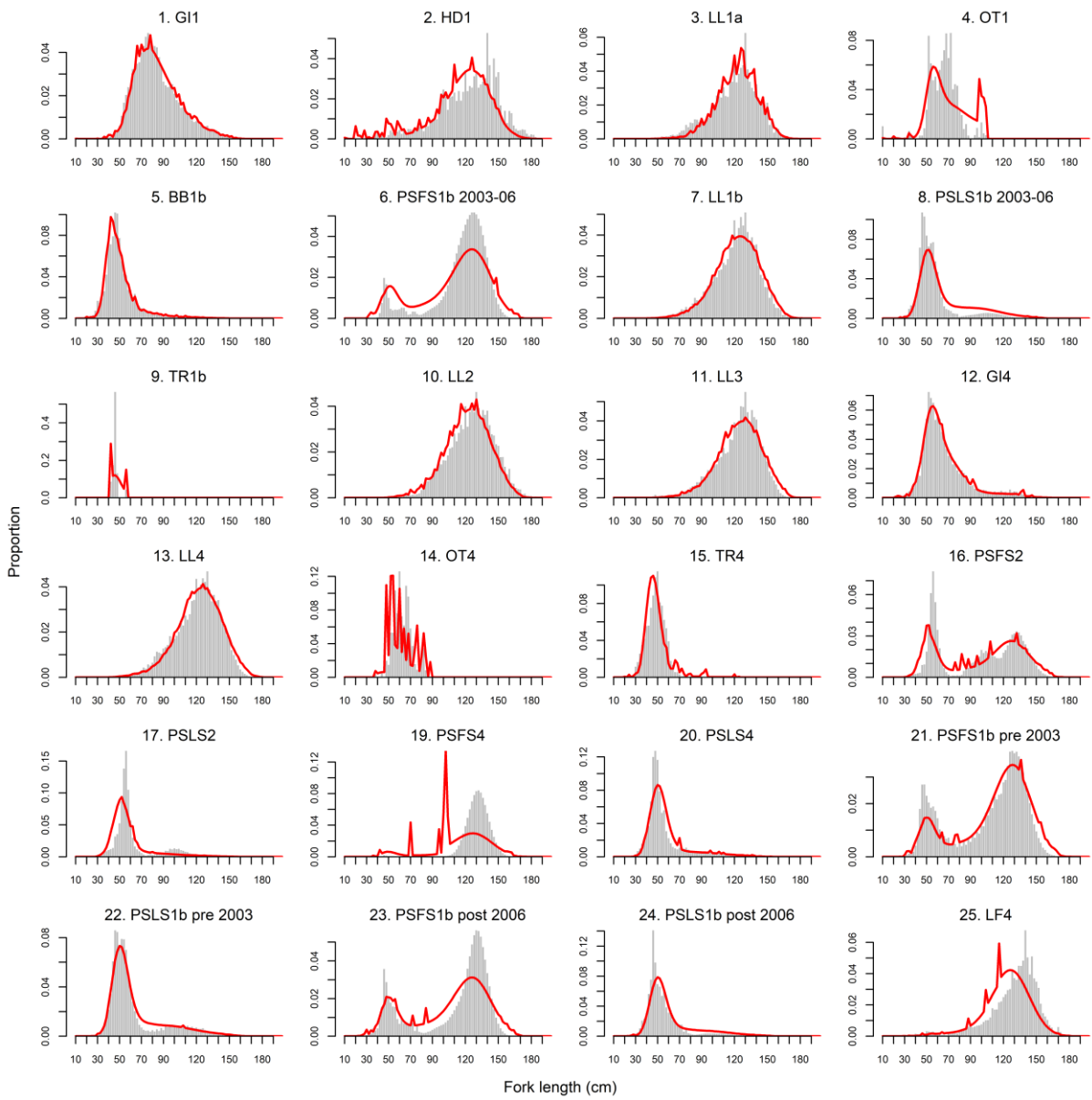


Figure 22: Observed (grey bars) and predicted (red line) length compositions (in 2 cm intervals) for each fishery aggregated over time.

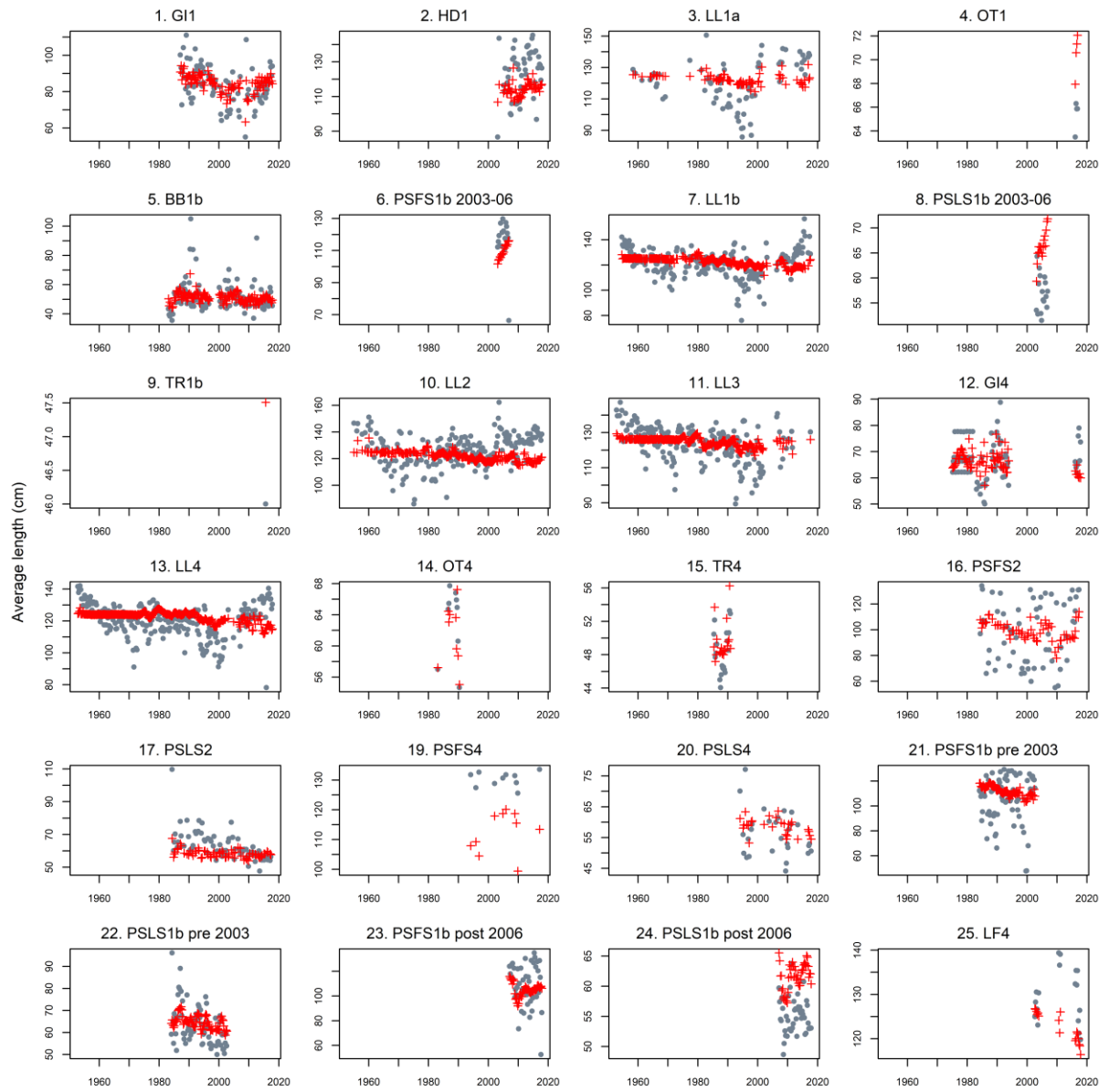


Figure 23: A comparison of the observed (grey points) and predicted (red points and line) average fish length (FL, cm) of yellowfin tuna by fishery for the main fisheries with length data.

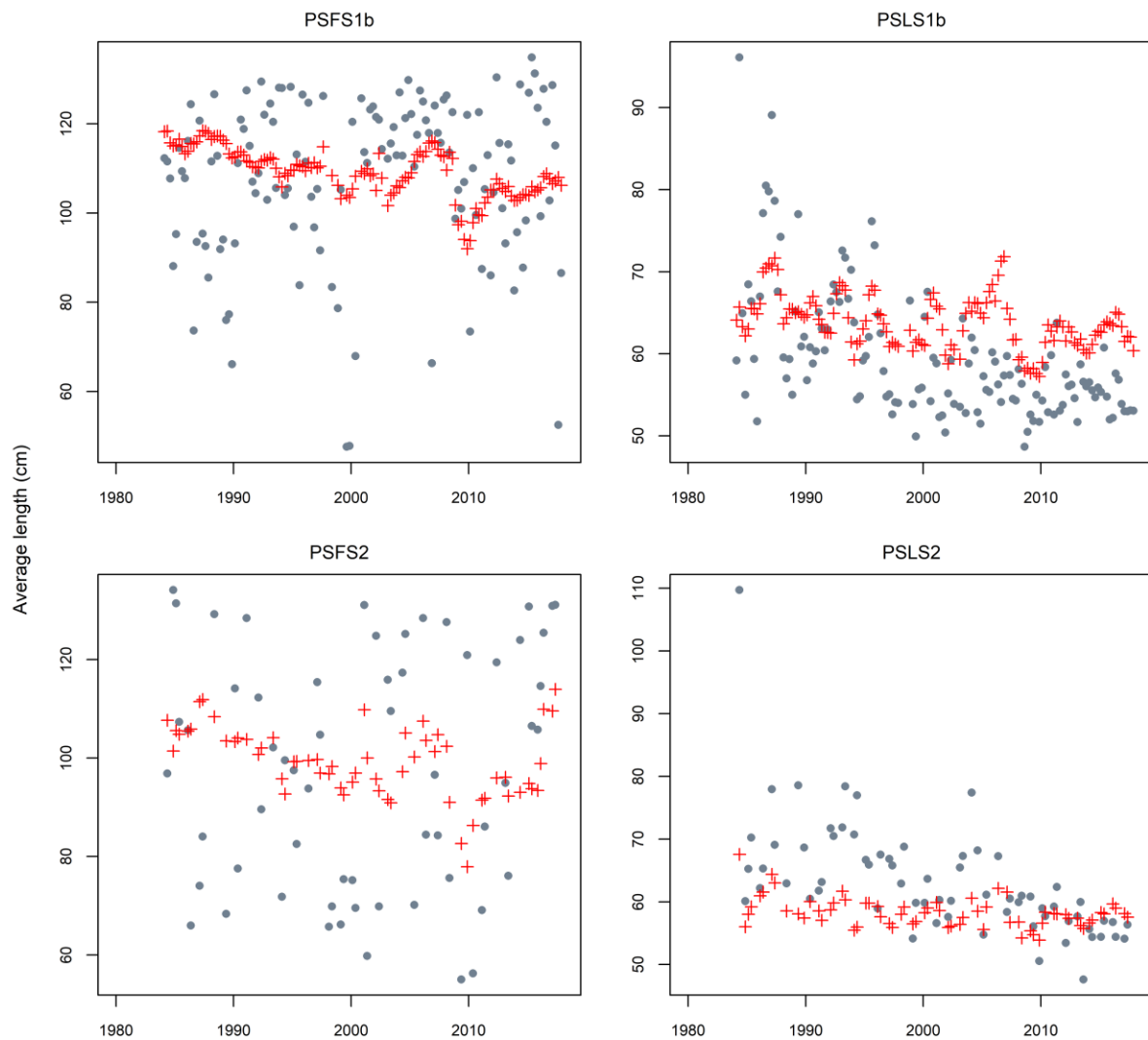


Figure 24: A comparison of the observed (grey points) and predicted (red points) average fish length (FL, cm) of yellowfin tuna by fishery for the main purse seine fisheries.

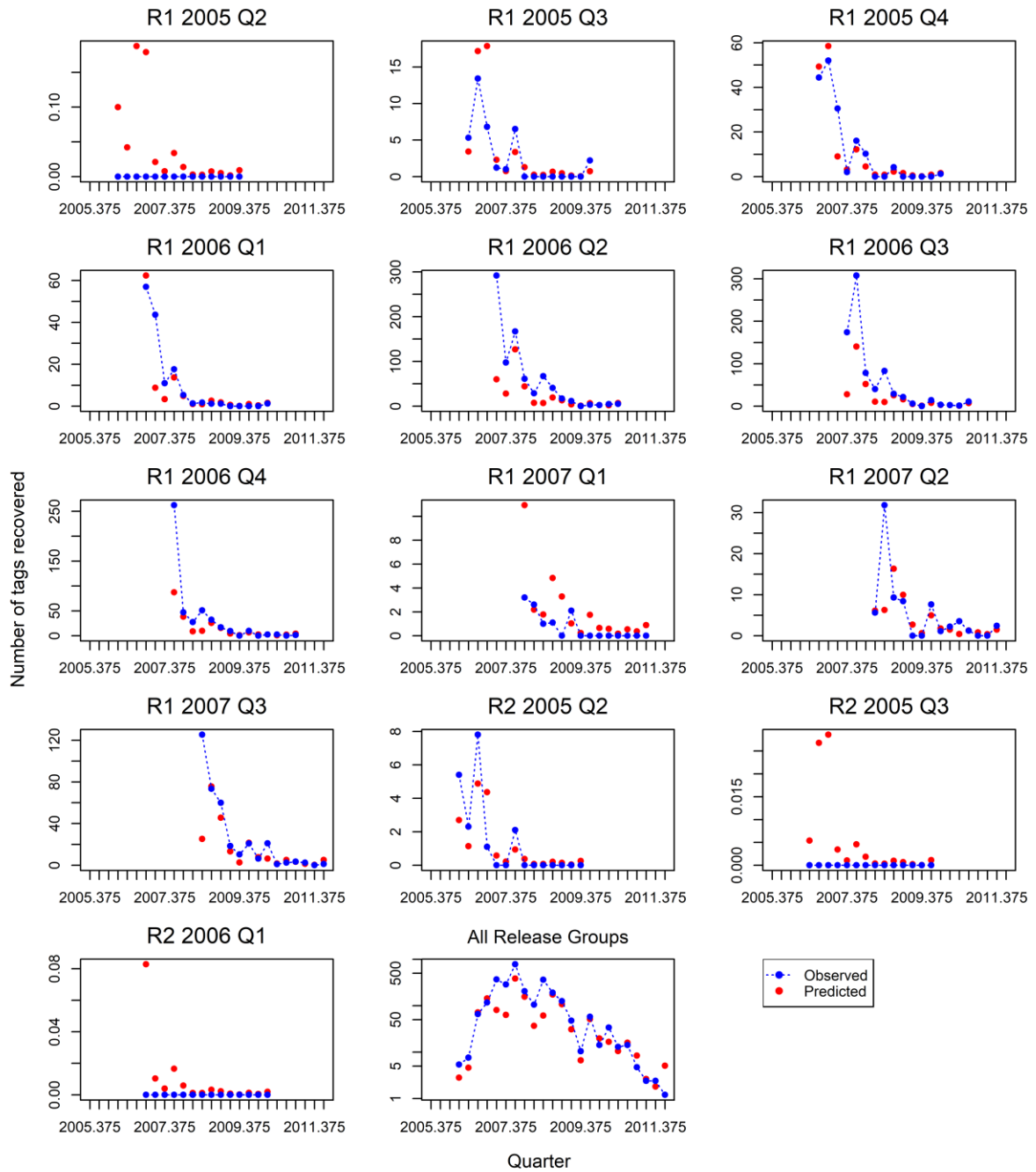


Figure 25: Observed and predicted number of tags recovered by quarter for the PSLS fishery in region 1b (PSLS 1b). Only tags at liberty after the three quarter mixing period are included. Tag recoveries are aggregated from the regional purse seine free-school and log fisheries.

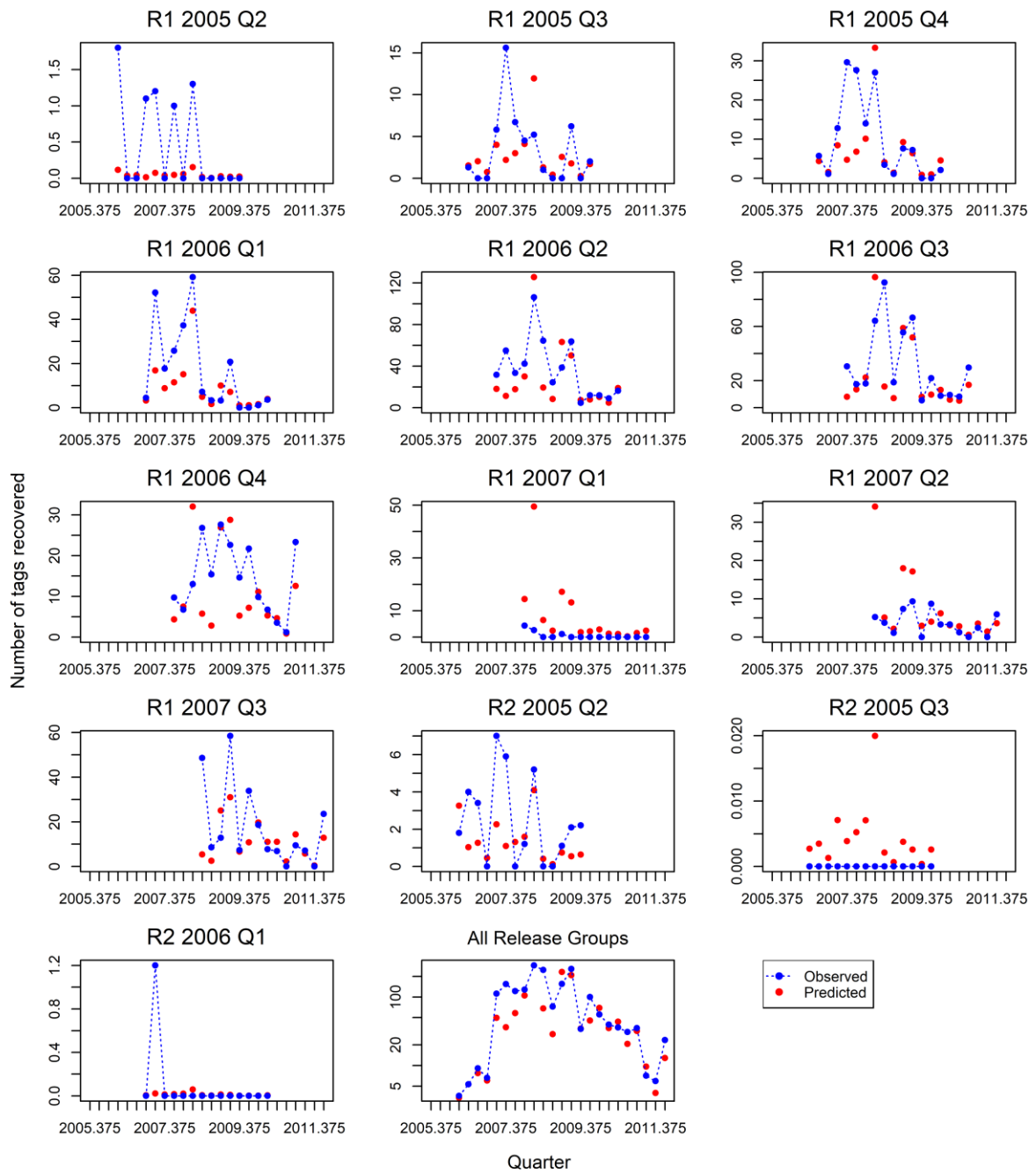


Figure 26: Observed and predicted number of tags recovered by quarter for the PSFS fishery in region 1b (PSFS 1b). Only tags at liberty after the three-quarter mixing period are included. Tag recoveries are aggregated from each release group (region, year, and quarter).

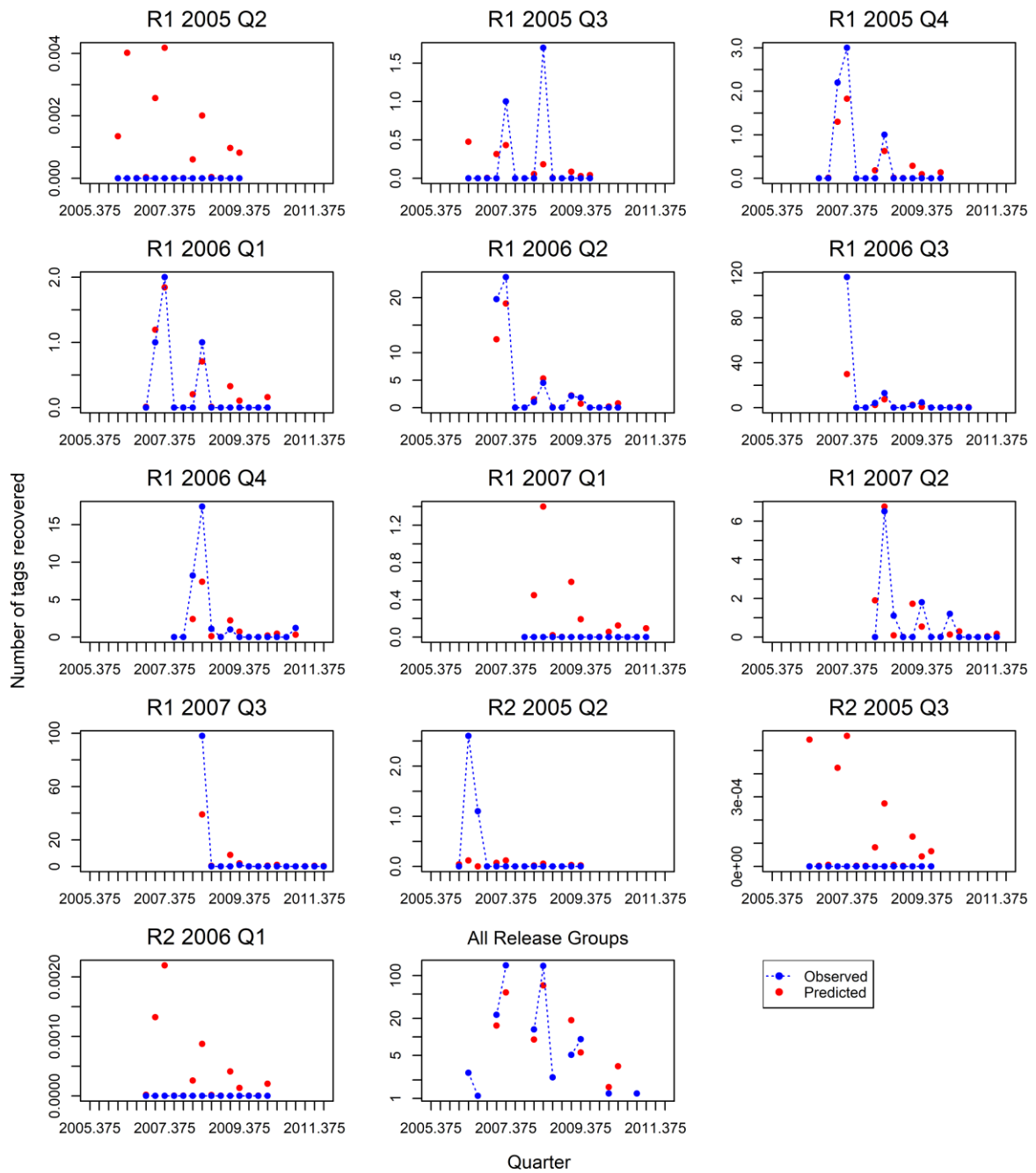


Figure 27: Observed and predicted number of tags recovered by quarter for the PSLS fishery in region 2 (PSLS 2). Only tags at liberty after the three-quarter mixing period are included. Tag recoveries are aggregated from each release group (region, year, and quarter).

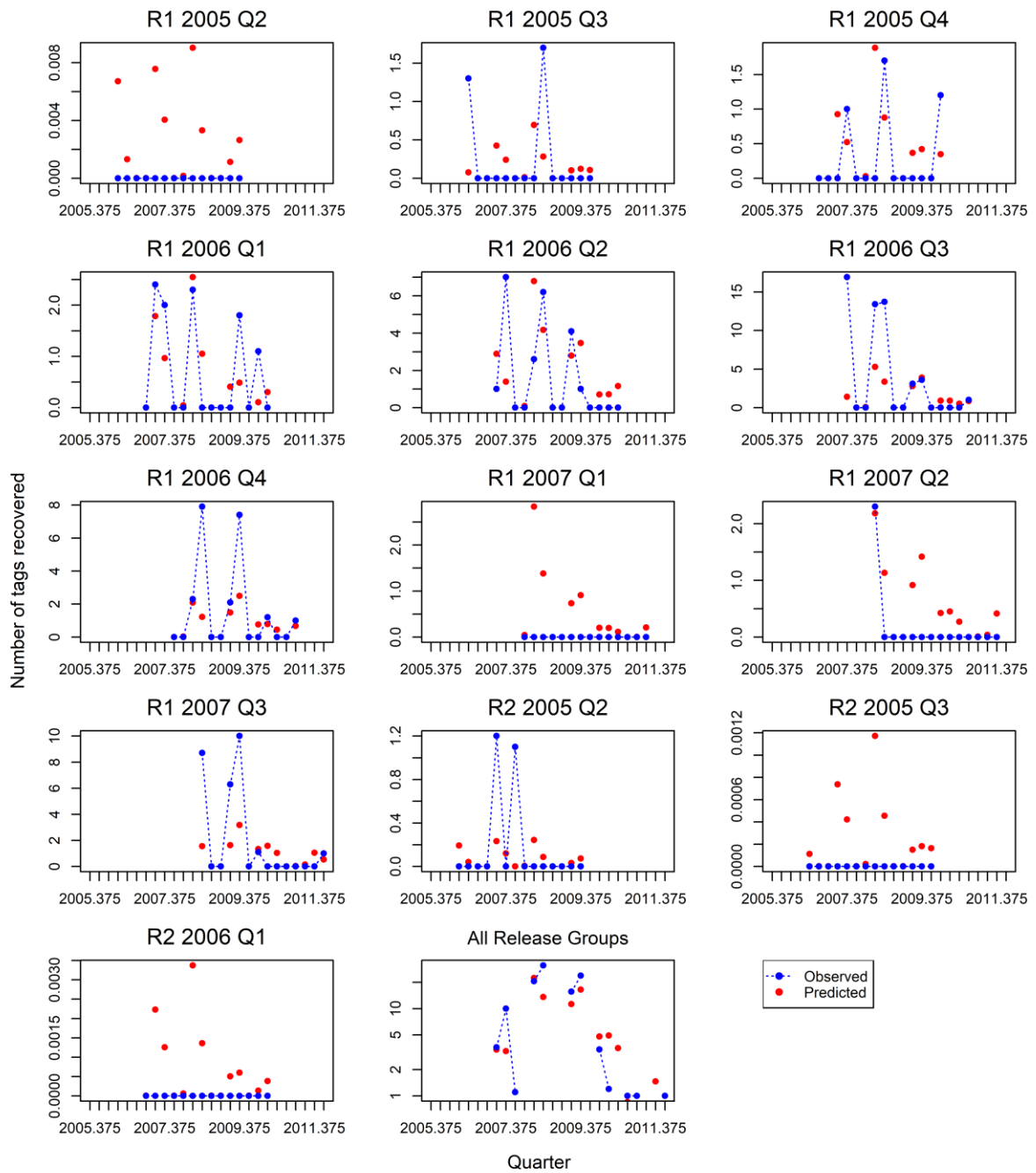


Figure 28: Observed and predicted number of tags recovered by quarter for the PSFS fishery in region 2 (PSFS 2). Only tags at liberty after the three-quarter mixing period are included. Tag recoveries are aggregated from each release group (region, year, and quarter).

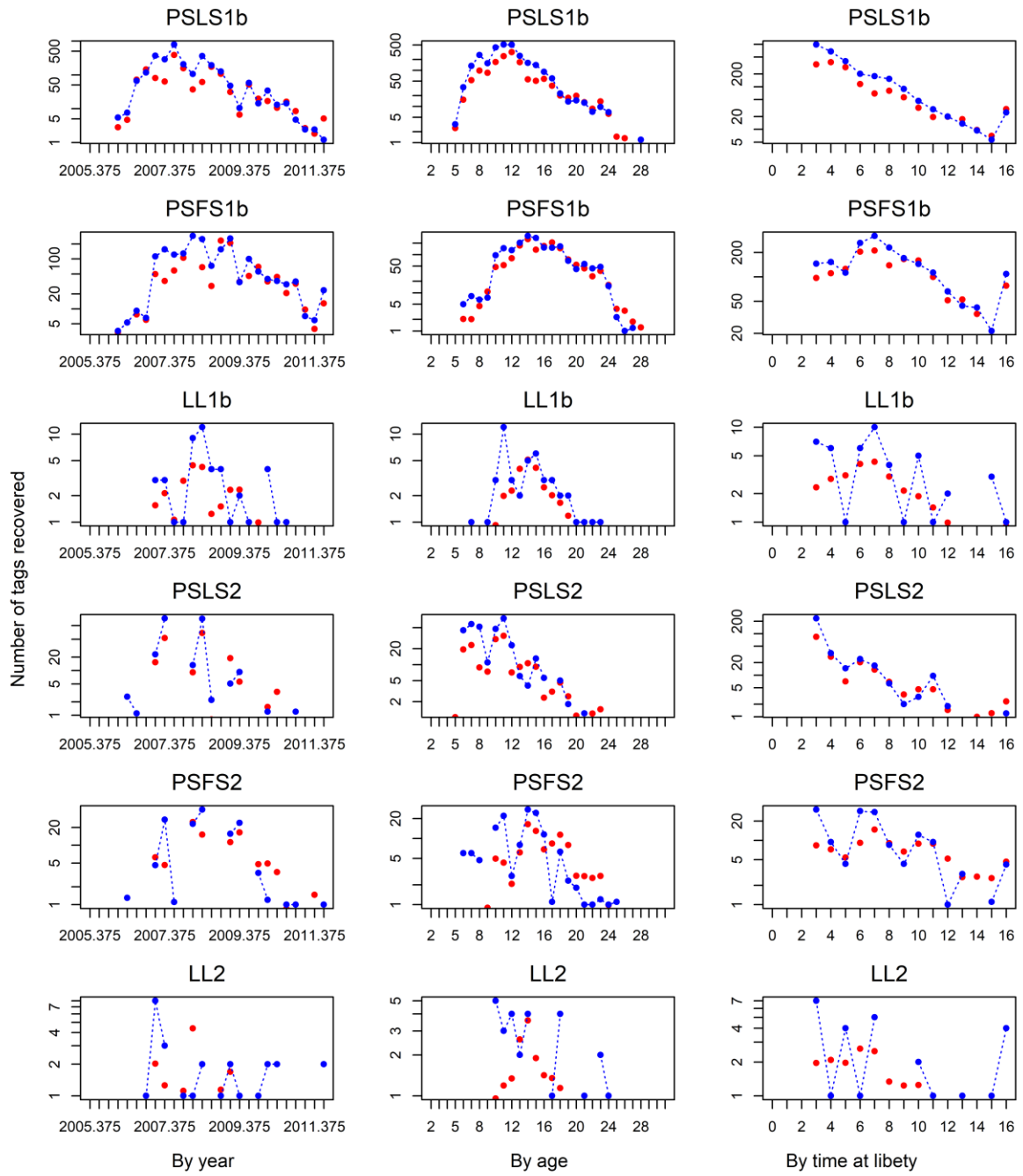


Figure 29: Observed and predicted number of tags recovered by year/quarter time-period (left), by age (mid), and by time at liberty (in quarters, right) for main fishery and region. Only tags at liberty after the three-quarter mixing period are included. Tag recoveries are aggregated for each of the regional fisheries.

5.3.2 Selectivity estimates

A common logistic selectivity function is estimated for the principal longline fisheries (LL 1a, 1b, 2–4) that attains full selectivity at age 17 quarters (Figure 30). The fresh tuna fishery (LF 4) is estimated to have a relatively similar selectivity to the principal longline fisheries, albeit slightly skewed towards older fish.

The associated purse-seine and baitboat fisheries have a high selectivity for juvenile fish, while the free-school purse-seine fishery selects substantially older fish. For all regions and time blocks, the selectivity of the free school and associated purse-seine fisheries was held constant among the method fisheries (Figure 30). The selectivity of associated purse-seine method is relatively broad compared to the modal structure of the length frequency data. The selectivity function encompasses the full range of age classes, including the older age classes, albeit with a relatively low selectivity.

Limited or no size data were available for a number of fisheries, specifically the artisanal fisheries (OT 1a & 4) and the troll fishery in regions 1b and 2 (TR 1b & 2). Consequently, selectivity for these fisheries is poorly estimated or, in the absence of size data, assumed equivalent to a fishery with the same gear code in another region. The model did not estimate a significant change of selectivity for gillnet fishery in region 1a, but estimated a relatively large shift of selectivity towards older fish for the handline fishery since 2005) (Figure 30).

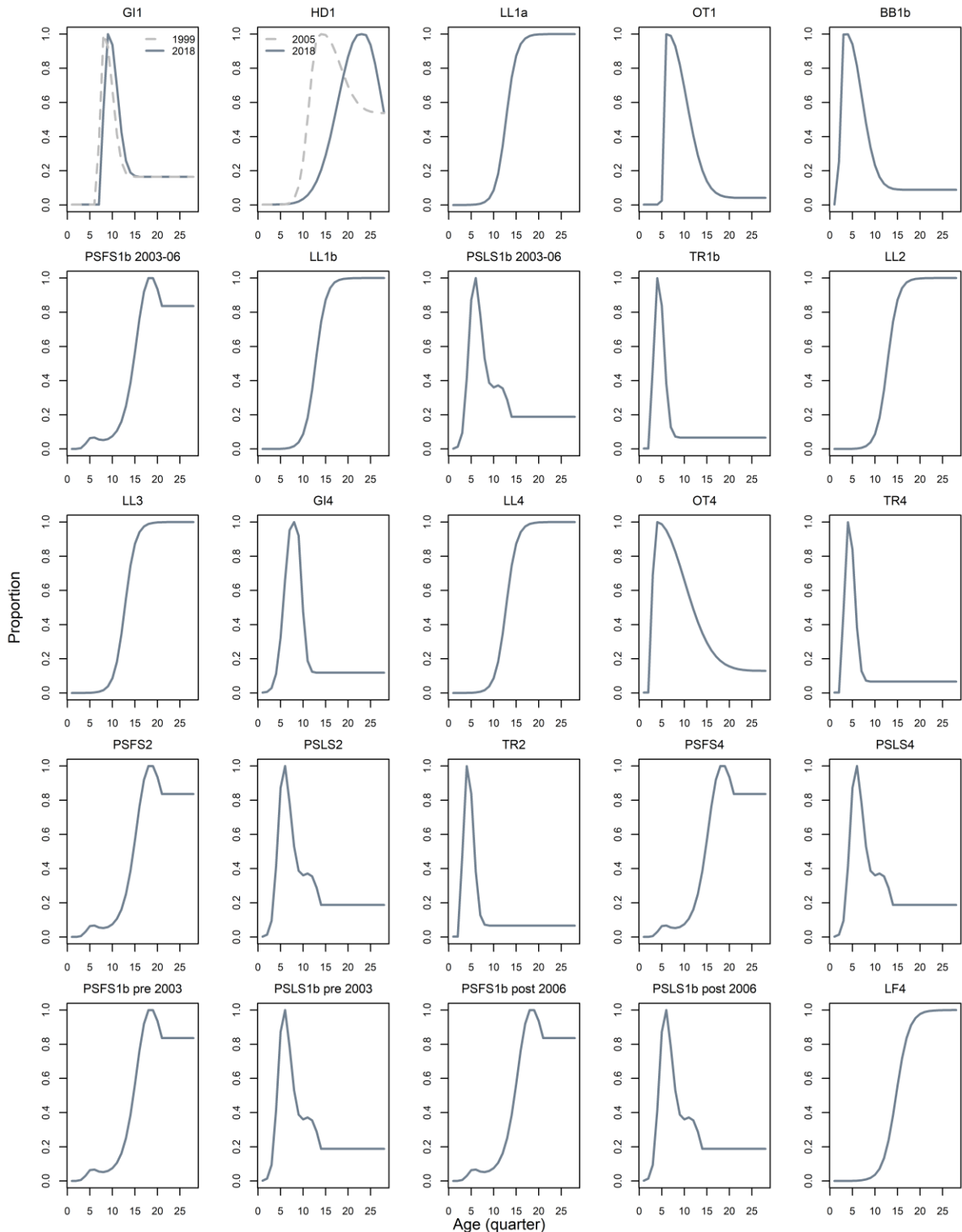


Figure 30: Age specific selectivity by fishery. Selectivity was estimated for time-blocks for the GI 1a fishery (before and after 2000) and the HD 1a fishery (before and after 2005)

5.3.3 Tag reporting rate

Tag reporting rates for the purse-seine fisheries within regions 1b and 2 were fixed at the prior value (1.00) (Figure 31, see Table 5 for details). For the other fisheries, limited information was available regarding tag reporting rates and fishery-specific reporting rates were estimated with virtually no constraints. The estimated tag reporting rates are for the period following the initial tag mixing phase (for tags at liberty for at least three quarters). The tag reporting rates estimated for the purse seine fisheries in region 4 were comparable to the base reporting rate of the main purse seine fisheries, although the reporting rates were very poorly determined.

For the other fisheries, the estimated reporting rates were generally low (less than 10%) or close to zero reflecting the small number of tags reported from these fisheries (post dispersal period). The main exception was the troll fishery in region 2 (TR 2) with a reporting rate of 60% (Figure 31). The moderate reporting rate for the LL 3 represents the prior value as there were no tag recoveries from the fishery (or region). Similarly, reporting rates from the other fisheries in region 4 (LL4, TR4, and OT4) were informed by a very small number of tag recoveries from a small population of tagged fish (Figure 31).

The estimates of fishery-specific tag reporting rates differ somewhat from those estimated by Carruthers et al (2015). These differences are likely to be primarily due to the different assumptions included in the two modelling approaches, especially related to the spatial stratification of the fisheries, spatial structure of the tag releases, and the duration of the tag mixing period.

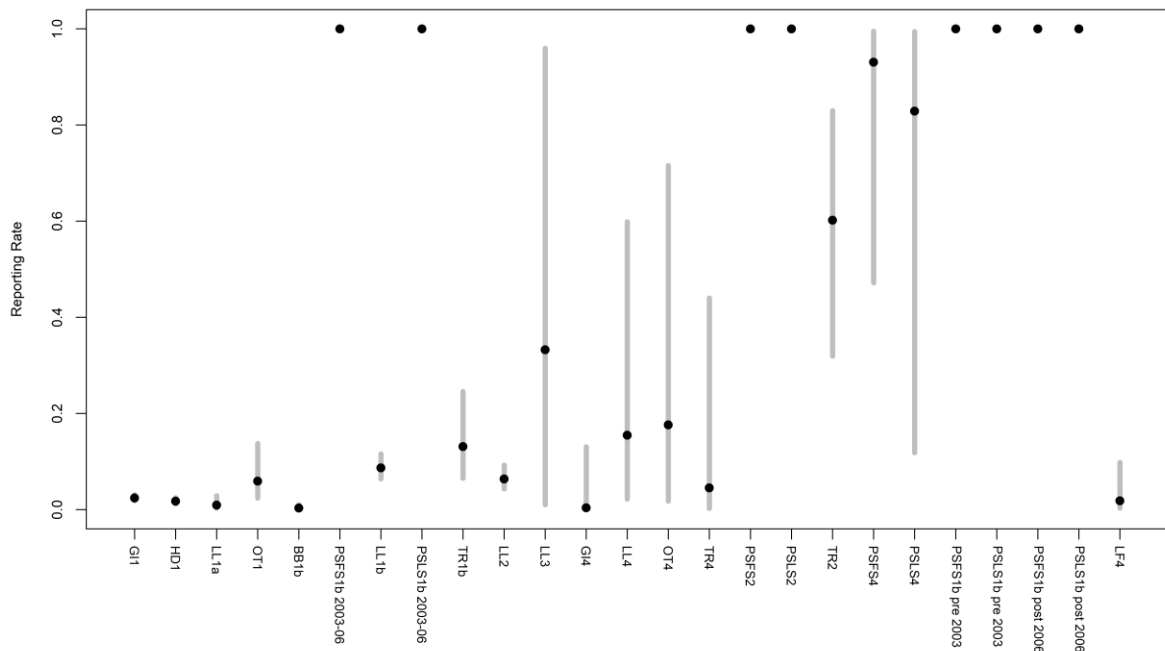


Figure 31: Tag-reporting rates by fishery (black circles) and 95% confidence intervals for the estimated fishery reporting rates. The reporting rates for the purse-seine fisheries in regions 1 and 2 were fixed at 1.

5.3.4 Recruitment parameters

The quarterly recruitment deviates indicate recruitment varies seasonally (Figure 32). Recruitment deviates were low during 2004–2006, especially during 2005. Recruitment deviates declined between 2011 and 2017.

Recruitment is parameterised to occur in region 1 and 4 only. The model estimates 60% and 40% of the total annual recruitment is assigned to regions 1 and 4, respectively. The proportion of total recruitment assigned to either region varies temporally during the estimation period (1977–2016) and, overall the proportion of recruitment allocated to region 1 during the estimation period is higher than the base level (and vice versa for region 4) (Figure 33).

Recruitment within the western region (R1) is characterised by relatively high recruitment during the mid-1980s and late 1990s–early 2000s and lower recruitment during the early 1990s and particularly low recruitment during 2004–2006 (Figure 34). Recruitment in Region 1 was above average during 2009–2016. These trends in recruitment also drive the trend in total recruitment for the Indian Ocean. Recruitment in region 4 fluctuated about the equilibrium level during 1972–1986 but was lower during the subsequent years, particularly 2005–2012 (Figure 34). Total recruitment declined considerably during 2012–2017, except for a peak in the last quarter of 2016.

Further analysis was conducted to investigate the low recruitment during the 2004–2006. The analysis involved removing the certain observational dataset (size composition, tagging data, and the LL CPUE indices) and re-estimating the recruitment deviations (Figure C22, Appendix C). For the LL CPUE indices, only indices from late 2000s onwards were excluded. The results suggested the recruitment pattern during the 2004 – 2006 was related to sharp decline in the CPUE index from the late 2000s in all regions as well as the inclusion of the tag data. However, neither the CPUE data nor the tagging data by itself were sufficient to fully explain the lower level of recruitment. The sharp decline in the LL CPUE for region 1 during the late 2000s was immediately following the exceptionally large catches taken by the PSFS fishery during 2004–2006. The reason that the tag data may have informed the recruitment pattern is not clear, possibly because the model have considerable flexibility in the estimation of recruitment deviates to account for the contrasting abundance information in the tag and CPUE data sets during this time period.

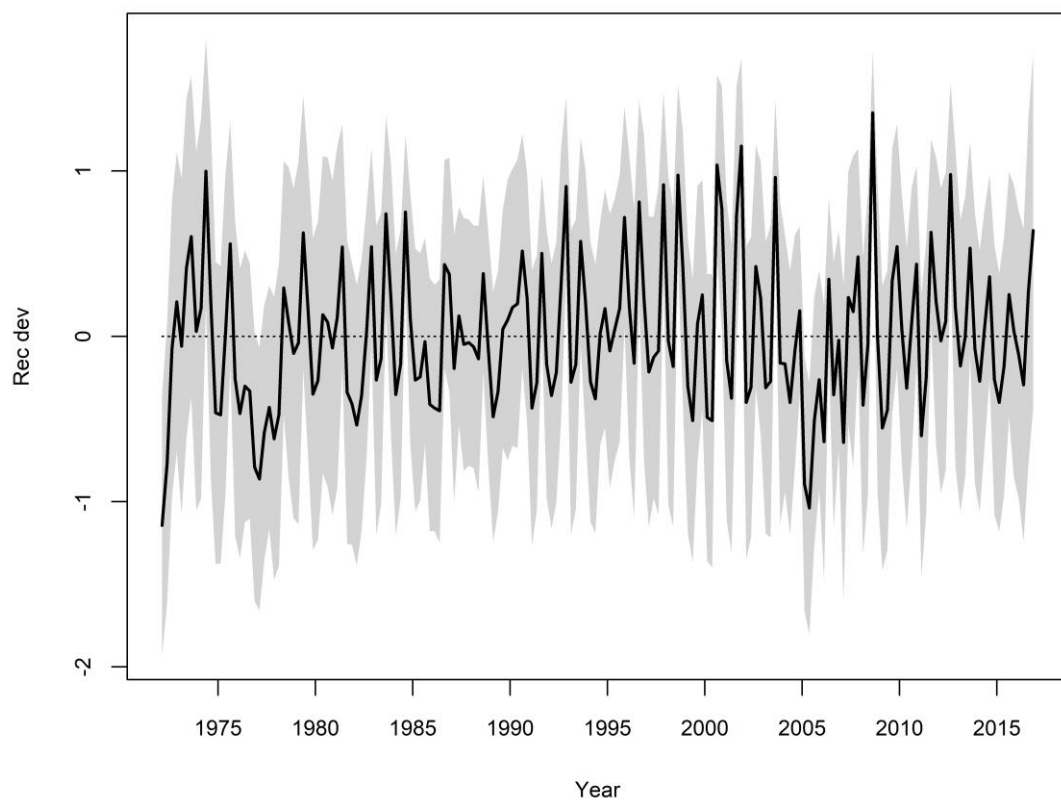


Figure 32: Recruitment deviates from the SRR and the associated 95% confidence interval.

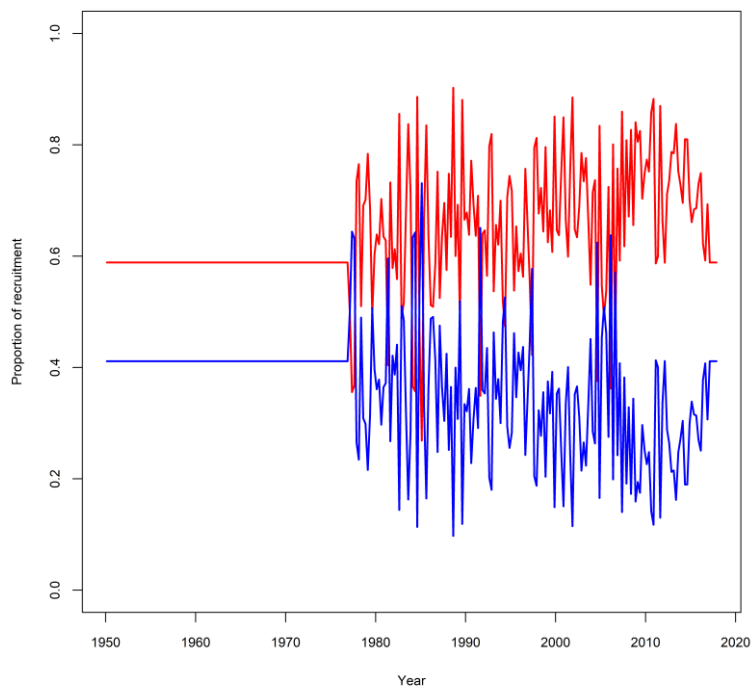


Figure 33: Proportion of the total quarterly recruitment assigned to region 1 (red) and region 4 (blue).

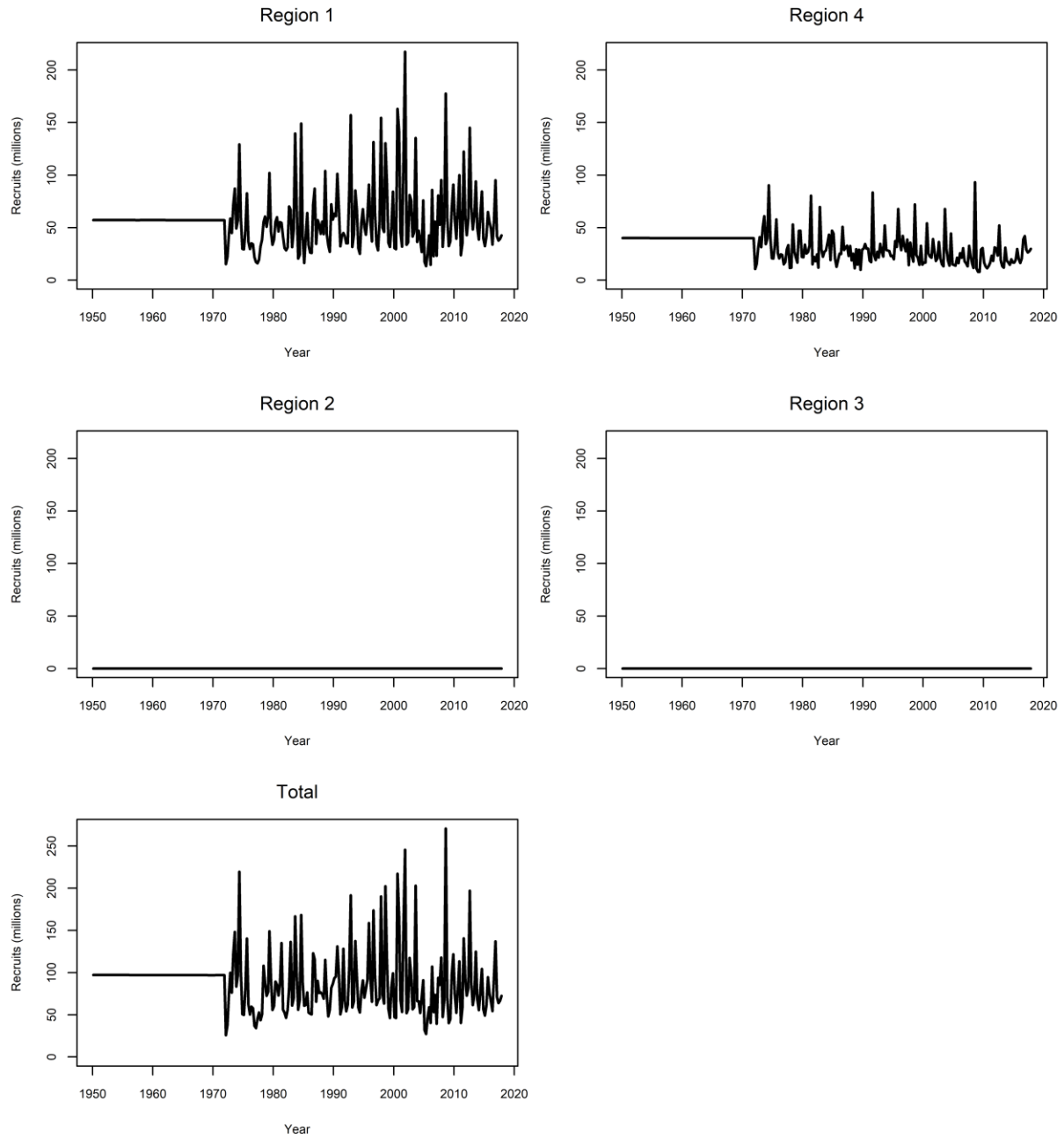


Figure 34: Estimated quarterly recruitment by region and for the entire IO.

5.3.5 Movement

The base model estimates that there is a high degree of connectivity between the two western regions (R1 and R2) and between the eastern regions (R3 and R4) but trivial longitudinal movement between regions 1 and 4 (Figure 35). Recruitment is restricted to regions 1 and 4. There is a very high movement rate estimated for juvenile fish from region 1 to region 2. There is also a similar reciprocal rate of movement (Figure 35), which is contrary to the estimates from the early assessment which suggested a lower movement rate for juvenile fish from R2 to R1 (Langley 2015). This difference is most likely due to the change in the prior information on the regional biomass distribution following the adoption of the revised regional weighting factors. Similarly, there is a high level of movement of juvenile fish between region 4 and region 3 (Figure 35). These movements are strongly correlated with the seasonal variation in SST in region 3 (*SST3* covariate) as is the northward movement of adult fish from region 3 (to region 4), presumably reflecting the seasonal variability in LL CPUE in region 3.

Overall, the environmental covariates do not have a strong longer term temporal effect on the realized migration coefficients. Similar level of movement rates was estimated when environment data were excluded from the assessment model. Attempts to estimate seasonal pattern in movement rates directly in the exploratory modelling using an annual-season model structure estimated broadly similar rates of movement in most regions.

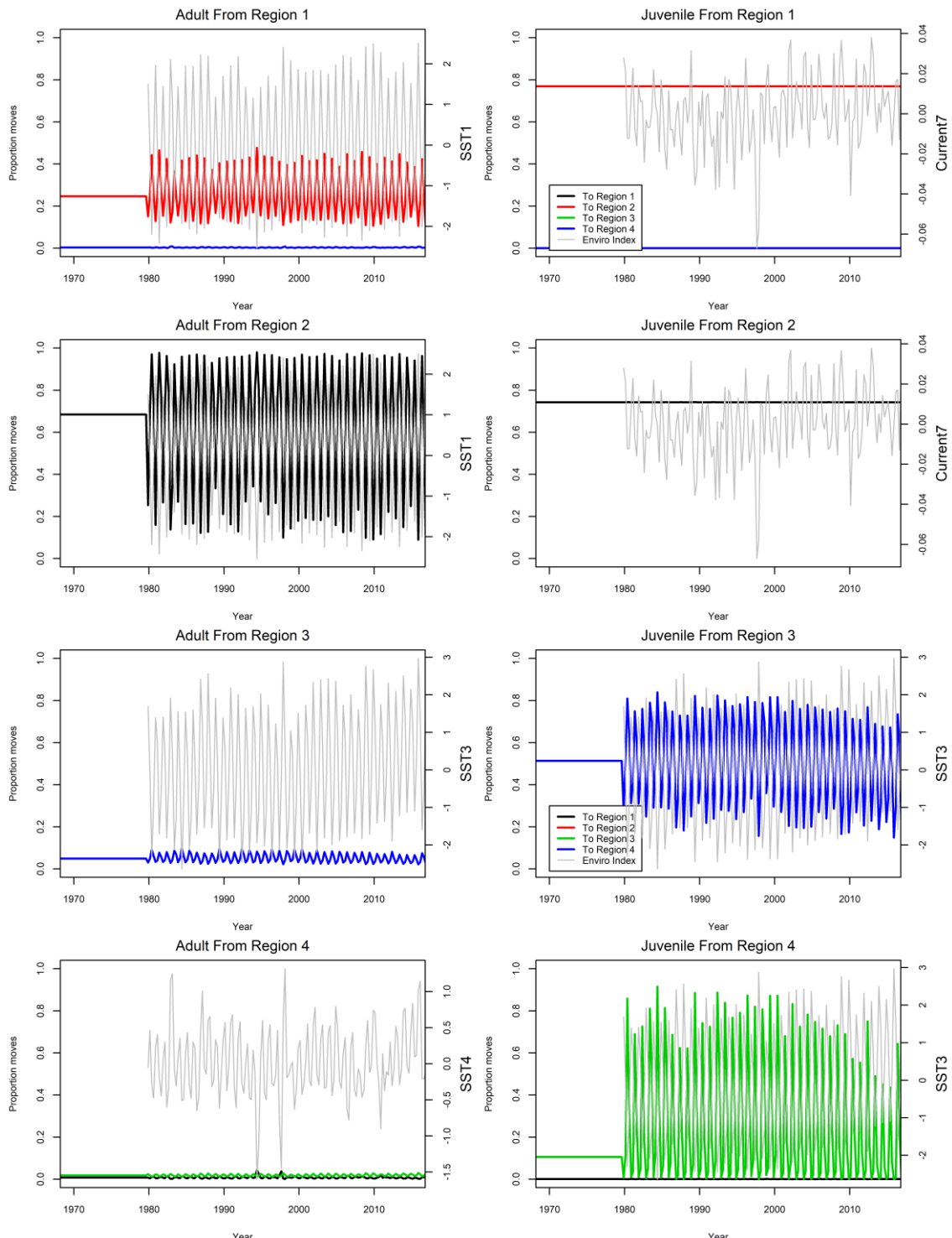


Figure 35: Quarterly movement coefficients and the corresponding environmental covariate (grey line).

5.3.6 Biomass

Total spawning biomass for the IO stock is estimated to have remained relatively high throughout the 1950s, 1960s and early 1970s (Figure 36) corresponding with the relatively low levels of catch during the period and the assumption of equilibrium recruitment. Total spawning biomass declined rapidly during the late 1980s to mid-1990s, recovered slightly during the late 1990s and early 2000s before declining to a low level in 2008–2009. Total spawning biomass recovered slightly during 2009–2011 and then declined to 2017. Current (2017) total spawning biomass is estimated to be close to the historically low level.

There are very narrow confidence intervals associated with the time-series of total spawning biomass (Figure 36). The high level of precision is likely to be a function of the key assumptions of the model, especially constant catchability and selectivity associated with the LL CPUE indices and the fixed biological parameters.

Relative trends in spawning biomass are broadly comparable for the four model regions (Figure 37), although the overall magnitude of the decline in biomass is substantially higher in Region 4. The biomass in this region declined steadily throughout the 1990s and 2000s following the trend in the regional LL CPUE indices. For the most recent years, region 4 biomass is estimated to be at a very low level (Figure 37).

Different to the previous assessment, the model estimates that a substantially smaller proportion (less than 20%) of the total spawning biomass is within Region 2, reflecting the changes in movement and recruitment dynamics following the adoption of a new regional weighting scheme. The lower biomass in region 2 appears to be more plausible as the region accounted for a relatively small proportion of the historical catch (less than 10%). However, there remains a strong linkage between region 1 and region 2, and the high level of mixing resulted in similar population trend between the two regions, which are monitored by the LL CPUE.

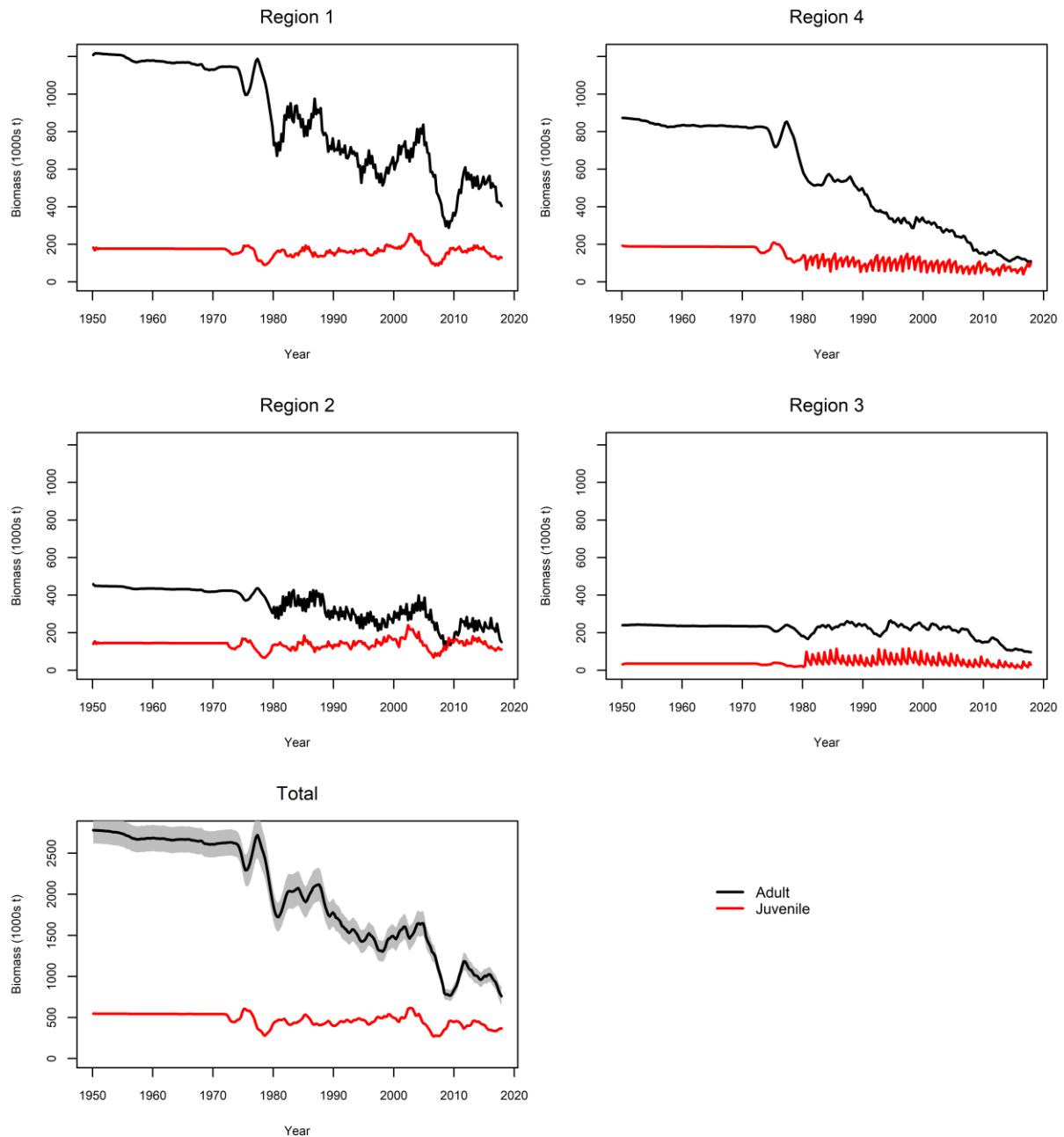


Figure 36: Spawning and juvenile biomass (thousand mt) by region and for the IO for the base-case analysis. The shaded areas indicate the approximate 95% confidence interval.

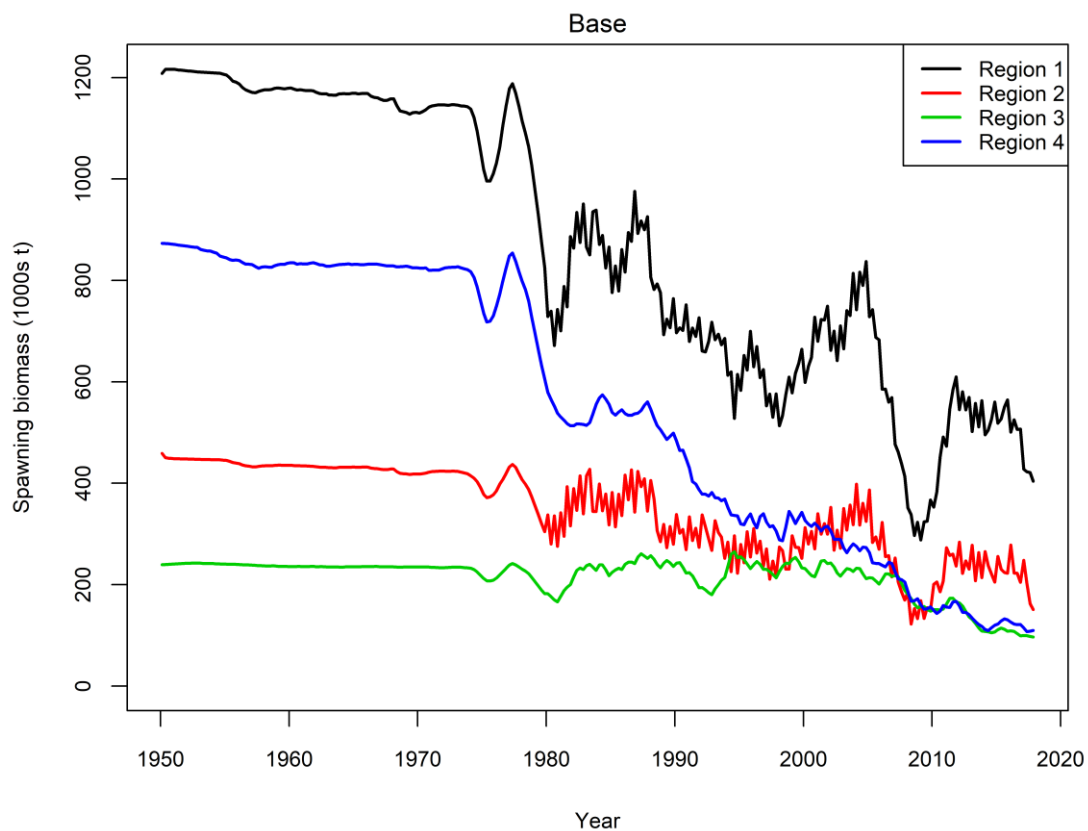


Figure 37: A comparison of the spawning biomass trajectory for the individual model regions.

5.3.7 Fishing mortality

Fishing mortality rates for each fishery are defined as apical fishing mortality rates; i.e. the fishing mortality for the fully selected age class (or age classes). The fishing mortality rates are an approximation of the Baranov continuous F (Methot & Wetzel 2013). Relatively high recent fishing mortality rates have been estimated for a number of fisheries in Region 1, specifically PSLS1b, PSFS1b, GI1, HD1 and BB1b (Figure 38). Fishing mortality rates for the PSLS1b fishery increased sharply in 2013 corresponding to relatively high catches from the fishery in the last two quarters of 2013.

In Region 4, recent fishing mortality rates from the LF4 fishery were high (Figure 38), although there remains great uncertainty in annual catches from the fishery during the last 10 years (Geehan & Setuadji 2008). The high fishing mortality rates correspond to the sharp decline in model biomass from the late 2000s and are also related to the selectivity of the fishery, with full selection occurring at age 18 quarters. The GI4 and the TR4 fisheries represent the other main sources of fishing mortality in Region 4 (Figure 38). Fishing mortality rates are estimated to be very low in both Region 2 and Region 3 (Figure 38). Fishing mortality estimated for some fisheries (e.g. LF) differed considerably to the previous assessment given the changes in the regional biomass distribution following the adoption of the revised regional weighting.

Spatially aggregated, age-specific fishing mortality rates are derived for each model time period (Methot & Wetzel 2013). Average total fishing mortality rates were derived for the last two years of the assessment model (2016 and 2017) and the resulting age specific mortality schedule was applied in the computation of the *MSY* reference points. Aggregated fishing mortality rates increased for the younger age classes and were relatively stable over the ages 4–14 quarters (Figure 39). Fishing mortality rates increased sharply for the 15–18 age classes and were highest for age classes 18–24.

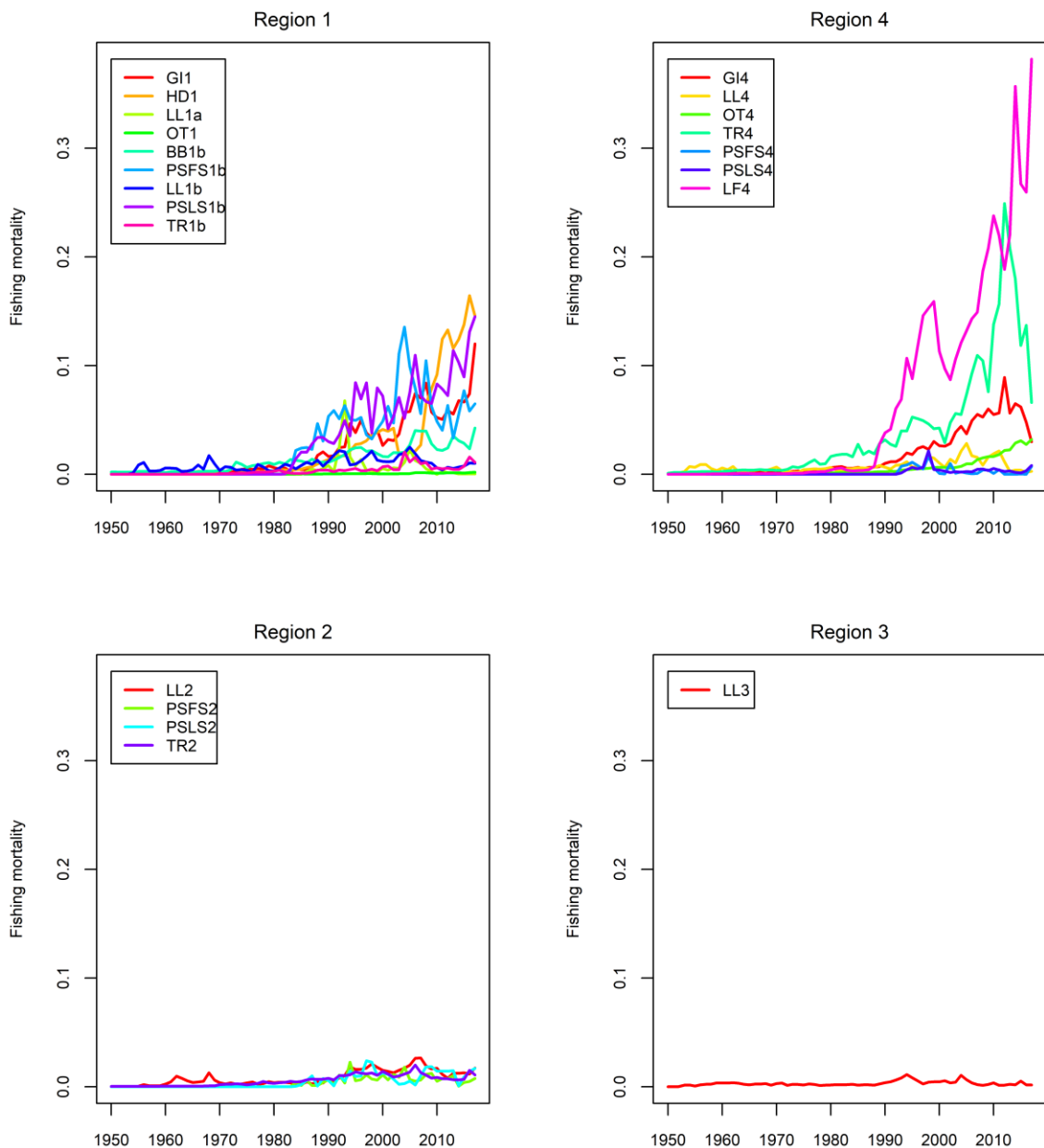


Figure 38:Trends in fishing mortality (quarterly) by fleet.

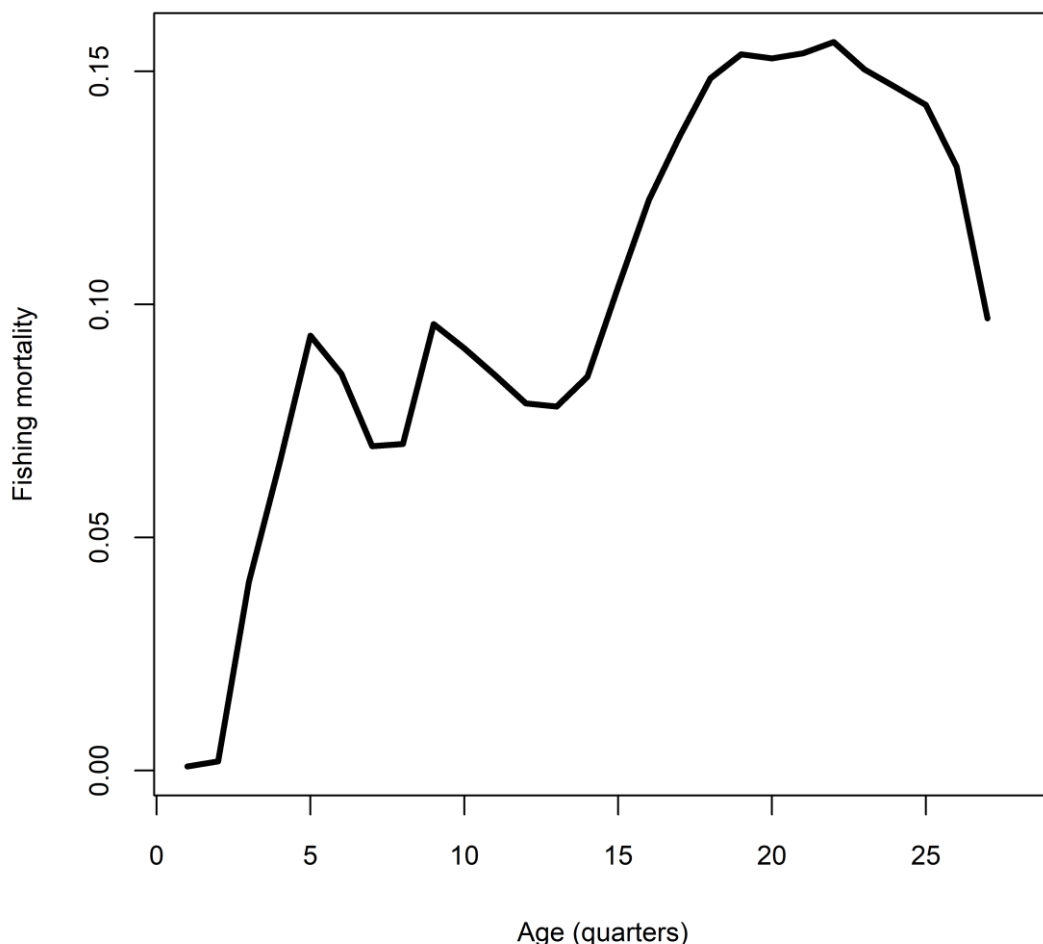


Figure 39. Fishing mortality (quarterly, average) by age class and region for the period used to determine the total F-at-age included in the calculation of MSY based reference points (2015 and 2016).

5.3.8 Fishery impact

A fishery impact analysis was conducted using a similar approach commonly used in the Eastern Pacific Ocean (Minte-Vera et al. 2016). This was essentially done by plotting the trajectory of spawning biomass overtime that would have occurred in the absence of historical fishing. Estimates of reduction in spawning biomass induced by fishing can be further attributed to specific fishery components (grouped by gear type across regions), so that the impact of different types of fishing activity on SSB can be compared (Figure 40). The fishery impact of a fishing activity is related to the both the historical level of catch (e.g. purse seine and gillnet fisheries), as well as selectivity pattern. The latter can be seen from Figure 40 which suggested both troll and baitboat fisheries appeared to have a higher impact than the handline fishery despite their relatively smaller overall catches—both fisheries were predominantly targeting smaller and younger fish. Overall impacts are distributed amongst the main fisheries, although highest impacts were attributable to the purse seine and gillnet fisheries.

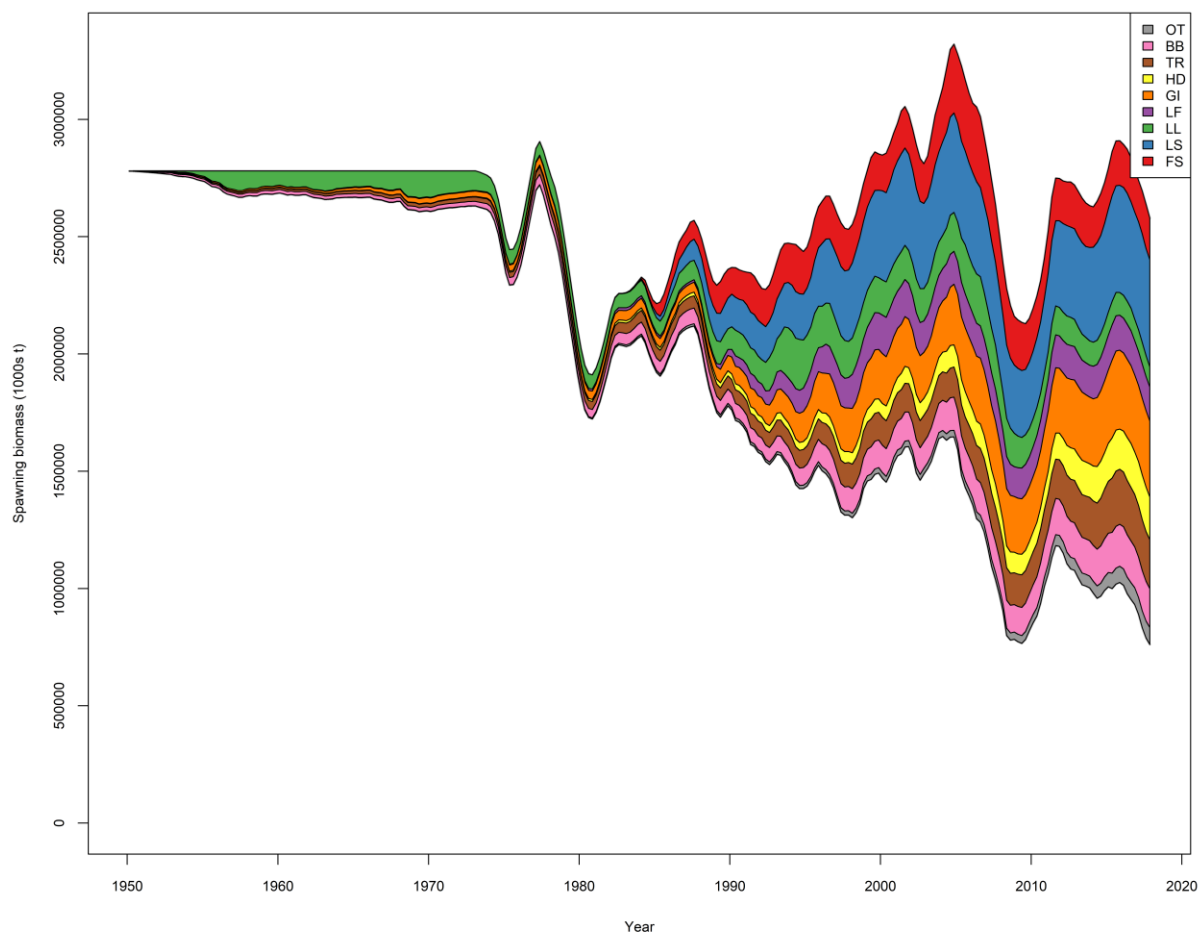


Figure 40: Estimates of reduction in spawning biomass due to fishing over all regions attributed to various fishery groups for the base model.

5.4 Sensitivity case

A range of model sensitivities (see Table 10) were undertaken to address the uncertainty related to various model assumptions (most options were examined during previous assessments, and they are still highly pertinent to the current assessment). Objective function values are summarised in Table 12. Key results are summarised in Table 13 (selected diagnostics are given in Appendix D) and are briefly discussed below:

Reference model

The reference model has the same configuration but excluded the size data 2015 – 2017 (see Section 6.2 for discussion). The estimated stock biomass was appreciably lower than the base model, particularly for recent years (See Figure 19).

SRR steepness (0.70, 0.90).

These are the range of values typically considered for the tropical tuna assessments. Very similar spawning biomass was estimated for alternative values of steepness (Figure 41). The low steepness yielded an estimate of a smaller maximum sustainable yield, which occurred at higher depletion level, and vice versa (Figure D1, Appendix D), but the difference is not considered to be great.

Environmental covariates on movement

NoEnviroMove represents a simpler parameterisation of the seasonal movement dynamics, and the exploratory modelling results indicated that the CPUE data was unlikely to inform estimation of seasonal movement pattern. The model yielded very similar estimate of spawning biomass as the base model (Figure 41)

Natural mortality

M_{low} option was also retained as a sensitivity, as it represents a possible lower bound for the range of credible values of natural mortality (Langley 2015). The model yielded more pessimistic estimates of biomass and stock status (Figure 41).

Tag data weighting

The previous assessments suggested there is conflict between the tag release/recovery data and the CPUE data, and the relative weighting of each data type influences the population scale parameter (R_0). Downweighting the tag data (10% of weight) yielded substantially higher level of stock biomass and (Figure 42), considerably higher estimate of MSY , and change in stock status relative to SB_{MSY} and F_{MSY} compared to base model. A likelihood profile analysis may provide further insights into the conflict between the CPUE and tag data.

Tag over-dispersion parameter

Increasing the value of the tag over-dispersion parameter from 7 to 70 does not appear to have an impact on model results (Figure 42, Table 13)

Tag mixing period

The fit to the time series of tag recoveries from purse seine fleets appeared to indicate the three quarters may not be sufficient to allow for adequate dispersal of tagged fish in the population. It is assumed that extending the tag mixing period is likely to have improved the degree of mixing. Models with tag mixing period assumed to be four or eight quarters improved the fit to the tag recoveries (post-mixing, Figure D2), and improved to fit to the CPUE indices for region 1b and 2 as well (Figure D3). The improvement in the fit to CPUE (as indicated in the more balanced residuals) is mostly related to that the model (e.g. *TagMix4Q*) estimated substantially lower movement rates between the region 1 and 2 especially for adults (Figure D4), resulting in a low level of mixing of populations between the two regions. The reason for this is not entirely clear, as extending the mixing period is not expected to substantially reduce the number of tags recovered in a region other than the region of release. This result may indicate the high degree of uncertainty associated with the movement dynamics, as well as potential inconsistency between the CPUE and tag observations which were further compounded by the assumed mixing period. Extended mixing period yielded higher estimates of biomass (*TagMix8Q* in particular).

Longline CPUE

The base model indicated that there is discrepancy between the two sets of western LL CPUE indices, especially in the more recent years – The model over-estimates CPUE to the Region 1 LL CPUE indices from the last 5 years and the opposite is the case for Region 2. Additional analysis that down-weighted the last 10 years of R1 CPUE indices in region 1b yielded more optimistic results, and the opposite is true when the R2 CPUE indices are similarly down-weighted.

The discrepancy in LL CPUE indices between R1 and R2 is not apparent in the CPUE indices derived using the Taiwanese logbook catch effort alone (Figure 41 of Ye et al. 2018). The steeper decline in the R1 LL indices may reflect higher depletion in the tropical area, but a negative bias in the indices is also possible (considering the low level of effort from the Japanese fleet following the piracy period). Thus, we conducted a sensitivity model (*CPUETWR1*, see Table 10) which included the Taiwanese CPUE time series for region 1 for the last 20 years (1998 – 2016, see Figure 41 of Ye et al. 2018). This model excluded the Joint LL R1 indices over the same data period.

The results from *CPUETWR1* estimated less decline in stock abundance between the late 1990s to the present, and a slightly high current biomass (Figure 43). The fit to the recent (Taiwanese) LL indices has more balanced residuals (Figure D4), although the negative trend persists for the early year (Joint) LL indices. The results were more consistent with the trend of the LL CPUE indices in region 2. The stock status was more optimistic than the base model with the current biomass estimated to slightly above Bmsy (Table 13).

Purse seine CPUE indices

The utility of the purse seine CPUE as an index of abundance is yet to be fully evaluated. The longer CPUE series from the free-swimming schools (FREE SCH) show an overall increasing trend over the data period (1986–2017), which contradicted the LL CPUE (Figure D5). The sensitivity model (*PS_CPUE*) configured to fit the PS indices (assuming a low CV of 0.1) show deteriorating fit to the LL CPUE in region 1b (Figure D5). The model estimated less decline in abundance and more optimistic stock status than the base model (Figure 44, Table 13).

Assuming a catchability increase of approximately 1.25% per year for the PS CPUE indices (suggested by Kolody (2018)) shift the long-term trend in PS FREE SCH CPUE indices more in line with the LL CPUE. *PS_CPUE_Q125* estimated similar biomass from late 1990s to the present but lower biomass in the early years (Figure 44). Overall the model estimated a slightly more optimistic stock status than the base model (Table 13) indicating a 1.25% catchability increase is probably not sufficient to fully reconcile the difference between the PS and LL CPUE indices.

An additional analysis (*PS_CPUE_estQ*) was conducted to estimate the potential catchability change in the PS FREE SCH CPUE indices, following the same approach by Kolody (2018). It involves setting the lambda of the PS CPUE index to zero so that it is uninformative in the model, and the departure of PS CPUE from the expected population trend (as reflected in the residuals in the fit) can be interpreted as the change in catchability (see Kolody (2018) for details). The model estimated a catchability increase of approximately 1.5% per year for the PS FREE SCH CPUE (Figure D6).

The shorter PS CPUE timeseries from effort on FAD schools appear to show a broadly similar trend to the LL indices in R1 over the last 10 years, except for the timing where the peak occurred in the series. The sensitivity model (*LLFAD*) that included only the PS FAD CPUE and all the other LL CPUE series yielded similar results to the base model (Table 13).

Table 12: Details of objective function components for the final set of stock assessment models and main sensitivities.

	TOTAL	CPUE	Length_comp	Tag_comp	Tag_negbin	Recruitment	Parm_priors	Parm_devs	Catch	Parm_softbounds
<i>base</i>	11506.4	-221.7	4291.3	5427.6	1976.8	-44.2	54.2	21.2	0.000005	0.006
<i>reference</i>	11049.9	-242.2	3871.5	5429.2	1957.2	-42.0	54.5	20.5	0.000056	0.006
<i>Steep70</i>	11452.4	-308.8	4286.2	5465.9	1978.5	-44.5	54.7	19.0	0.000006	0.006
<i>Steep90</i>	11504.6	-221.3	4279.7	5429.6	1977.8	-51.0	63.5	25.0	0.000007	0.006
<i>Mlow</i>	11527.9	-293.9	4349.9	5509.7	1904.8	-23.3	61.2	18.9	0.000021	0.007
<i>NoEnviroMove</i>	11487.2	-241.6	4271.7	5434.7	1985.0	-50.1	73.8	12.3	0.000008	0.006
<i>TagDwt01</i>	4637.5	-319.8	4178.0	562.7	207.5	-61.0	46.2	22.5	0.000001	0.006
<i>TagOD70</i>	12137.0	-218.4	4313.1	5420.2	2597.9	-43.9	46.7	20.2	0.000004	0.006
<i>TagMix4Q</i>	9691.2	-285.4	4242.9	4028.6	1679.2	-51.5	57.5	18.6	0.000015	0.006
<i>TagMix8Q</i>	6321.9	-198.7	4209.3	1356.3	928.7	-58.2	72.3	10.8	0.000003	0.006
<i>CPUETWR1</i>	11427.4	-291.8	4265.6	5416.9	1996.5	-36.1	54.1	20.9	0.000014	0.006
<i>PS_CPUE</i>	11350.0	-425.7	4254.3	5433.8	2028.7	-31.3	60.6	28.4	0.000008	0.005
<i>PS_CPUE_Q125</i>	11368.1	-441.0	4298.6	5450.1	1999.9	-33.2	72.3	20.4	0.000008	0.005
<i>LLFAD</i>	11421.1	-392.2	4343.5	5473.0	1974.1	-45.4	47.6	19.2	0.000021	0.006

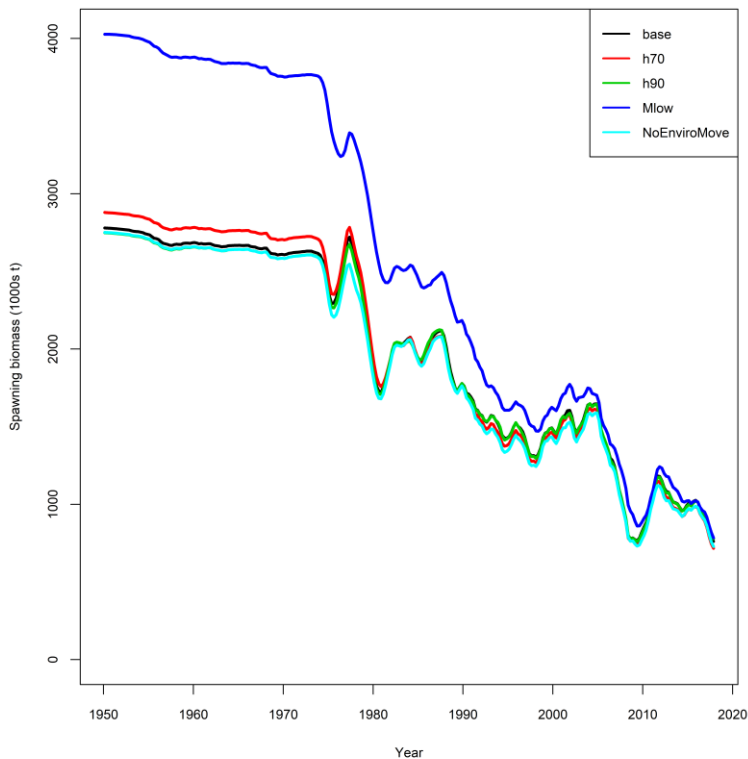


Figure 41: Spawning biomass trajectories from the base model and model sensitivities related to spatial and steepness, natural mortality, and movement assumptions.

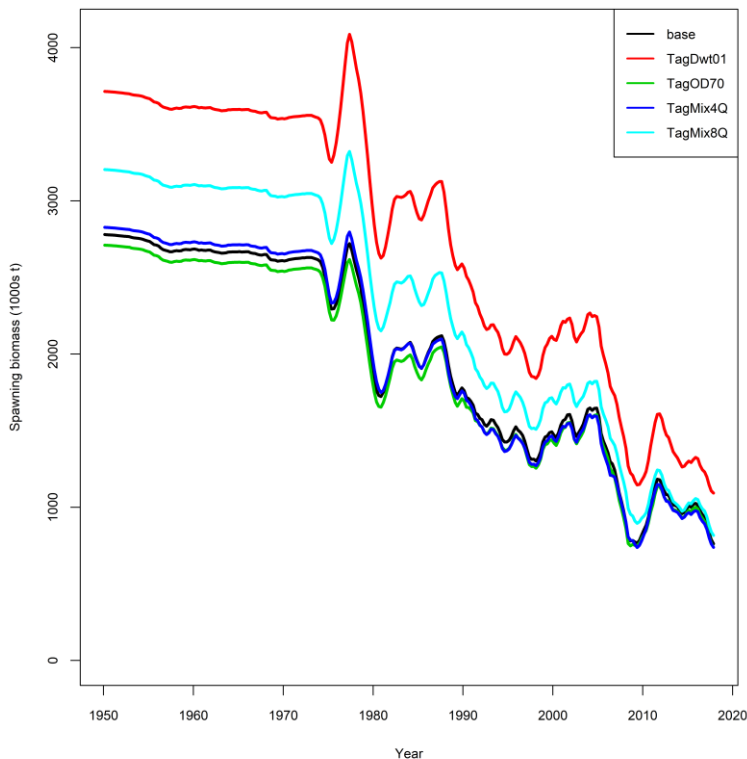


Figure 42: Spawning biomass trajectories from the base model and model sensitivities related to tagging data weighting, and over-dispersion parameter (OD), and mixing period assumptions.

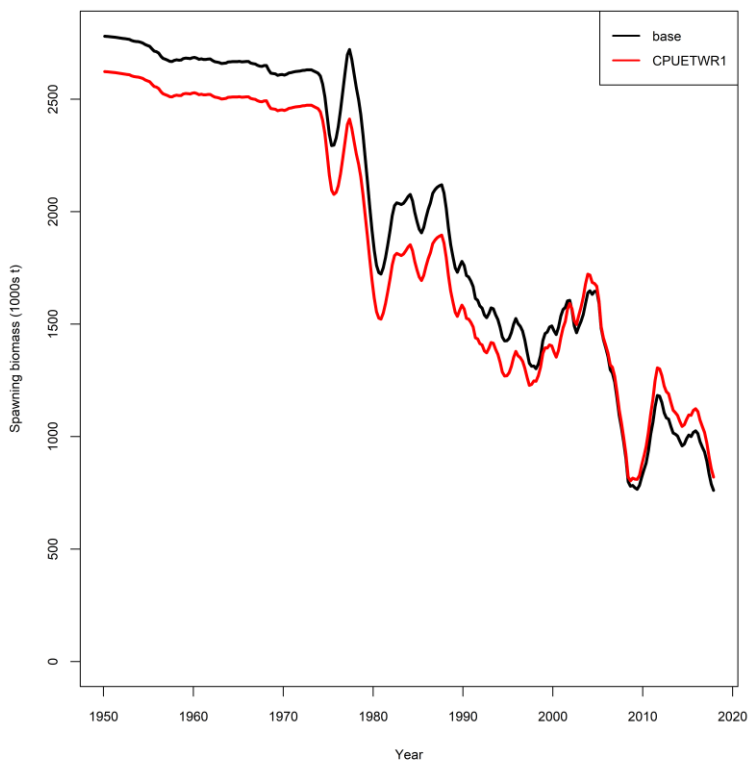


Figure 43: Spawning biomass trajectories from the base model and model sensitivity that included the Taiwanese LL CPUE 1998 – 2016 in region 1 (*CPUETWR1*).

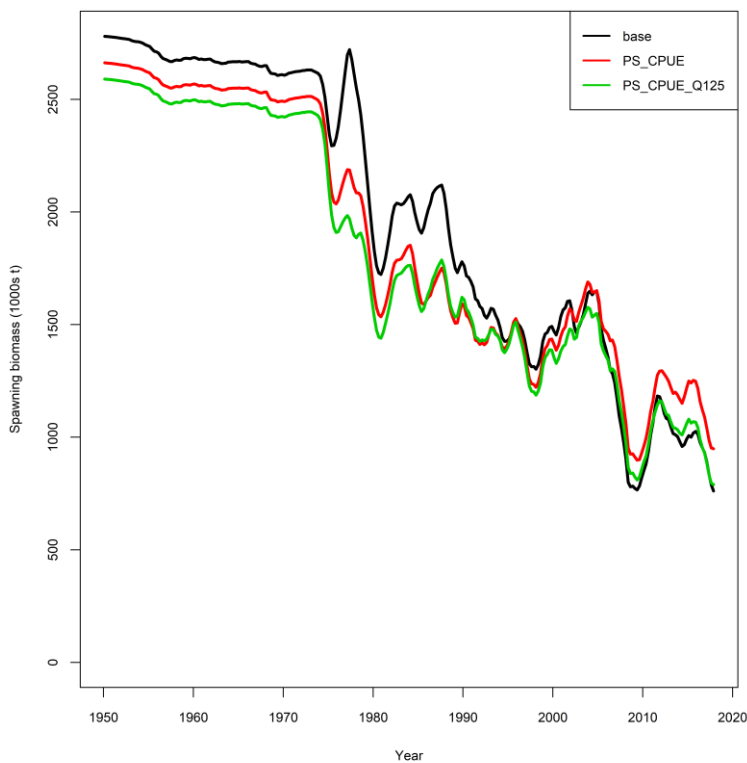


Figure 44: Spawning biomass trajectories from the base model and model sensitivities that included the PS CPUE indices.

6. STOCK STATUS

6.1 Current status and yields

Current (2017) stock status was defined relative to the *MSY* based biomass (SB_{MSY}) and fishing mortality (F_{MSY}) reference points. The yield analysis incorporates the SRR into the equilibrium biomass. The base model and model sensitivities assumed the value of steepness (0.80), except for the two sensitivity models assuming the low (0.7) and high (0.9) values.

Equilibrium yield and biomass (spawning) were computed as a function the 2016–2017 average fishing mortality-at-age (Figure 39). The estimate of *MSY* for the base model is 377,000 mt (Table 13). This level of yield is somewhat lower than the average level of catch from 2013–2017 (400,000 mt). The estimate of *MSY* is considerably lower for the model sensitivity with lower natural mortality (*MSY* 302,000 mt) and is considerably higher for the model with lower tag weighting option (*MSY* 450,000 mt).

For the base model option, the annual trends in F_t/\tilde{F}_{MSY} and SB_t/\tilde{SB}_{MSY} were computed for each year (t) included in the model (1950–2017) (Figure 45 & Figure 46). Prior to 1990, exploitation rates were low and adult biomass remained well above \tilde{SB}_{MSY} . In the early 1990s, F_t/\tilde{F}_{MSY} increased and biomass levels declined before stabilizing during the mid-1990s–early 2000s. Overall fishing mortality rates increased sharply in 2005 in line with the large increase in catches during 2004/2005. Adult biomass declined considerably in the subsequent years, attributable to a period of very low recruitment during 2004–2006 and declined below the SB_{MSY} level in 2008. The stock rebounded during 2009–2012 before declining below the SB_{MSY} level again in 2015–2017 (Figure 45 & Figure 46).

Fishing mortality rates increased and exceeded the F_{MSY} level in 2012 following the recent increase in annual catch (Figure 45 & Figure 46). The estimate of current fishing mortality is not well determined although there is only a small probability that fishing mortality is below the F_{MSY} level (for the base model) (Figure 45 & Figure 46).

For the base model, adult biomass is estimated to be at 87% of the SB_{MSY} level and current fishing mortality rates are 12% higher than the F_{MSY} level (Table 13). Most of the other model options also estimated that the stock is in an overfished state ($SB/SB_{MSY} < 1.0$) and that overfishing is occurring ($F/F_{MSY} > 1.0$) (Figure 47, Table 13). Both *Steep90* and *TagDwt01* estimated that overfishing is not occurring. Both *CPUETWR1* and *PS_CPUE* estimated the stock is not overfished. Of all models explored, *PS_CPUE* estimated the current stock status to be in the green quadrant of the KOBE plot. The extent of the stock depletion varies considerably amongst the model options (SB/SB_{MSY} 0.61–1.09).

The overall stock status conclusions do not differ substantially from the previous assessment; current (2017) spawning biomass is estimated to be below SB_{MSY} ($SB_{2017}/SB_{MSY} = 0.87$) and fishing mortality is estimated to be above F_{MSY} ($F_{2017}/F_{MSY} = 1.12$).

Table 13: Estimates of management quantities for the stock assessment model options and model sensitivities. Current yield (mt) represents yield in 2015 corresponding to fishing mortality at the FMSY level. The 95% confidence intervals for the current stock status metrics are provided for the base model.

Option	SB_0	SB_{MSY}	SB_{MSY}/SB_0	SB_{2017}	SB_{2017}/SB_0	SB_{2017}/SB_{MSY}	F_{2017}/F_{MSY}	MSY
<i>base</i>	2,779,850	935,463	0.34	818,276	0.29	0.87 (0.82–0.73)	1.12 (0.90–1.37)	377,084
reference	2,577,250	880,554	0.34	770,197	0.30	0.87	1.34	367,224
<i>Steep70</i>	2,879,390	1,059,770	0.37	777,507	0.27	0.73	1.48	356,100
<i>Steep90</i>	2,749,230	870,231	0.32	828,768	0.30	0.95	0.92	396,452
<i>Mlow</i>	4,027,410	1,378,380	0.34	846,263	0.21	0.61	2.23	302,809
<i>NoEnviroMove</i>	2,751,510	1,005,620	0.37	788,429	0.29	0.78	1.31	360,482
<i>TagDwt01</i>	3,713,970	1,295,410	0.35	1,135,555	0.31	0.88	0.87	449,340
<i>TagOD70</i>	2,710,930	918,727	0.34	795,051	0.29	0.87	1.15	373,835
<i>TagMix4Q</i>	2,827,060	964,217	0.34	789,062	0.28	0.82	1.17	370,074
<i>TagMix8Q</i>	3,203,990	1,151,140	0.36	868,736	0.27	0.75	1.28	408,608
<i>CPUETWR1</i>	2,622,500	875,537	0.33	889,477	0.34	1.02	1.08	348,979
<i>PS_CPU</i>	2,662,080	896,861	0.34	981,431	0.37	1.09	0.89	348,332
<i>PS_CPU_Q125</i>	2,590,020	894,570	0.35	825,441	0.32	0.92	1.16	347,955
<i>LLFAD</i>	2,769,110	986,751	0.36	808,035	0.29	0.82	1.17	386,070

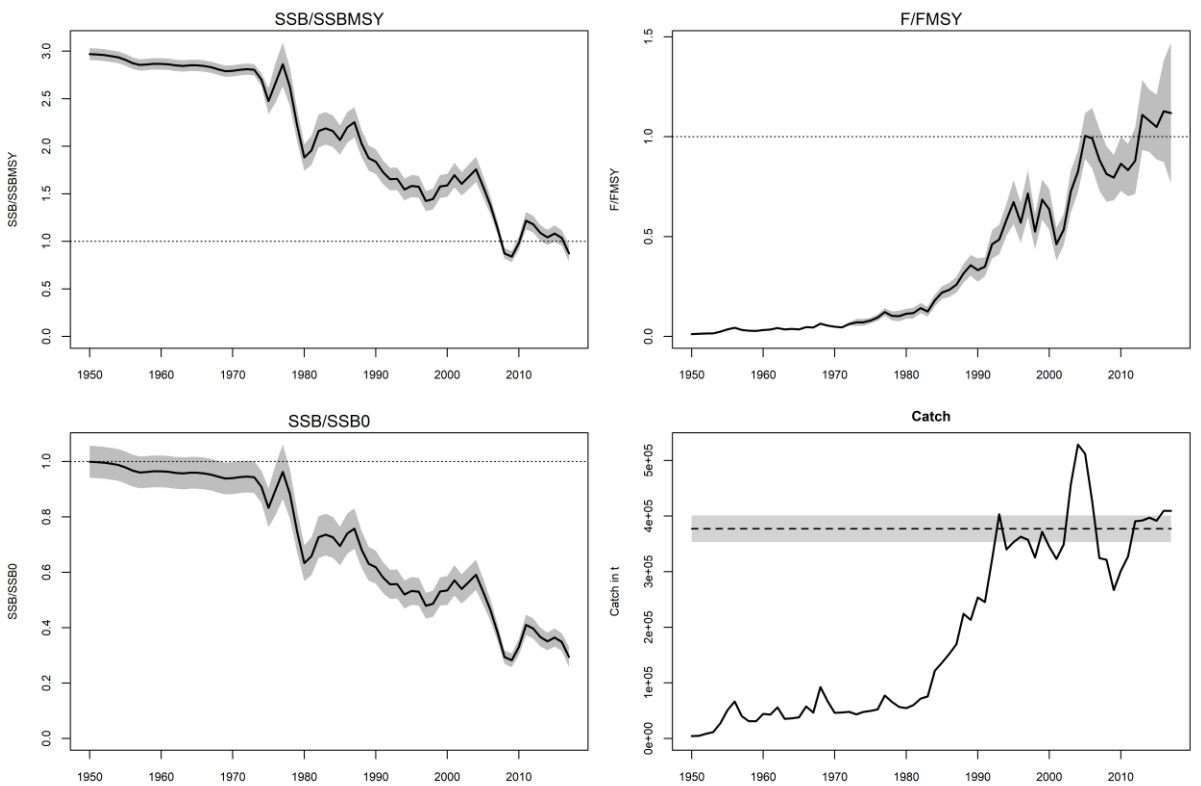


Figure 45: Stock status summary for the Indian Ocean yellowfin for base model. Thick black lines shaded areas represent 5th and 95th percentiles. In the catch plot, dotted lines represent estimate of MSY, the shaded area represents 5th and 95th percentiles

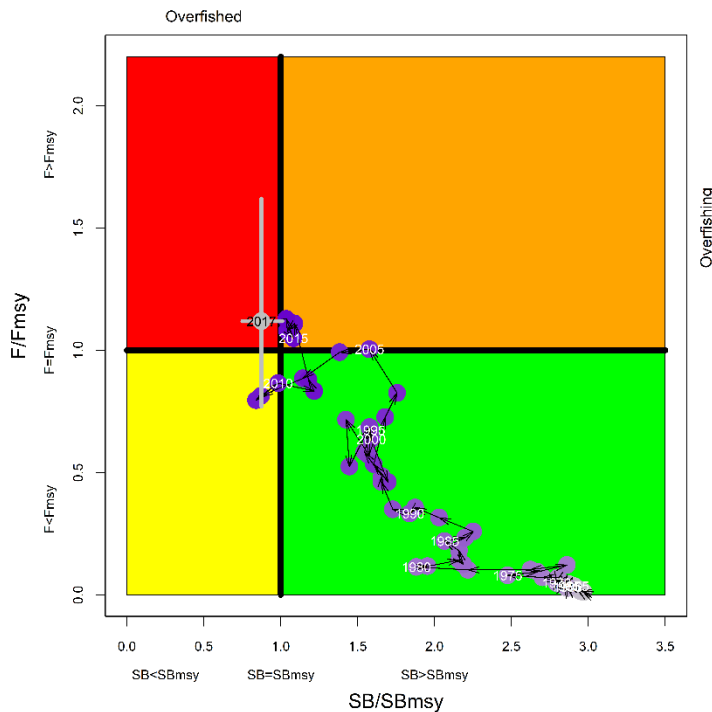


Figure 46: Annual stock status, relative to SB_{MSY} (x-axis) and F_{MSY} (y-axis) reference points for the base model. The grey lines represent the 95% confidence interval associated with the 2017 stock status.

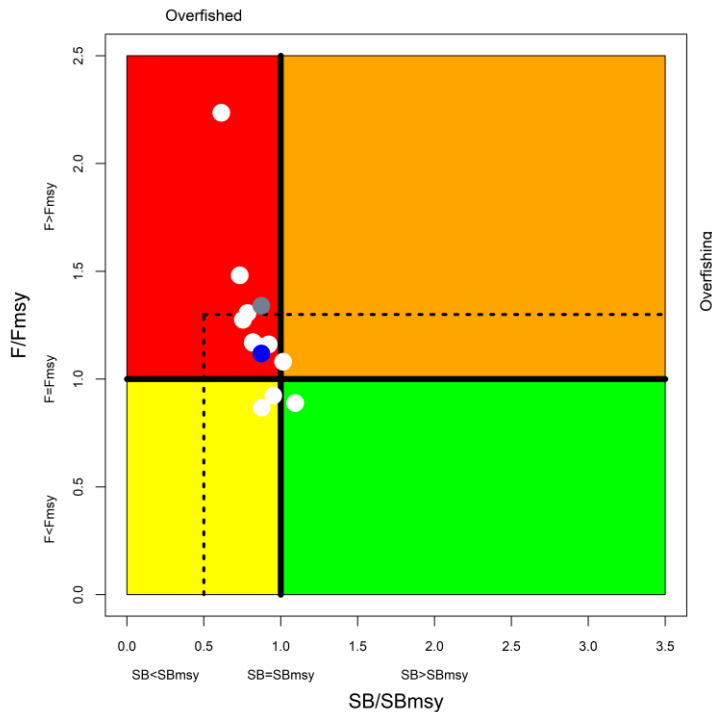


Figure 47: current stock status, relative to SB_{MSY} (x-axis) and F_{MSY} (y-axis) reference points for the base model (blue), the reference model (grey), and a range of sensitivity models (white, see Table 10). The dashed lines represent limit reference points for IO yellowfin tuna ($SB_{lim} = 0.5 SB_{MSY}$ and $F_{lim} = 1.4 F_{MSY}$).

6.2 Retrospective analysis

Retrospective analysis is diagnostic approach to evaluate the reliability of parameter and reference point estimates and to reveal systematic bias in the model estimation. It involves fitting a stock assessment model to the full dataset. The same model is then fitted to truncated datasets where the data for the most recent years are sequentially removed. The retrospective analysis was conducted to the base model for the last 5 years of the assessment time horizon to evaluate whether there were any strong changes in model results. The selected period was intended to avoid removing any tag recovery data. The analysis involves sequentially removing 4 quarters of data at each trial.

The analysis conducted to the base model indicated some level of retrospective patterns, where model predictions indicated lower level of SSB, and higher exploitation rate, lower (recent) recruitment variability when up to 5 years of data were sequentially removed (Figure 48).

Further investigation suggested the retrospectives appeared to be related to the addition of most recent size composition data (given the large influence of the recent size data revealed during the simple model updates. See Section 5.1). A reference model was therefore configured which has the same model options as the base model but excluded the size composition data from 2015– 2017. The retrospectives of the the reference model were very stable (Figure 49). The reference model estimated a similar depletion level to the base model but higher exploitation rate ($SSB/SSB_{MSY} = 0.87$ and $F/F_{MSY} = 1.34$, see Table 13).

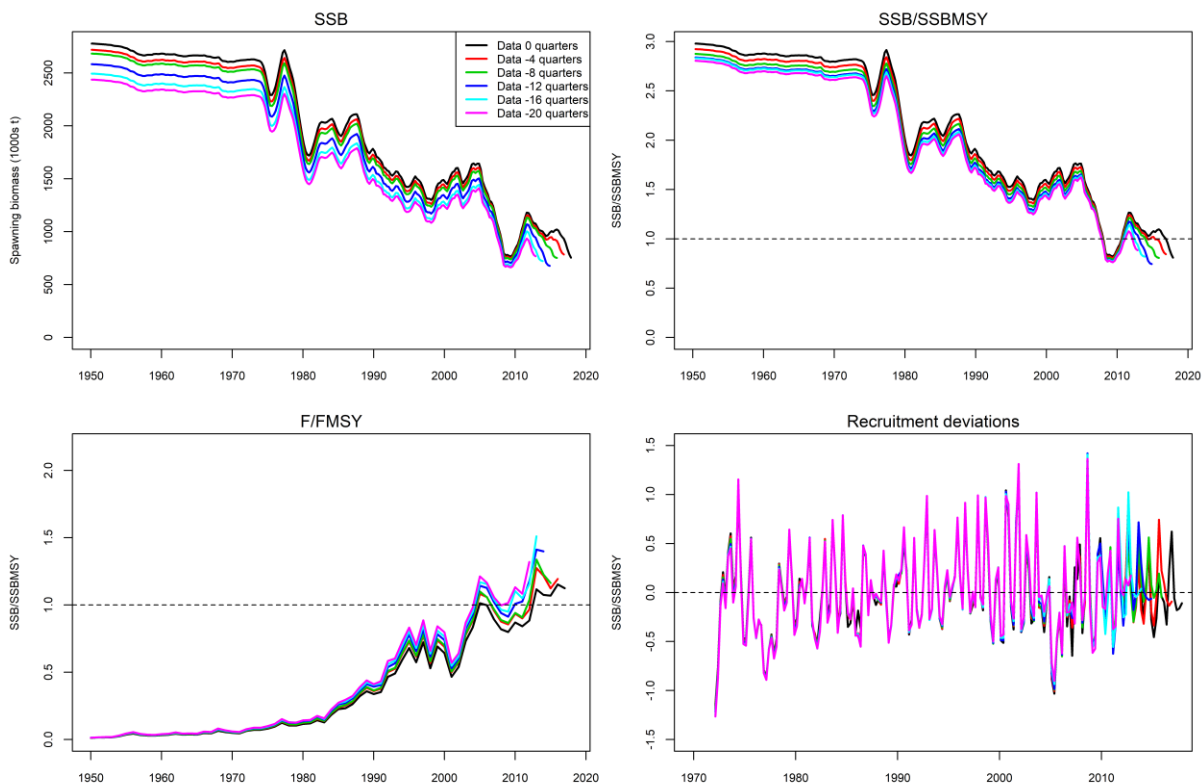


Figure 48: Retrospective analysis summary for the Indian Ocean yellowfin for base model.

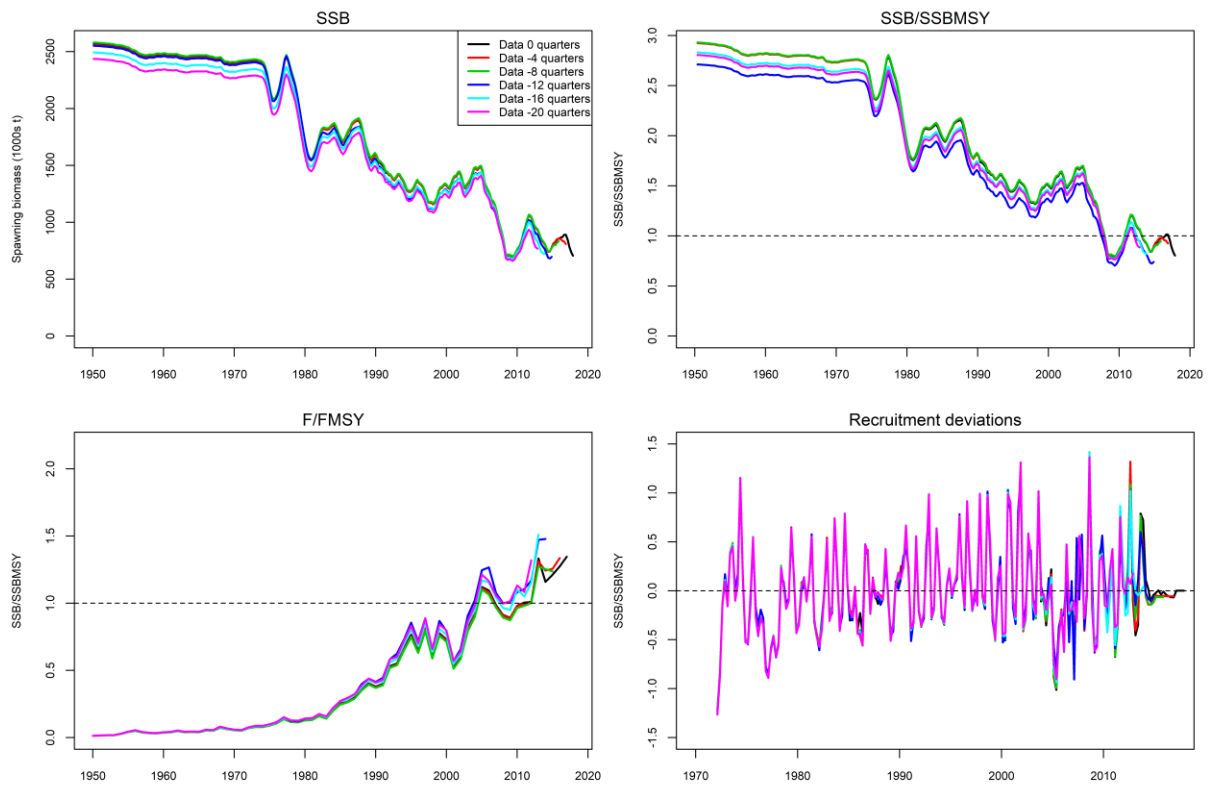


Figure 49: Retrospective analysis summary for the Indian Ocean yellowfin for reference model.

6.3 Projection

Stock projections were conducted for both the base model and the reference model. We further note that the projections are preliminary and are only intended for the comparison of model performance. The projections were conducted for a 10 year period (2018–2027) at a constant level of catch as a multiple of the fishery catches in 2015 (391,587 mt). Five levels of catch were investigated representing 100% to 60% of the 2015 catch level. Recruitment during the projection period was at the equilibrium level. The uncertainty associated with the projected biomass was derived from the covariance matrix. For each stock scenario, the probability of the biomass being below the SB_{MSY} level was determined after 3 years (2020), 5 years (2022) and 10 years (2027).

The uncertainty associated with the projected biomass promulgates rapidly reflecting the uncertainty associated with the equilibrium recruitment level (Figure 50). For the base model, a 20% catch reduction relative to 2015 level would allow the stock to rebuild to be above the SB_{MSY} level at the end of the 10 year projection period with a probability greater than 50% (Table 14). Reference model indicated up to 30% catch reduction is required for the stock to recover to be above the SB_{MSY} level at the end of the 10 year projection period with a high probability (Table 14)

K2SM probabilities are provided with options to reduce fishing mortality with a view to recover the stocks in the green zone of the Kobe Plot with levels of probability ranging from 60% to 90% by 2026. The base model indicates that this would require the maximum annual catches have to be set to between 280,000 – 325, 000 t (Table 15). The reference case indicates the maximum annual catches need to be further reduced to 250,000 – 280,000 t (Table 15).

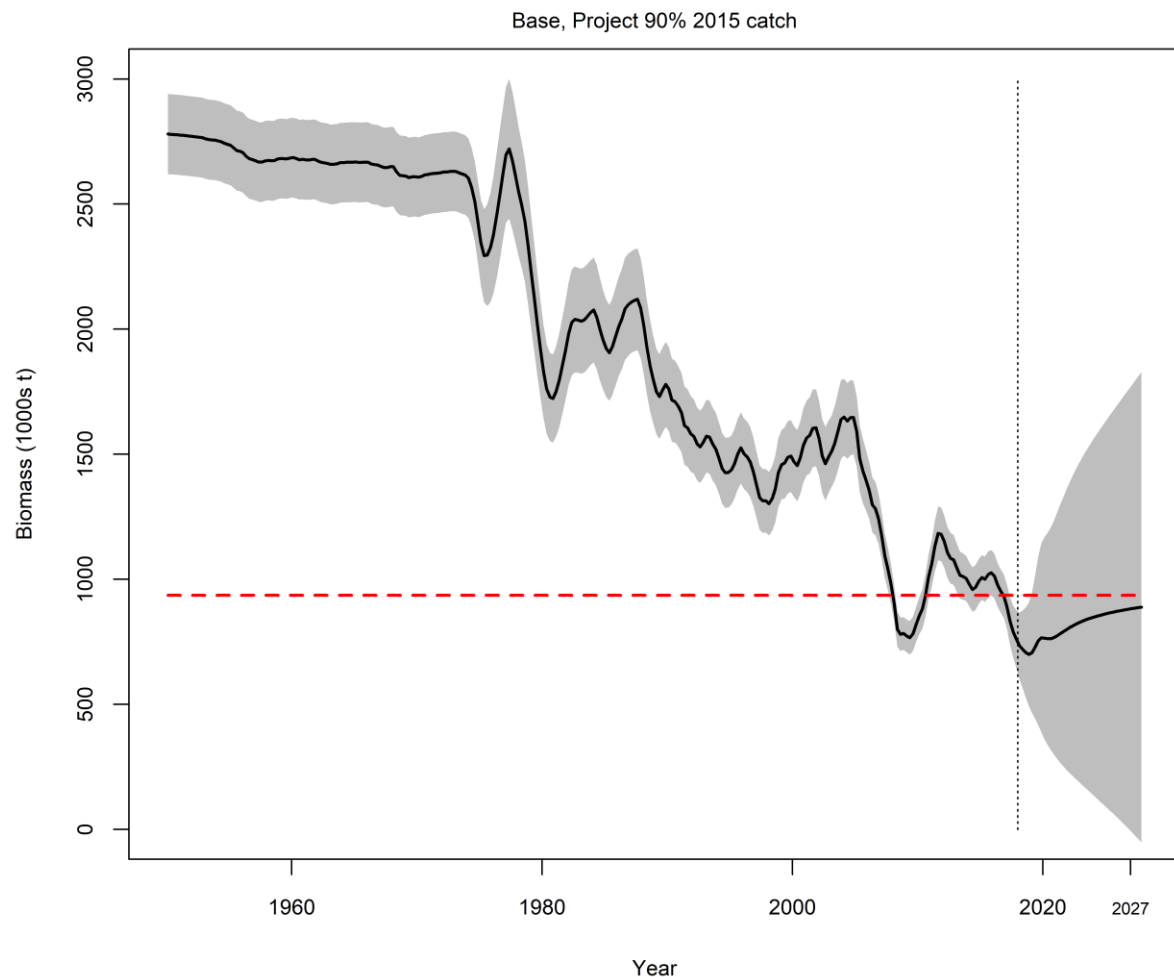


Figure 50: Spawning biomass trajectory for the base model option with a 10-year projection (2018–2027) assuming a constant level of catch at 90% of the 2015 catch level (i.e. 391,587 t in 2015). The grey area represents the 95% confidence interval. The red horizontal line represents the SB_{MSY} level.

Table 14: Projected stock status: spawning biomass relative to SB_{MSY} and the probability of being below SB_{MSY} , fishing mortality relative to F_{MSY} and the probability of being above F_{MSY} in 3-, 5- and 10 years for five alternative levels of catch (relative to 2015) for the base model. A value of zero for SB/SB_{MSY} indicates that catches exceeded the stock biomass (the stock crashed), or the estimated variance was implausibly high.

Model option	Catch	3 years (2020)		5 year (2022)		10 year (2027)	
		SB/SB_{MSY}	$\Pr(SB < SB_{MSY})$	SB/SB_{MSY}	$\Pr(SB < SB_{MSY})$	SB/SB_{MSY}	$\Pr(SB < SB_{MSY})$
base	100%	0.714	0.908	0.666	0.849	0.508	0.524
	90%	0.817	0.822	0.873	0.645	0.947	0.547
	80%	0.918	0.642	1.061	0.421	1.326	0.215
	70%	1.019	0.479	1.237	0.238	1.596	0.055
	60%	1.119	0.278	1.404	0.129	1.825	0.016
reference		SB/SB_{MSY}	$\Pr(SB < SB_{MSY})$	SB/SB_{MSY}	$\Pr(SB < SB_{MSY})$	SB/SB_{MSY}	$\Pr(SB < SB_{MSY})$
	100%	0.52	0.98	0.00	1.00	0.00	1.00
	90%	0.63	0.93	0.58	1.00	0.00	1.00
	80%	0.74	0.87	0.83	0.70	0.86	0.56
	70%	0.85	0.73	1.05	0.47	1.38	0.16
	60%	0.95	0.61	1.24	0.24	1.67	0.03

Table 15: Probability (percentage) of achieving the KOBE green quadrat from 2018-2027 for a range of constant catch projections for the base model of the IO yellowfin assessment. Highlighted zeroes indicate that catches exceeded the stock biomass (the stock crashed), or the estimated variance was implausibly high

Catch Year	2018	2019	2020	2021	2022	2023	2024	2025	2026	2027
<u>Base</u>										
400,000	0.00	0.01	0.02	0.02	0.03	0.13	0.00	0.00	0.00	0.00
385,000	0.00	0.01	0.03	0.04	0.05	0.07	0.11	0.00	0.00	0.00
370,000	0.00	0.03	0.06	0.08	0.10	0.11	0.12	0.13	0.14	0.16
355,000	0.00	0.05	0.11	0.14	0.18	0.19	0.20	0.21	0.22	0.23
340,000	0.00	0.07	0.17	0.23	0.27	0.30	0.34	0.37	0.40	0.42
325,000	0.00	0.10	0.24	0.32	0.39	0.46	0.52	0.58	0.62	0.65
310,000	0.00	0.15	0.33	0.42	0.53	0.63	0.68	0.73	0.76	0.79
295,000	0.00	0.24	0.40	0.50	0.62	0.69	0.75	0.79	0.83	0.86
280,000	0.00	0.26	0.48	0.63	0.74	0.80	0.85	0.89	0.90	0.93
265,000	0.00	0.39	0.50	0.63	0.73	0.80	0.85	0.90	0.92	0.94
250,000	0.01	0.36	0.64	0.77	0.85	0.90	0.93	0.95	0.96	0.97
Catch Year	2018	2019	2020	2021	2022	2023	2024	2025	2026	2027
<u>Reference</u>										
400,000	0.00	0.00	0.00	0.00	0.00	0.00	0.00	0.00	0.00	0.00
385,000	0.00	0.00	0.01	0.00	0.00	0.00	0.00	0.00	0.00	0.00
370,000	0.00	0.00	0.01	0.00	0.00	0.00	0.00	0.00	0.00	0.00
355,000	0.00	0.01	0.01	0.03	0.00	0.00	0.00	0.00	0.00	0.00
340,000	0.00	0.01	0.02	0.04	0.07	0.00	0.00	0.00	0.00	0.00
325,000	0.00	0.01	0.03	0.07	0.10	0.13	0.15	0.20	0.00	0.00
310,000	0.00	0.02	0.07	0.13	0.17	0.19	0.21	0.22	0.23	0.24
295,000	0.00	0.04	0.12	0.22	0.27	0.31	0.36	0.40	0.43	0.47
280,000	0.01	0.06	0.18	0.32	0.41	0.49	0.58	0.64	0.70	0.74
265,000	0.01	0.08	0.26	0.43	0.56	0.67	0.74	0.79	0.84	0.87
250,000	0.02	0.11	0.35	0.55	0.70	0.78	0.83	0.88	0.90	0.93

7. DISCUSSION

This report presents a preliminary stock assessment for Indian Ocean yellowfin tuna using a spatially disaggregated, age structured model that integrates multiple sources of fisheries and biological data. It represents an update and refinement of the 2016 assessment model using newly available data. In addition to the revised and updated fishery and environmental data, the assessment incorporated minor revisions to the previous base case model following scrutiny of the model configurations, adopted a revised regional weighting scheme that is more consistent with the historical catches, and further revised the procedure to process the tag data for incorporation into the assessment. A range of exploratory and sensitivity models are also presented to explore the impact of key data sets and model assumptions on the stock assessment conclusions.

We note that the models presented in the assessment (including the base model and sensitivities) are for the purpose of facilitating the discussions of model diagnostics and performance and are not intended as the final model(s) for providing management advice (which shall be determined by the Working Party on Tropical Tunas after deliberations of all model options explored during the assessment).

The base model indicated stock biomass declined substantially since 2012, driven by high catch levels and declining recruitment. Current (2017) total spawning biomass is estimated to be close to the historically low level. The overall stock status conclusions do not differ substantially from the previous assessment. Current spawning biomass is estimated to be below SB_{MSY} ($SB_{2017}/SB_{MSY} = 0.87$) and fishing mortality is estimated to be above F_{MSY} ($F_{2017}/F_{MSY} = 1.12$). Most sensitivity model options also estimated that the stock is in an overfished state ($SB/SB_{MSY} < 1.0$) and that overfishing is occurring ($F/F_{MSY} > 1.0$), although the extent of the stock depletion varies considerably amongst the model options. Current catches are higher than the estimated MSY from the base model (377,000 t) and are unlikely to be sustainable.

Stock projections were conducted to evaluate the impact of the alternative levels of catch relative to 2015 catches. **The projections are not intended to provide a reliable prediction of future stock status due to the simplifying assumptions of equilibrium recruitment (from SRR), constant catch and unlimited fishing mortality. Instead, the projections are provided to give an indication of the relative performance of the stock at different levels of catch. In addition, the projections are not based on the final model options (yet to be discussed and agreed by the Working party on Tropical Tuna).** For the base model, the stock slowly recovered to SB_{MSY} at a catch level of 80% of the 2015 catch. To recover the stocks to the green zone of the Kobe Plot with levels of probability higher than 60% by 2026 would require the maximum annual catches to be set to less than 325,000 t. Higher catch reductions are required to achieve these targets for a reference model which did not include the size composition data for the last three years.

As earlier assessments, the models presented here, while providing a reasonable fit to some key data sets (e.g., the CPUE indices), also show some signs of poor fit (e.g. tag data). There are conflicts amongst observational datasets, noticeably between the CPUE and tag data, and the model estimates are sensitive to the relative weighting of these data. Estimates of movement rates were informed by prior information on regional biomass distribution derived from an external analysis of CPUE data and were also influenced by model configurations. The nature and extent of the dispersal of tagged fish remains a key uncertainty in the assessment. The retrospective pattern in base model may undermine the predictive capabilities of the model.

In general, the current assessment models provide a good fit to the main data sets. The CPUE indices represent the primary source of information regarding abundance and, consequently, the main conclusions of the assessment are dependent on the reliability of these indices. Temporal trends appear to vary within regions, with greater decline in CPUE in tropical areas close to the equator. Similar spatial patterns have been observed in Atlantic fisheries, with larger declines in catch rates in tropical

areas (Hoyle et al. 2018b). The trend may be associated with greater depletion of areas subject to more purse seine fishing (Hoyle et al. 2018b). It is difficult for the model to fully account for the difference in temporal trend between region 1 and 2, given the current population dynamics (high degree of mixing of the populations between the two regions, as estimated by the model). The difference in temporal trend within regions might be better explained by the long-term trend in movement rates, which was not captured by the environment covariates. On the other hand, the LL CPUE indices are based on a joint analysis of the Japanese, Korean, and Taiwanese logbook where the Taiwanese data are included only from 2005 onwards and the Japanese effort were low following the piracy period (Hoyle et al. 2018a, b). The discrepancy in LL CPUE indices between R1 and R2 is not apparent in the CPUE indices derived using the Taiwanese logbook catch effort alone. The trend is also not seen in the EU purse seine CPUE on free schools (although the utility of PS CPUE needs further evaluation). There is the possibility of the low CPUE indices in region 1 could be reflective of fishing operation (post piracy) and/or a change in the fleet composition rather than abundance.

The distribution of tags throughout the wider IO appears to have been relatively limited and tag recoveries from beyond region 1 and 2 are unlikely to inform the model regarding movement rates. The regional weighting of LL CPUE provides information on the relative abundance amongst regions, and thus inform the model on movement and recruitment. Hoyle & Langley (2018) reviewed the estimation of the regional weighting of LL CPUE for IO tropical and temperate tuna from regional catch rates and areas. The revised estimates are based on a standardisation model that has incorporated fleet and seasonal effects and are derived from a period when the targeting was considered relatively stable and fishing is widely distributed. The revised regional weighting resulted in a biomass distribution that appears to be more consistent with the regional catch history, although the results cannot be validated independently. Alternative estimates from Hoyle & Langley (2018) were also explored in the assessment. In general, the regional weighting scheme did not appear to have any appreciable impact on the estimates of the overall stock biomass, but they influenced estimation of movement rates and recruit allocation, therefore have direct implications on the estimates of fishing mortality and stock depletion at the regional level.

The assessment model was unable to fit the early size data from the longline fisheries - the rate of decline appears too rapid to represent change in the size structure of the population, given the size of the catches. The substantial decline in the mean sizes captured during the 1950s period appeared to be consistent with the juvenilization hypothesis. Hoyle et al. (2017) suggested that the size reduction is not due to sampling in areas with smaller fish, but to reduction in the average size of fish across all locations. Further investigation is also required to understand the decline in mean length through in the 1990s and early 2000s, which was mainly driven by the length data from the Taiwanese Fleet. This period coincides with the years when the logbook coverage of the Taiwanese fleet was the lowest (less than 10%) whereas most samples may have come from vessels primarily targeting albacore tuna. The assessment model should include size composition data from the main fleets and areas where size data are most consistent with catch and CPUE, a practice adopted for the most recent IO bigeye tuna assessment (Langley 2016b). Further refinement of the fishery definitions may be justified if there are substantial differences in the length composition of the catches from main fleets. But this requires more representative sampling for individual constituents.

Investigations conducted in the assessment suggested that the recruitment anomaly in 2004 – 2006 is primarily attributed to the sharp decline of LL CPUE in the late 2000s, as well as the influence of the tag data. The mechanism as to how the tag data may have affected the recruitment pattern is not clear, possibly relating to the contrasting abundance information in the tag and CPUE data sets. Although the size composition data did not appear to contribute to the estimation of low recruitment in 2004 – 2006, the level of low recruits is consistent with marked increase in the average length of fish sampled from the PSFS fishery during this period. The period of lower recruitment may be a direct consequence of high catches of adult fish. As the stock assessment model attributes the recent (2008–2009) drop in spawning biomass to a period of very low recruitment during the preceding period (2004–2006) rather than a direct result of the higher levels of catch during the peak period, the estimates of

recent levels of fishing mortality and recruitment are likely to be considerably more uncertain than the estimation of the overall change in stock abundance (Langley 2015).

The current assessment model also assumes that natural mortality and growth are equivalent for both sexes. The differential sex ratio of the larger fish in the population indicates that either natural mortality rates for older female fish are likely to be higher or males are grower faster than females, (Fonteneau 2005, Maunder & Aires-da-Silva 2012). Evidence from tag data indicate possible differential growth between and females (Evenson 2015). The two-sex model for males provides a mechanism to explain the difference in sex-ratio widely observed in the length samples. However, the model simply assumes differential asymptotic length, whereas it is more likely that growth rates are different between two sexes (the estimates of sex-specific growth rates by Eveson 2015 were unlikely to be accurate give the low sample size). Stock assessment of yellowfin in other oceans often assumes sex-specific natural mortality (Aires-Da-Silva and Maunder 2012) which might better explain why fish greater than 160 cm are virtually all males. But without direct observations, it is difficult to quantify or derive sex-specific natural mortality for IO yellowfin.

There also remains considerable uncertainty associated with the overall level of natural mortality. The values assumed in the *base* and *Mlow* assessment models probably represents a reasonable range to reflect the uncertainty associated with natural mortality. The *Mlow* model option yields a considerably more pessimistic estimate of current stock status compared to the *base* model options. The Lorenzen parameterisation considered in the preliminary modelling is biologically appealing, but the very high level of natural mortality for the younger ages appeared to contradict the evidence from tag data, and as previous analysis of tag data indicated low natural morality for fish younger than 12 quarters. Estimates of the overall stock productivity appeared to be insensitive to the functional relationship between natural mortality age; the model yielded almost identical biomass estimates when the Lorenzen mortality vector was rescaled to the mean of the base level natural mortality.

The PS CPUE indices was first considered for the yellowfin assessment in 2016 (Langley 2016a). CPUE from purse seine fisheries is particularly difficult to standardize given the rapid development of new technologies. Kolody (2018) suggested a catchability increase of approximately 1.25% per year (based on effort on FAD schools) should be assumed when incorporating standardised PS effort for yellowfin in the assessment. An update that that analysis within the current assessment estimated a slightly higher catchability increase (1.5% per year) for the effort on free-swimming schools. Future assessments should continue to evaluate the utility of the PS CPUE as indices of abundance.

The assessment considered an alternative spatial structure which further partitions the western equatorial region in view of evidence of potential differences in the population within the region (Hoyle et al. 2018a). This additional stratification helps minimise the potential bias introduced by incomplete mixing of tagged fish within the western equatorial region and is also consistent with what was adopted for the most recent bigeye assessment, which could facilitate management analyses for the tropical tuna species. However, neither the CPUE nor the model has revealed significant differential depletion between the sub-regions. The marginal improvement in the fit to the time series of tag data in western equatorial region does not appear to justify the additional complexity introduced by the additional stratification (more model parameters relating to movement, recruitment, etc). The five-region model didn't yield significantly different results. Therefore, we recommend retaining the current four-region spatial structure for the future assessment.

However, the nature and extent of the dispersal of tagged fish remains as key uncertainty to the assessment. Fish may be fully mixed at a local scale but not at the regional scale. Violation of the assumption of homogeneous mixing of tagged fish at the relevant spatial scale will introduce bias into the estimation of fish abundance and other management quantities. IOTC has commenced a project that aims to evaluating potential stock assessments bias induced by the tag data due to the possibly non-random tag movement or distribution of fishing efforts. Results from that study can be used to improve the ways in which the tag data are modelled in the assessment.

The assessment explored an alternative temporal structure which permits the seasonal movement dynamics to be explicitly incorporated within the model. The annual/season model yielded broadly similar results to the model iterated on the quarterly time step. However, the seasonal pattern in migration rates estimated in the model was not able to explain the variability exhibited in the LL CPUE. Additional investigation by replacing the CPUE index with the index included in an early assessment (developed from the Japanese longline data alone) show some improvement, yet the model was still not able to fully capture the magnitude of the variations in the CPUE. This may indicate the variation in the CPUE may not contain sufficient information that would allow the model to elucidate seasonal migration pattern among regions. For example, the lowest catch rates generally occur in the third quarter in the tropical equatorial regions (R1b and R4), but these do not usually correspond to the high catch rates in the temperate region (R2 and R3) region the Temporal region. Relative longline CPUE in Region 1b tended to higher than Region 2 (CPUE R1/CPUE R2) in the second quarter, but the trend was reversed in recent years. In addition, the seasonality of the catches in the western temporal region are not consistent with the LL CPUE.

The uncertainty in model outputs include statistical uncertainty quantified from the covariance of the parameter estimation. The level of uncertainty in key management quantities is likely to be underestimated due to constraint of model assumptions especially on constant catchability, selectivity and the fixed biological parameters. Uncertainty associated with structural assumptions and model data can be characterised using the "grid approach" which explores the interactions among a suite of models on a combination of parameter values and model specifications (ISSF 2018). Due to the very large computational load of running the grid (each model requiring significant running time, typically 2-5 hours.), this approach was not attempted in the current assessment. The use of the grid 'approach' to quantify the structural uncertainty could be explored in future assessments of yellowfin tuna.

8. ACKNOWLEDGMENTS

We are grateful to the many people that contributed to the collection of this data historically, analysts involved in the CPUE standardization, and to Rick Methot, Ian Taylor and other developers for providing the SS3 software, for useful discussions on the various modelling options of the SS3 software.

9. REFERENCES

- Behringer, D. W., Xue, Y. 2004. Evaluation of the global ocean data assimilation system at NCEP: The Pacific Ocean. Eighth Symposium on Integrated Observing and Assimilation Systems for Atmosphere, Oceans, and Land Surface, AMS 84th Annual Meeting, Washington State Convention and Trade Center, Seattle, Washington, 11–15.
- Carruthers, T., Fonteneau, A. Hallier, J.P. 2015. Estimating tag reporting rates for the tropical fleets of the Indian Ocean. *Fisheries Research* 163 85–97.
- Chassot, E. 2014. Are there some small yellowfin tunas caught in free-swimming schools? IOTC-2014-WPDCS-10-INF05.
- Chassot, E., Dubroca, L., Delgado de Molina, A., Assan, C., Soto, M., Floch, L., Fonteneau, A. 2012. Decomposing purse seine CPUEs to estimate an abundance index for yellowfin free-swimming schools in the Indian Ocean during 1981–2011. IOTC-2012-WPTT-14-33.
- Chassot E, Assan C, Esparon J., Tirant A, Delgado d, Molina A, Dewals P, Augustin E, Bodin N. 2016. Length-weight relationships for tropical tunas caught with purse seine in the Indian Ocean: Update and lessons learned. IOTC-2016-WPDCS12-INF05.
- Dammannagoda, S.T., Hurwood, D.A., Mather, P.B. 2008. Evidence for fine geographical scale

- heterogeneity in gene frequencies in yellowfin tuna (*Thunnus albacares*) from the north Indian Ocean around Sri Lanka. *Fisheries Research* 90: 147–157.
- De Montaudoin, X., Hallier, J.P., Hassani, S. 1991. Length-weight relationships for yellowfin (*Thunnus albacares*) and skipjack (*Katsuwonus pelamis*) from Western Indian Ocean. ITPP Coll. Vol. Work. Doc. 4: 47–65.
- Dortel, E., Sardenne, F., Bousquet, N., Rivot, E., Million, J., Croizier, G. Le., Chassot, E. 2014. An integrated Bayesian modeling approach for the growth of Indian Ocean yellowfin tuna: Fish. Res. (2014), <http://dx.doi.org/10.1016/j.fishres.2014.07.00>.
- Eveson, P., Million, J., Sardenne, F., Le Croizier, G. 2012. Updated growth estimates for skipjack, yellowfin and bigeye tuna in the Indian Ocean using the most recent tag-recapture and otolith data. IOTC-2012-WPTT14-23.
- Edwards, C.T.T., DeBruyn, P., Million, J., Hillary, R.M. 2010. Updated analysis of 2006/07 RTTP-IO tagging data for Skipjack. IOTC-2010-WPTT-26.
- Francis, R.I.C.C. 1992. Use of risk analysis to assess fishery management strategies: a case study using orange roughy (*Hoplostethus atlanticus*) on the Chatham Rise, New Zealand. *Can. J. Fish. Aquat. Sci.* 49: 922–930.
- Francis, R.I.C.C. 2011. Data weighting in statistical fisheries stock assessment models. *Canadian Journal of Fisheries and Aquatic Sciences* 68: 1124–1138.
- Fonteneau, A. 2005. An overview of yellowfin (*Thunnus albacares*) tuna stocks fisheries and stock status worldwide. IOTC-2005-WPTT-21.
- Fonteneau, A. 2008. A working proposal for a Yellowfin growth curve to be used during the 2008 yellowfin stock assessment. IOTC-2008-WPTT-4.
- Fournier, D.A., Hampton, J., Sibert, J.R. 1998. MULTIFAN-CL: a length-based, age-structured model for fisheries stock assessment, with application to South Pacific albacore, *Thunnus alalunga*. *Can. J. Fish. Aquat. Sci.* 55: 2105–2116.
- Fu, D. 2017. Indian ocean skipjack tuna stock assessment 1950–2016 (stock synthesis). IOTC-2017–WPTT19–47_rev1.
- Carruthers, T., Fonteneau, A., Hallier, J. P. 2015. Estimating tag reporting rates for tropical tuna fleets of the Indian Ocean. *Fishery research* 2015. 163.
- Gaertner, D., Hallier, J.P. 2008. Tag Shedding by Tropical Tunas in the Indian Ocean: explanatory analyses and first results.
- Gaertner, D., Hallier, J.P. 2015. Tag shedding by tropical tunas in the Indian Ocean and other factors affecting the shedding rate. *Fisheries Research*. 2015/163.
- Gaertner, D., Chassot, E., Fonteneau, A., Hallier, J.P., Marsac, F. 2009. Estimate of the non-linear growth rate of yellowfin tuna (*Thunnus albacares*) in the Atlantic and in the Indian Ocean from tagging data. IOTC-2009-WPTT-17.
- Geehan, J., Setuadji, B. 2018. Revision to the IOTC scientific estimates of Indonesia's fresh longline catches. OTC-2018-WPB16-22.
- Greehan, J., Hoyle, S. 2013. Review of length frequency data of the Taiwanese distant water longline fleet. IOTC-2013-WPTT15-41.
- Geehan, J., Pierre, L., Herrera, M. 2013. Data revisions to nominal catch for IOTC species. Busan, Republic of Korea, 29–30 November 2013. IOTC–2013–WPDCS09–14.
- Hampton, J., Fournier, D.A. 2001. A spatially-disaggregated, length-based, age-structured population model of yellowfin tuna (*Thunnus albacares*) in the western and central Pacific Ocean. *Mar. Freshw. Res.* 52:937–963.
- Harley, S.J. 2011. Preliminary examination of steepness in tunas based on stock assessment results. WCPFC SC7 SA IP-8, Pohnpei, Federated States of Micronesia, 9–17 August 2011.
- Herrera, M., Peirre, L., Geehan, J., Million, J. 2012. Review of the statistical data and fishery trends for tropical tunas. IOTC-2012-WPTT14-07.
- Hillary, R.M., Million, J., Anganuzzi, A., Areso, J.J. 2008a. Tag shedding and reporting rate estimates for Indian Ocean tuna using double-tagging and tag-seeding experiments. IOTC-2008-WPTDA-04.
- Hillary, R.M., Million, J., Anganuzzi, A., Areso, J.J. 2008b. Reporting rate analyses for recaptures

- from Seychelles port for yellowfin, bigeye and skipjack tuna. IOTC-2008-WPTT-18.
- Hoenig, J.M. 1983. Empirical use of longevity data to estimate mortality rates. *Fishery Bulletin* 82: 898–903.
- Hoyle, S. 2012. Tagger effects – models to estimate tag loss and mortality for stock assessment. Indian Ocean Tuna Tagging Symposium, Grand Baie International Conference Centre, Royal Road, Grand Baie, MAURITIUS, 30 October – 2 November 2012.
- Hoyle, S.D., Langley, A. 2018. Indian Ocean tropical tuna regional scaling factors that allow for seasonality and cell areas. IOTC-2018-WPM09-13.
- Hoyle, S.D., Okamoto, H., Yeh, Y., Kim, Z., Lee, S.4 and Sharma, R. (2015) IOTC–CPUEWS–02 2015: Report of the Second IOTC CPUE Workshop on Longline Fisheries, April 30th–May 2nd, 2015. IOTC–2015–CPUEWS02–R[E]: 128pp.
- Hoyle, S.D., Kitakado, T., Matsumoto, T., Kim, D.N., Lee, S.I., Ku, J.E., Lee, M.K., Yeh, Y., Chang, S.T., Govinden, R., Lucas, J., Assan, C., Fu, D. 2017a. IOTC–CPUEWS–04 2017: Report of the Fourth IOTC CPUE Workshop on Longline Fisheries, July 3th–7th, 2017. IOTC–2017–CPUEWS04–R. 21 p.
- Hoyle, S.D., Satoh, K., Matsumoto, T. 2017b. Selectivity changes and spatial size patterns of bigeye and yellowfin tuna in the early years of the Japanese longline fishery. IOTC-2017-WPTT19-34.
- Hoyle, S.D., Kitakado, T., Yeh, Y.M., Wang, S.P., Wu, R.F., Chang, F.C., Matsumoto, T., Satoh, K., Kim, D.N., Lee, S.I., Chassot, E., and Fu, D. IOTC–CPUEWS–05 2018a: Report of the Fifth IOTC CPUE Workshop on Longline Fisheries, May 28th–June 1st, 2018. IOTC–2018–CPUEWS05–R. 27 pp.
- Hoyle, S.D., Chassot, E., Fu, D., Kim, D.N., Lee, S.I., Matsumoto, T., Satoh, K., Wang, S.P., Yeh, Y.M., Kitakado, T. 2018b. Collaborative study of yellowfin tuna CPUE from multiple Indian Ocean longline fleets in 2018. IOTC–2018–WPM09–12.
- Lan, K.W., Lee, M.A., Nishida, T., Lu, H.J., Weng, J.S., Chang, Y. 2012. Environmental effects on yellowfin tuna catch by the Taiwan longline fishery in the Arabian Sea, International Journal of Remote Sensing, 33:23, 7491–7506, DOI: 10.1080/01431161.2012.685971.
- Lorenzen, K. 1996. The relationship between body weight and natural mortality in juvenile and adult fish: a comparison of natural ecosystem and aquaculture. *Journal of Fish Biology*, 42:627–647.
- Itano, D.G. 2000. The reproductive biology of yellowfin tuna (*Thunnus albacares*) in Hawaiian waters and the western tropical Pacific Ocean: project summary. SOEST 00-01 JIMAR Contribution 00-328. Pelagic Fisheries Research Program, JIMAR, University of Hawaii.
- IOTC 2008a. Report of the First Session of the IOTC Working Party on Tagging Data Analysis, Seychelles, 30 June to 4 July 2008. IOTC-2008-WPTDA-R[E].
- IOTC 2008b. Report of the 10th session of the IOTC Working Party on Tropical Tunas, Bangkok, Thailand, 23 to 31 October 2008. IOTC-2008-WPTT-R[E].
- IOTC 2009. Report of the 11th session of the IOTC Working Party on Tropical Tunas, Mombasa, Kenya, 15–23 October 2009. IOTC-2009-WPTT-R[E].
- IOTC 2010. Report of the 12th session of the IOTC Working Party on Tropical Tunas, Victoria, Seychelles, 18–25 October 2010. IOTC-2010-WPTT-R[E].
- IOTC–SC18 2015. Report of the 18th Session of the IOTC Scientific Committee. Bali, Indonesia 23–27 November 2015. IOTC–2015–SC18–R[E]: 175 pp.
- IOTC–WPTT17 2015. Report of the 17th Session of the IOTC Working Party on Tropical Tunas. Montpellier, France, 23–28 October 2015. IOTC–2015–WPTT17R.
- IOTC-2017-WPTT19-DATA13 - Equations.pdf file
- ISSF 2018. Report of the 2018 ISSF Stock Assessment Workshop: Review of Current t-RFMO Practice in Stock Status Determinations. ISSF Technical Report 2018-15. International Seafood Sustainability Foundation, Washington, D.C., USA
- Katara, I., Gaertner, D., Marsac, F., Grande, M., Kaplan, D., Urtizberea, A., Guery, L., Depetris, M., Duparc, A., Floch, L., Lopez, J., Abascal, F. 2018 Standardisation of yellowfin tuna CPUE for the EU purse seine fleet operating in the Indian Ocean. IOTC–2018–WPTT20–36.
- Kleiber, P., Hampton, J., Fournier, D.A. 2003. MULTIFAN-CL Users' Guide. <http://www.multifan-cl.org/userguide.pdf>.

- Kolody, D. 2011. Can length-based selectivity explain the two stage growth curve observed in Indian Ocean YFT and BET. IOTC–2011–WPTT13–33.
- Kolody, D. 2018. Estimation of Indian Ocean Skipjack Purse Seine Catchability Trends from Bigeye and Yellowfin Assessments. IOTC–2018–WPTT20–xx.
- Kunal, S.P., Kumar, G., Menezes, M.R., Meena, R.M. (2013). Mitochondrial DNA analysis reveals three stocks of yellowfin tuna *Thunnus albacares* (Bonnaterre, 1788) in Indian waters. *Conserv Genet* (2013) 14:205–213.
- Langley, A. 2012. An investigation of the sensitivity of the Indian Ocean MFCL yellowfin tuna stock assessment to key model assumptions. IOTC-2012-WPTT-14-37.
- Langley, A. 2015. Stock assessment of yellowfin tuna in the Indian Ocean using Stock Synthesis. IOTC-2012-WPTT-17-30.
- Langley, A. 2016a. An update of the 2015 Indian Ocean Yellowfin Tuna stock assessment for 2016. IOTC-2016-WPTT18-27.
- Langley, A. 2016b. Stock assessment of bigeye tuna in the Indian Ocean for 2016 — model development and evaluation. IOTC-2016-WPTT18-20.
- Langley, A., Hampton, J., Kleiber, P., Hoyle, S. 2007. Stock assessment of yellowfin tuna in the western and central Pacific Ocean, including an analysis of management options. WCPFC SC3 SA WP-1, Honolulu, Hawai'i, 13–24 August 2007.
- Langley, A., Hampton, J., Herrera, M., Million, J. 2008. Preliminary stock assessment of yellowfin tuna in the Indian Ocean using MULTIFAN-CL. IOTC-2008-WPTT-10.
- Langley, A., Herrera, M., Hallier, J.P., Million, J. 2009. Stock assessment of yellowfin tuna in the Indian Ocean using MULTIFAN-CL. IOTC-2009-WPTT-11.
- Langley, A., Herrera, M., Million, J. 2010. Stock assessment of yellowfin tuna in the Indian Ocean using MULTIFAN-CL. IOTC-2010-WPTT-12.
- Langley, A., Herrera, M., Million, J. 2011. Stock assessment of yellowfin tuna in the Indian Ocean using MULTIFAN-CL. IOTC-2011-WPTT-13.
- Langley, A., Herrera, M., Million, J. 2012a. DRAFT Stock assessment of yellowfin tuna in the Indian Ocean using MULTIFAN-CL. IOTC-2012-WPTT-14-38.
- Langley, A., Herrera, M., Million, J. 2012b. Stock assessment of yellowfin tuna in the Indian Ocean using MULTIFAN-CL. IOTC-2012-WPTT-14-38.
- Langley, A., Million, J. 2012. Determining an appropriate tag mixing period for the Indian Ocean yellowfin tuna stock assessment. IOTC-2012-WPTT-14-31.
- McAllister, M.K.; Ianelli, J.N. 1997. Bayesian stock assessment using catch-at-age data and the sampling-importance resampling algorithm. *Can. J. Fish. Aquat. Sci.* 54: 284–300.
- McKechnie, S., Pilling, G., Hampton, J. 2017. Stock assessment of bigeye tuna in the western and central Pacific Ocean. WCPFC-SC13-2017/SA-WP-05 Rev1
- Matsumoto, T. 2012. Japanese longline CPUE for yellowfin tuna in the Indian Ocean up to 2011 standardized by general linear model. IOTC-2012-WPTT14-35.
- Maunder, M.N., Aires-da-Silva, A. 2012. A review and evaluation of natural mortality for the assessment and management of yellowfin tuna in the eastern Pacific Ocean. External review of IATTC yellowfin tuna assessment. La Jolla, California. 15–19 October 2012. Document YFT-01-07.
- Maunder, M.N., Watters, G.M. 2001. A-SCALA: An age-structured statistical catch-at-length analysis for assessing tuna stocks in the eastern Pacific Ocean. Background Paper A24, 2nd meeting of the Scientific Working Group, Inter-American Tropical Tuna Commission, 30 April – 4 May 2001, La Jolla, California.
- Marsac, F. 2012. Outline of climate and oceanographic conditions in the Indian Ocean over the period 2002–2012. IOTC-2012-WPTT14-9.
- Methot, R.D. 2013. User manual for Stock Synthesis, model version 3.24f.
- Methot, R.D., Wetzel, C.R. 2013. Stock synthesis: A biological and statistical framework for fish

- stock assessment and fishery management. *Fisheries Research* 142 (2013) 86–99.
- Minte-Vera, C.V., Aires-da-Silva, Alexandre, Maunder., M. N. 2016. Status of yellowfin tuna in the eastern pacific ocean in 2016 and outlook for the future. SAR-18-2-YFT-assessment-2016. IATTC.
- Nishida, T., Shono, H. 2005. Stock assessment of yellowfin tuna (*Thunnus albacares*) resources in the Indian Ocean by the age structured production model (ASPM) analyses. IOTC-2005-WPTT-09.
- Nishida, T., Shono, H. 2007. Stock assessment of yellowfin tuna (*Thunnus albacares*) in the Indian Ocean by the age structured production model (ASPM) analyses. IOTC-2007-WPTT-12.
- Ochi, D. et al 2015. Japanese longline CPUE for yellowfin tuna in the Indian Ocean up to 2014 standardized by general linear model. IOTC-2015-WPTT17-XX.
- Suzuki, Z. 1993. A review of the biology and fisheries for yellowfin tuna (*Thunnus albacares*) in the western and central Pacific Ocean. In Shomura, R.S.; Majkowski, J.; Langi S. (eds). Interactions of Pacific tuna fisheries. Proceedings of the first FAO Expert Consultation on Interactions of Pacific Tuna Fisheries. 3–11 December 1991. Noumea, New Caledonia. Volume 2: papers on biology and fisheries. FAO Fisheries Technical Paper. No. 336, Vol.2. Rome, FAO. 1993. 439p.
- Satoh, K. 2014. Exploration of area stratification for CPUE standardization of yellowfin tuna by Japanese longline. IOTC-2014-WPTT16-48.
- Yeh, Y.M., Chang, S.T. 2012. CPUE standardizations for yellowfin tuna caught by Taiwanese longline fishery in the Indian Ocean using generalized liner model. IOTC-2012-WPTT14-36.
- Yeh, Y.M., Hoyle, S. Chang, S.T. Updated CPUE standardizations for bigeye and yellowfin tuna caught by Taiwanese longline fishery in the Indian Ocean using generalized linear model. IOTC-2018-WPTT20-35.
- Zudair, I., Murua, H., Grande, M., Bodin, N. 2013. Reproductive potential of yellowfin tuna (*Thunnus albacares*) in the western Indian Ocean. *Fish. Bull.* 111:252–264.

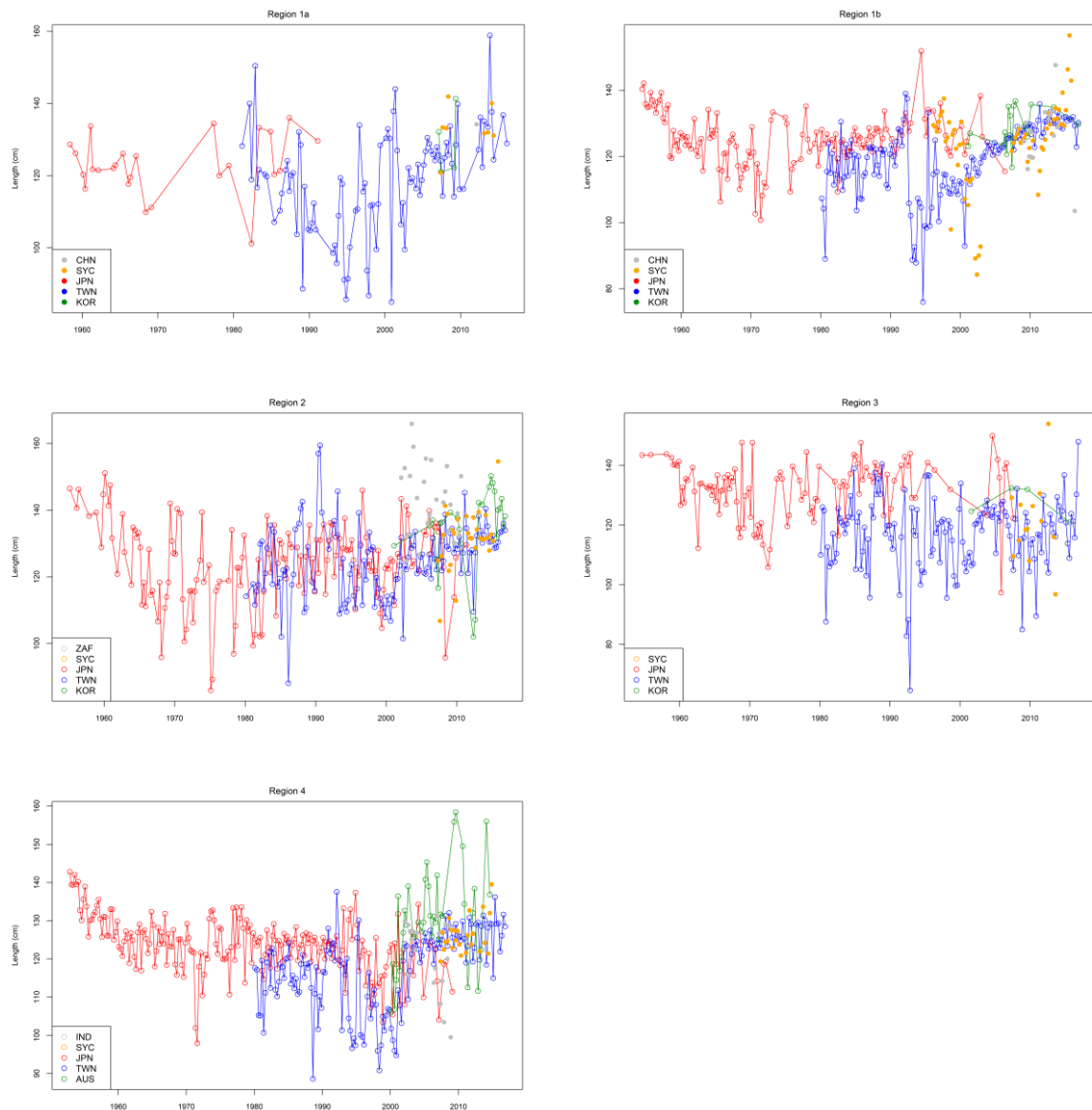
APPENDIX A: ADDITIONAL PLOTS OF LONGLINE LENGTH COMPOSITION DATA

Figure A1: Average length of yellowfin tuna (FL, cm) of fish sampled from the longline fishery in region 1a, 1b, 2, 3, and 4, by fleet nationality and year/quarter.

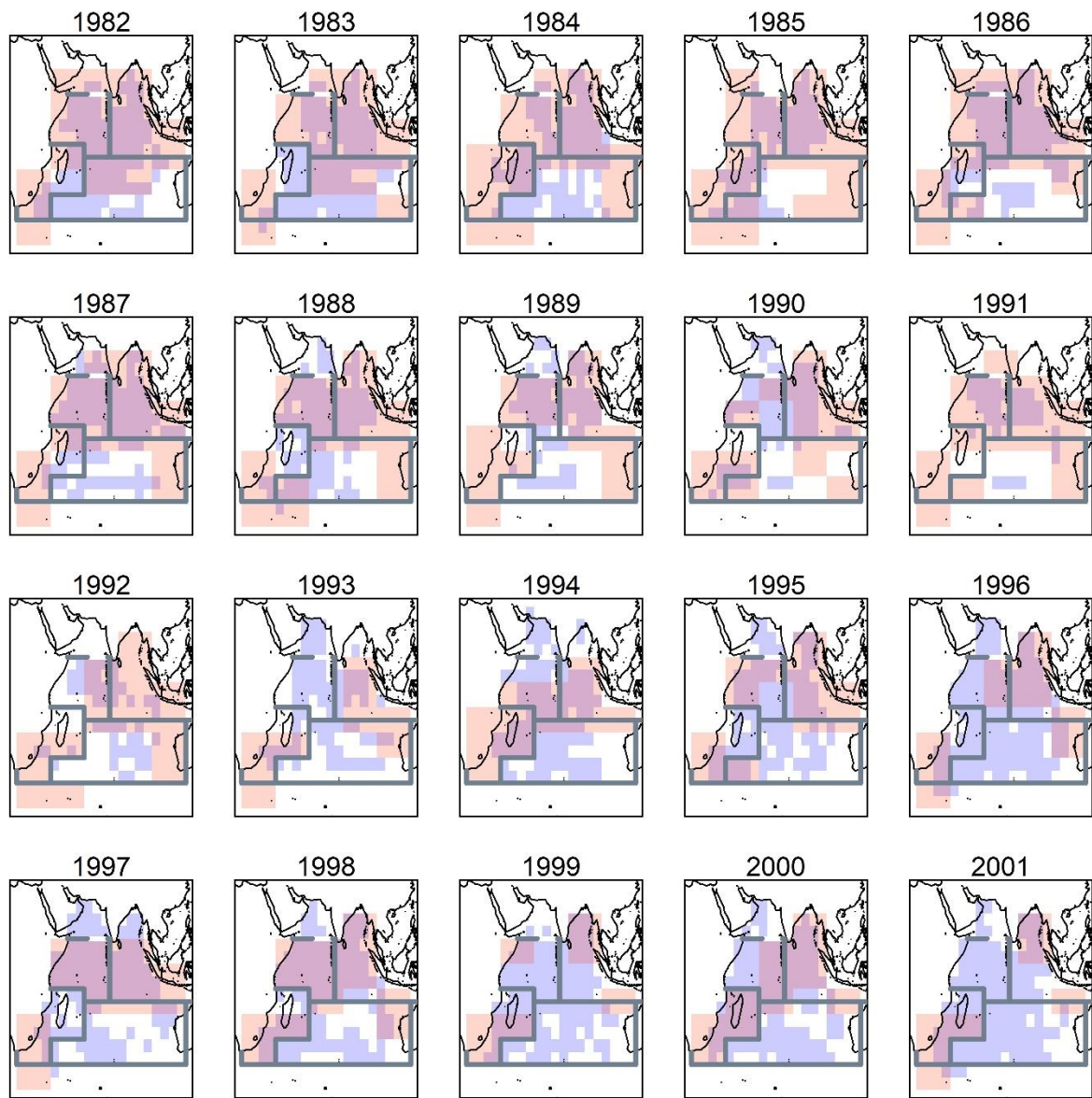


Figure A2: Spatial distribution of length composition samples of yellowfin tuna collected by Japanese and Taiwanese Fleet between 1983 and 2002. The Japanese data were reported by 10 by 20 latitude and longitude (red), and the Taiwanese samples were reported by 5 by 5 latitude and longitude (blue).

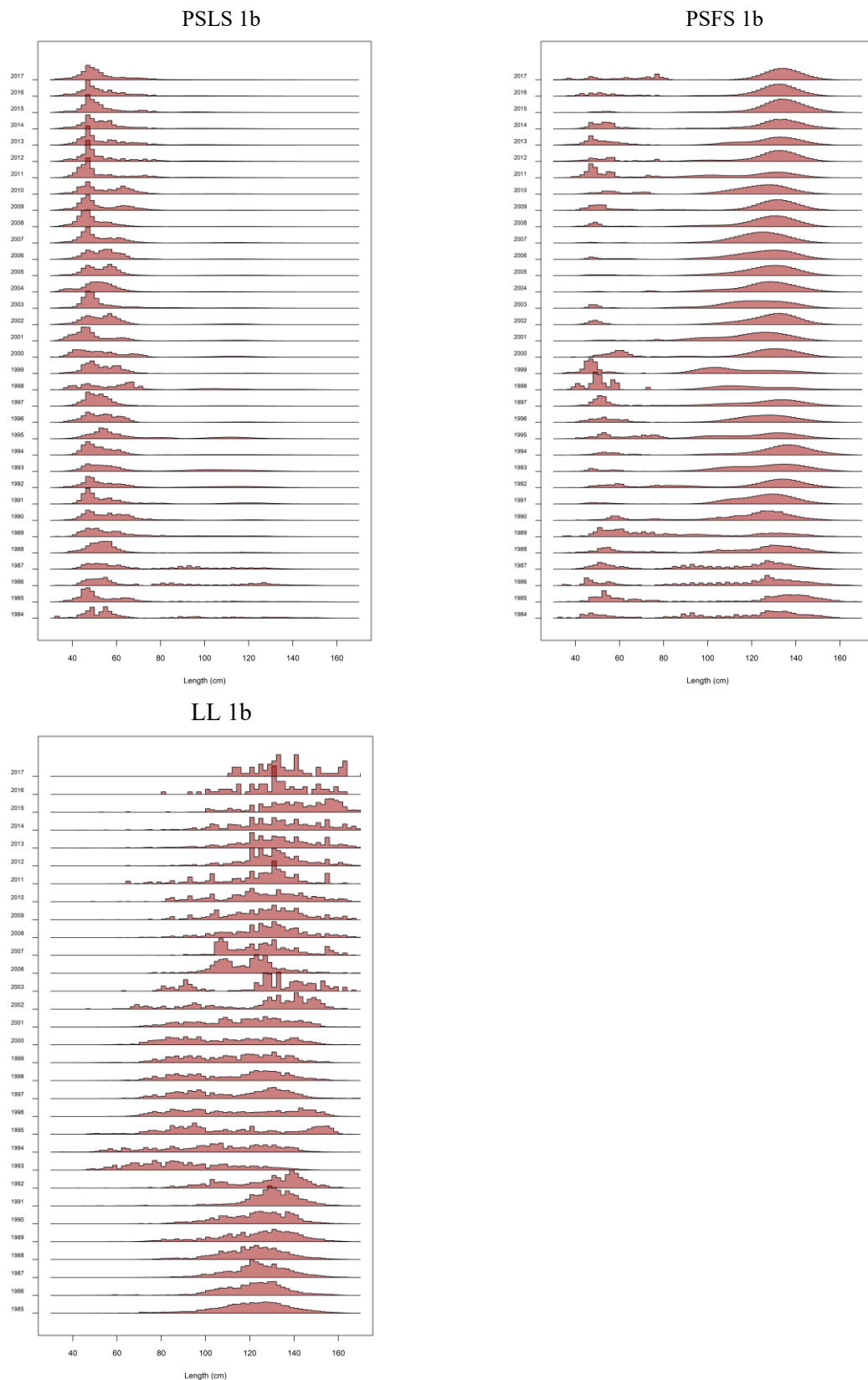


Figure A3: time series of size distribution from the purse seine sets on associated schools (PSLS), free schools (PSFS), and the longline fishery in the western equatorial regions (region 1b).

APPENDIX B: ANALYSIS OF TAG RECAPTURE DATA FROM THE RTTP-IO PROGRAM

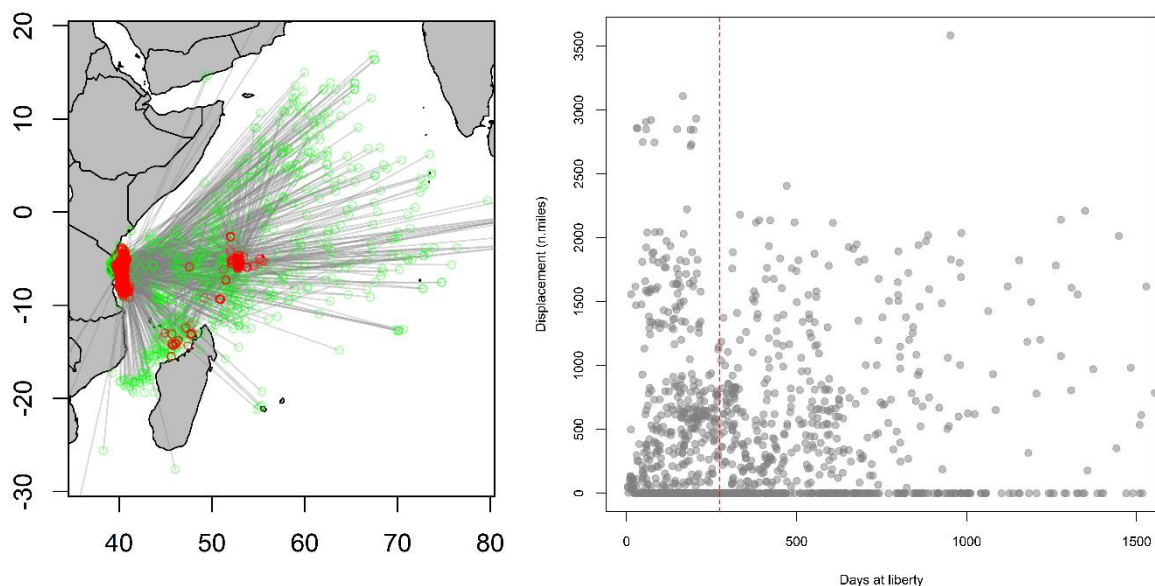


Figure B1. Net movement of tags between release and recapture (left) and displacement vs. days at liberty for a subset of tag recaptures from the RTTP-IO program. Only tag recaptures that have different (directional) bearing (and maximum net displacement for those of the same bearing) are included. Red circles indicate releases and green circles indicate recaptures.

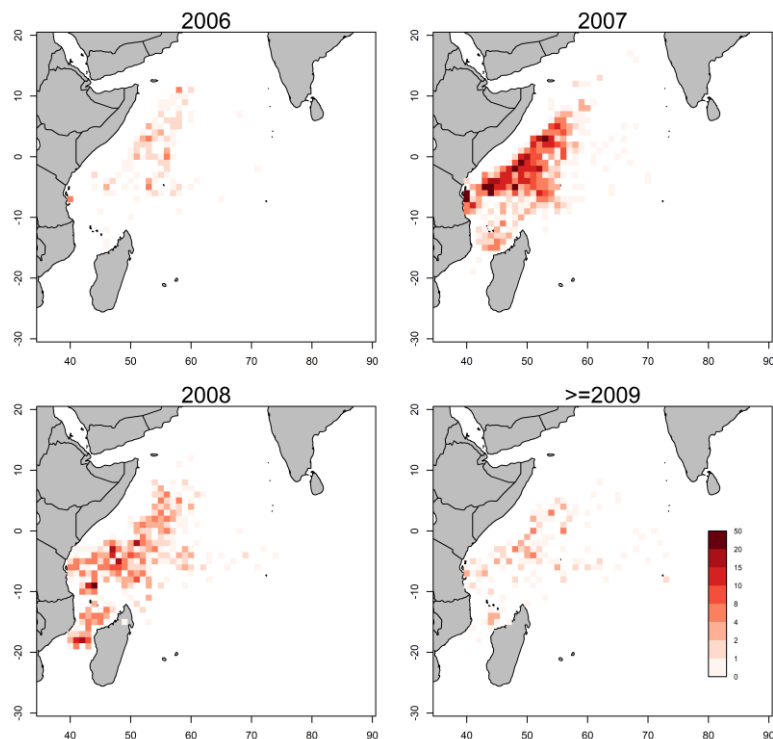


Figure B2: Spatial distribution (1 degree cell) of number of yellowfin RTTP tag recoveries of fish at liberty for at least 3 quarters, from the purse seine fisheries in the western tropical region.

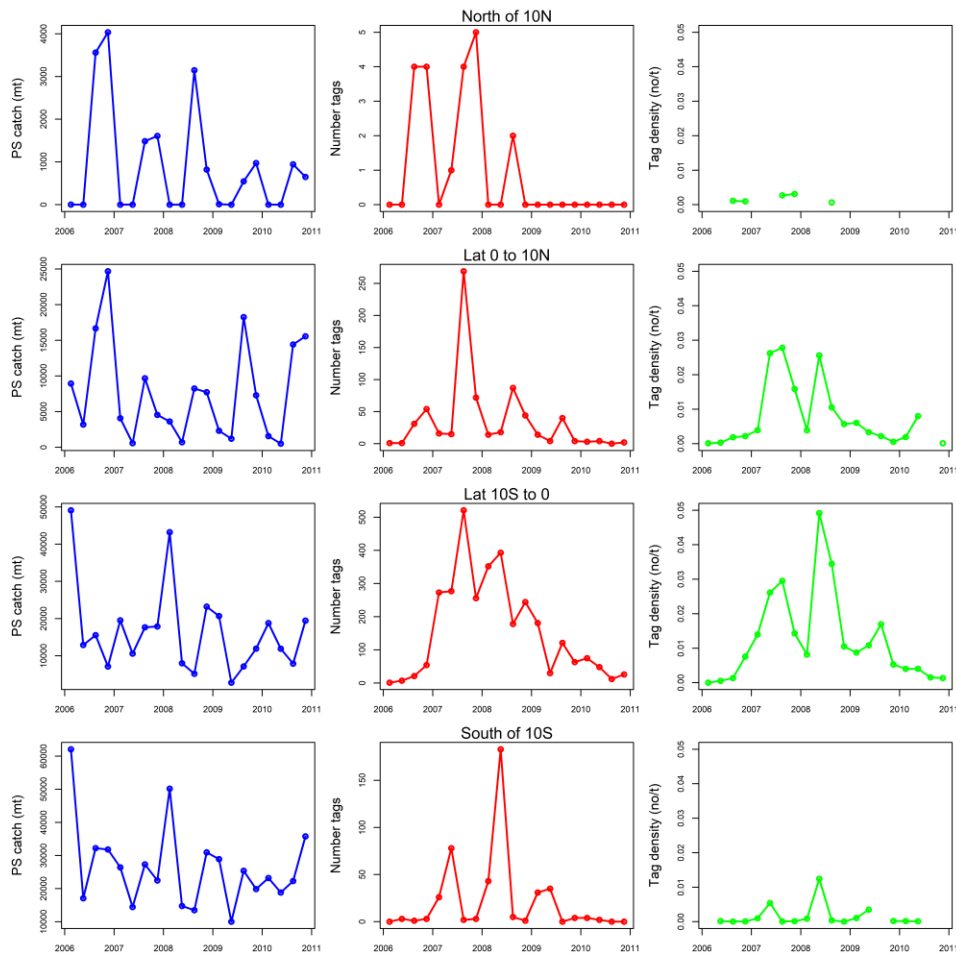


Figure B3: Quarterly yellowfin tuna catch (t) and number of tags recovered by the purse seine fishery in region 1 by latitudinal band. Only tags at liberty for at least 3 quarter mixing periods are included. The tag recovery density (tags/catch) is also presented for each latitudinal band.

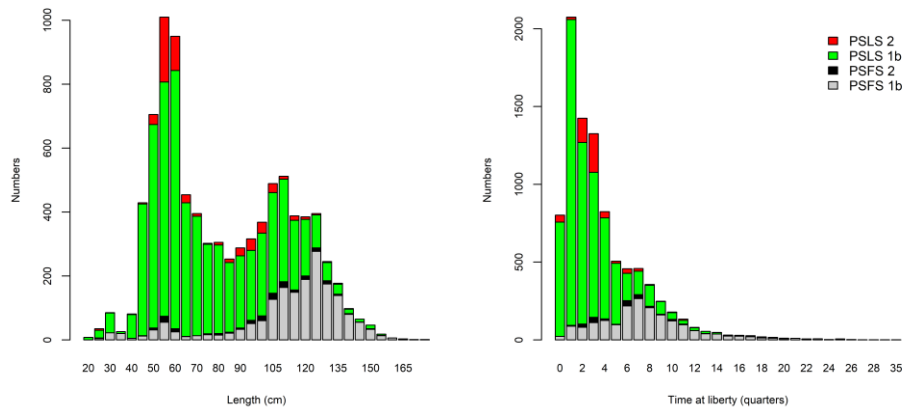


Figure B4: Distribution of yellowfin tag recoveries by length (left) and by time-at-liberty (right) for the purse seine free school and purse sein FAD schools in region 1b and 2. Purse seine tag recoveries have been corrected for reporting rate.

APPENDIX C: RESULTS FROM THE EXPLORATORY MODELLING

Table A1. Maximum Posterior Density (MPD) estimates of the main stock status indicators from the exploratory model option.

	<i>SB₀</i>	<i>SB_{MSY}</i>	<i>SB_{MSY}/SB₀</i>	<i>SB₂₀₁₇</i>	<i>SB₂₀₁₇/SB₀</i>	<i>SB₂₀₁₇/SB_{MSY}</i>	<i>F₂₀₁₇/F_{MSY}</i>	<i>MSY</i>
eRevised2018	2,706,490	931,111	0.34	811,632	0.30	0.87	1.27	399,018
e7594m8	2,727,820	946,665	0.35	829,346	0.30	0.88	1.25	401,436
e8000m8	2,672,020	934,931	0.35	795,391	0.30	0.85	1.30	403,456
eMlow	3,968,280	1,354,480	0.34	799,634	0.20	0.59	2.32	331,446
eMlorenzen	2,581,150	816,958	0.32	715,639	0.28	0.88	1.30	386,019
eGrowthDortel	2,458,640	839,812	0.34	597,878	0.24	0.71	1.77	353,975
eTwosex	1,200,040	414,038	0.35	358,606	0.30	0.87	1.30	393,465
eMaturityLogistic	2,693,050	917,615	0.34	816,732	0.30	0.89	1.19	391,610
eTagALK	2,609,440	915,893	0.35	749,822	0.29	0.82	1.40	394,769
eTagNewProc	2,755,860	954,062	0.35	844,366	0.31	0.89	1.22	408,112
eSelPSregion	2,702,950	962,799	0.36	769,564	0.28	0.80	1.38	401,980
eSelTimeVarying	2,902,580	1,030,610	0.36	871,537	0.30	0.85	1.23	396,660
eRegion5	2,864,490	1,060,900	0.37	937,074	0.33	0.88	1.21	381,354
eYearSeason	2,311,260	756,347	0.33	637,720	0.28	0.84	1.29	415,222

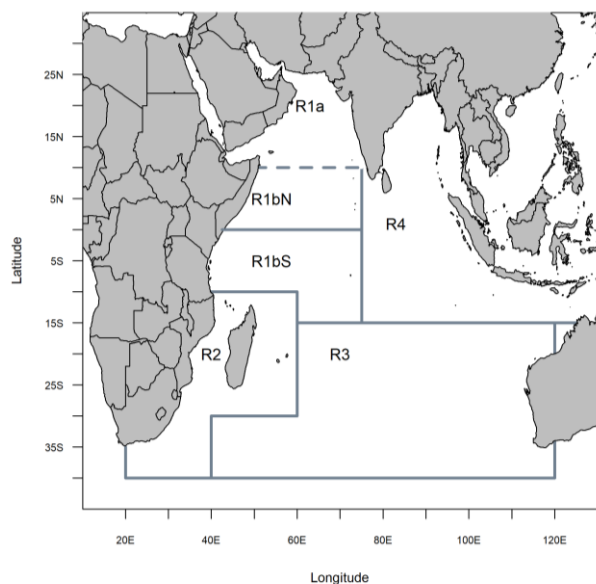


Figure C1: Alternative spatial stratification of the Indian Ocean for the exploratory five-region model sensitivity.

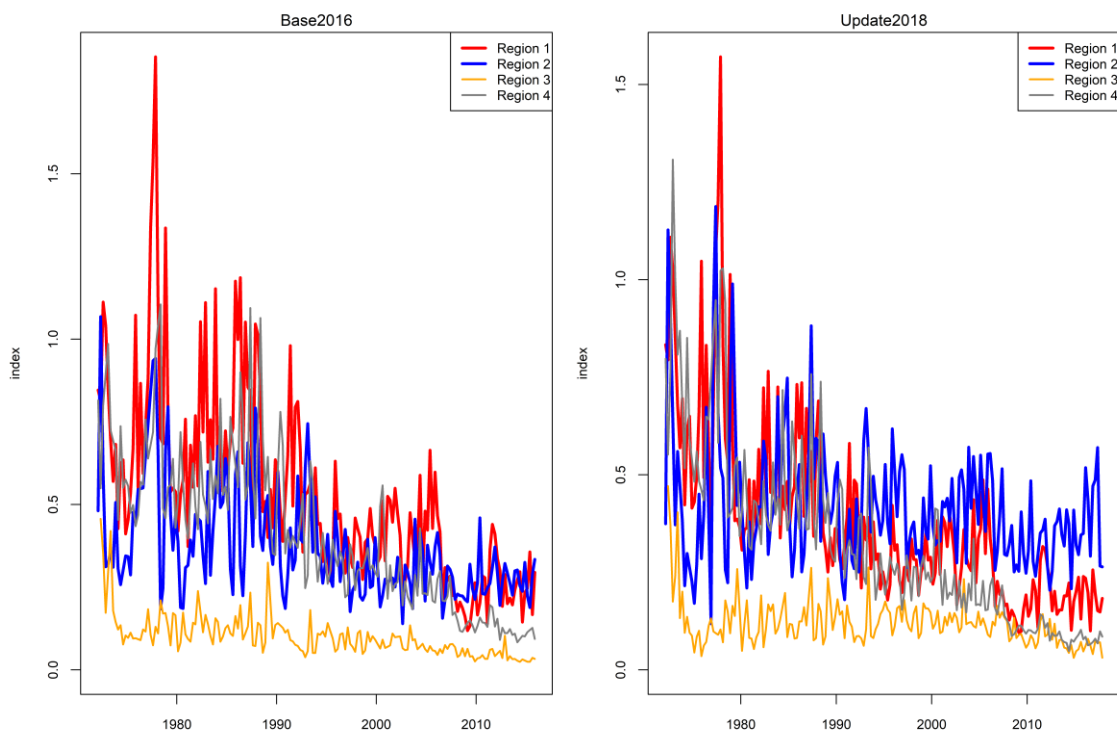


Figure C2: A comparison of regional CPUE indices between the 2016 base case and the ‘Update2018’ model. CPUE indices from both models were weighted by the regional scaling factors used for the 2016 assessment.

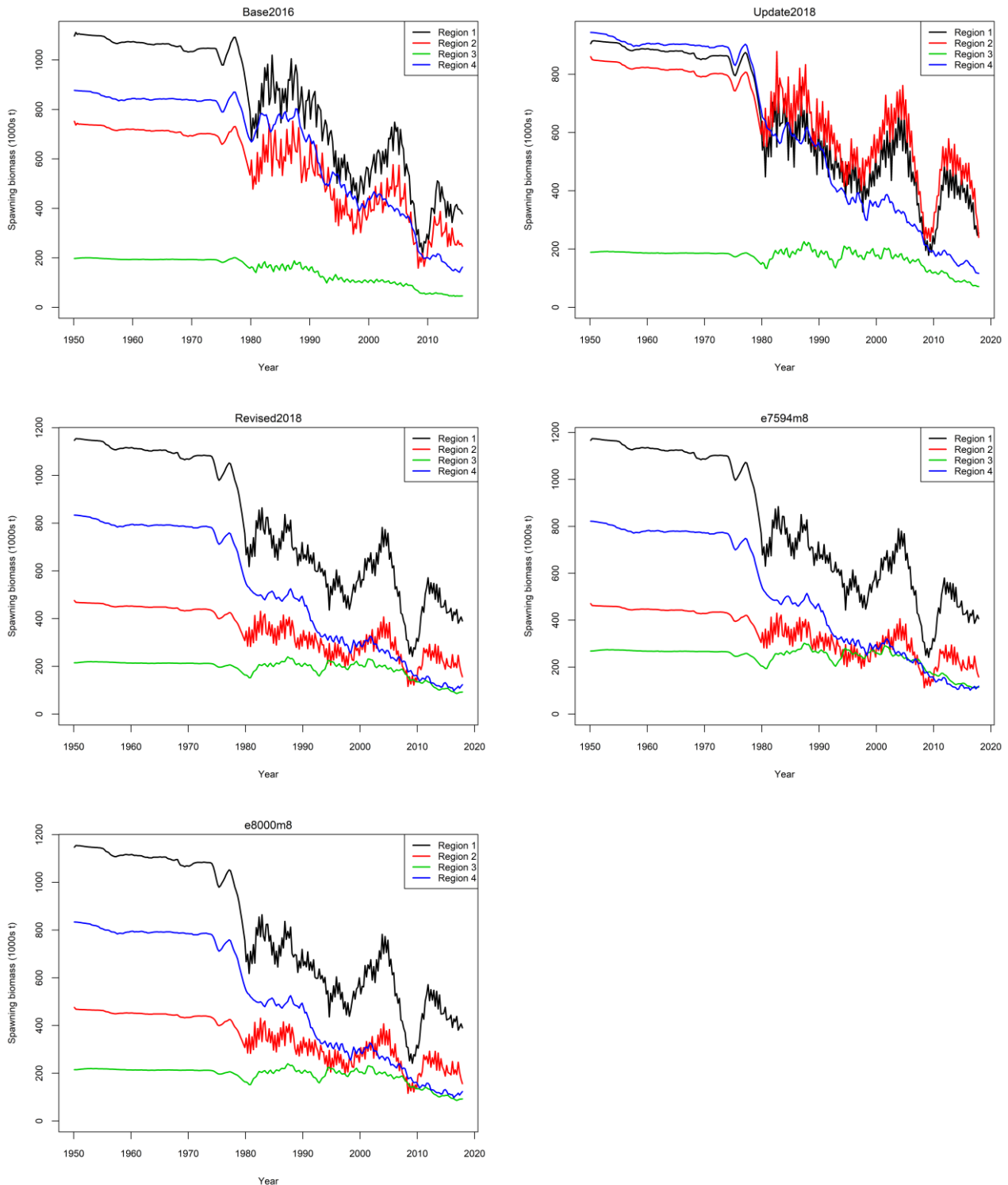


Figure C3: Regional spawning biomass trajectories from the exploratory revised model and a range of exploratory model sensitivities related to regional weighting assumptions.

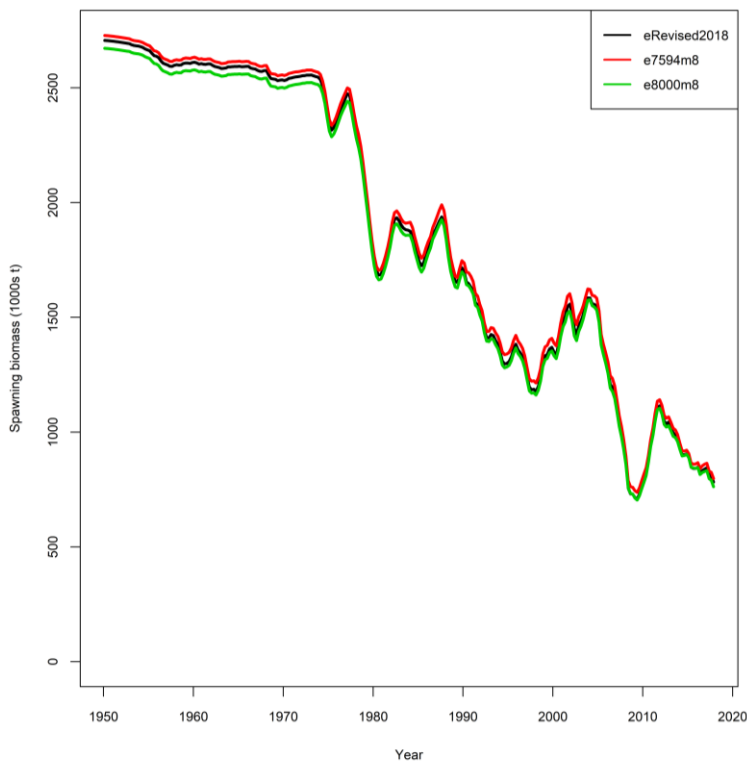


Figure C4: Spawning biomass trajectories from the exploratory revised model and a range of exploratory model sensitivities related to regional weighting assumptions.

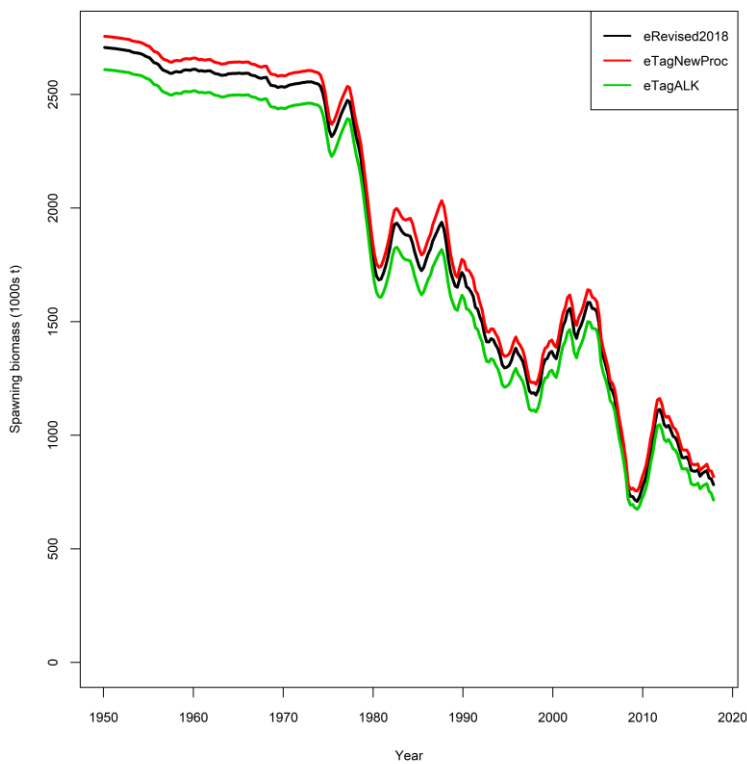


Figure C5: Spawning biomass trajectories from the exploratory revised model and a range of exploratory model sensitivities related to alternative approaches to process tagging data

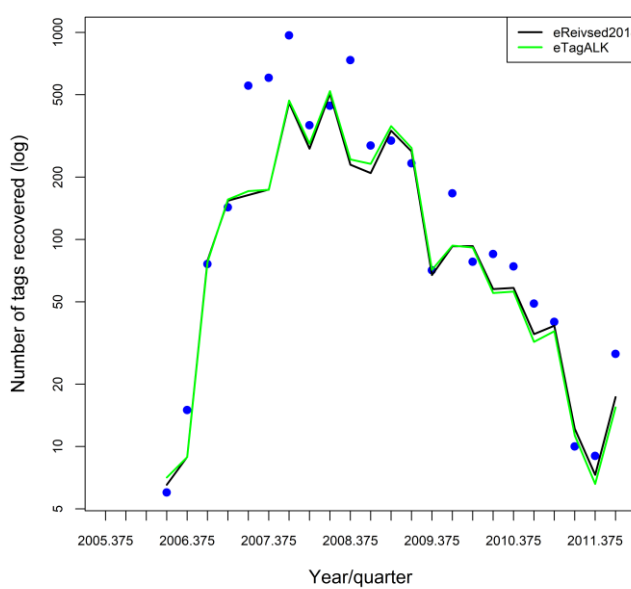


Figure C6: A comparison of the fits to the tag recoveries for the exploratory revised model and the model using the age-length-key approach to assign age to tag-at-release (*eTagALK*). The dots are observed tag recoveries and the lines are model predictions. Only tags at liberty after the three-quarter mixing period are included. Tag recoveries are aggregated for all fisheries.

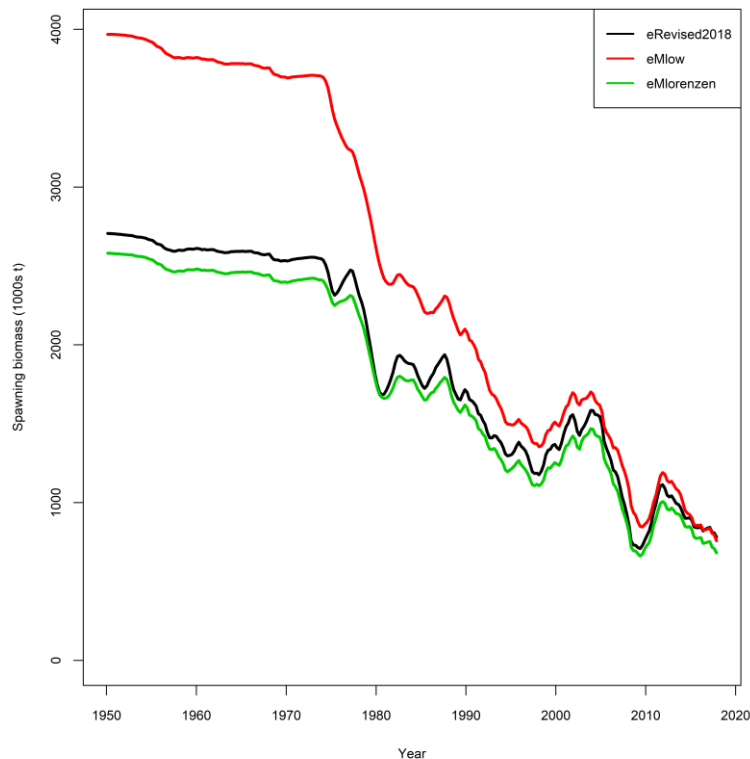


Figure C7: Spawning biomass trajectories from the exploratory revised model and a range of exploratory model sensitivities related to natural mortality assumptions.

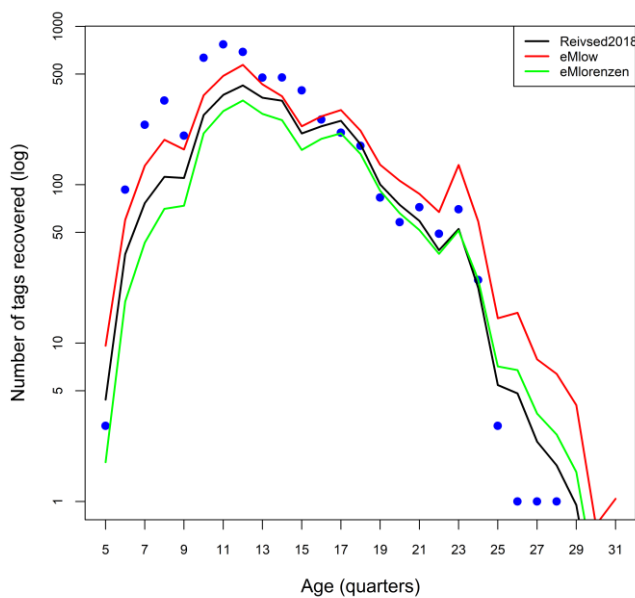


Figure C8: A comparison of the fits to the tag recoveries for the exploratory revised model and exploratory sensitivity models related assumptions on natural mortality. The dots are observed tag recoveries and the lines are model predictions (in log scale). Only tags at liberty after the three-quarter mixing period are included. Tag recoveries are aggregated for all fisheries.

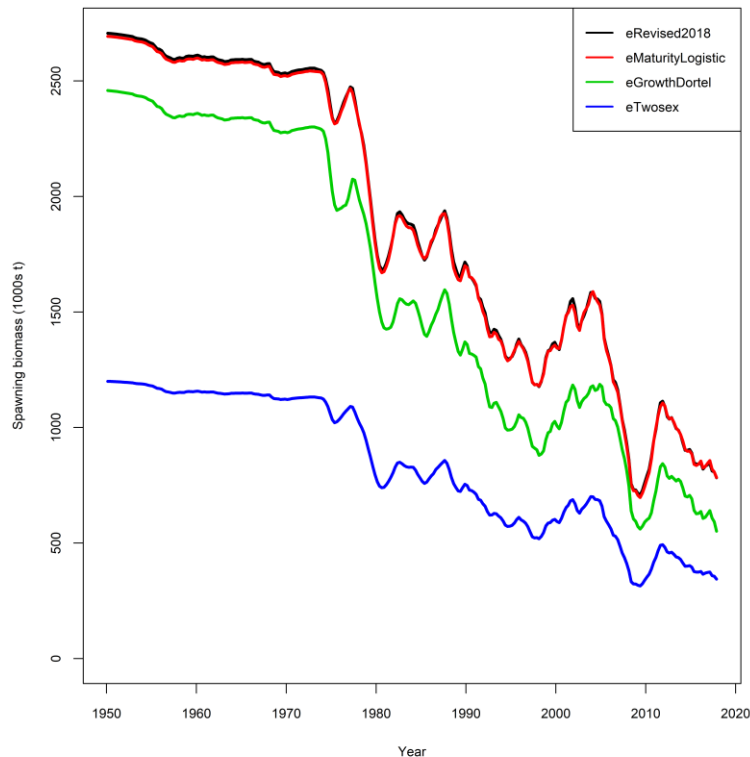


Figure C9: Spawning biomass trajectories from the exploratory revised model and a range of exploratory model sensitivities related to biological parameter assumptions.

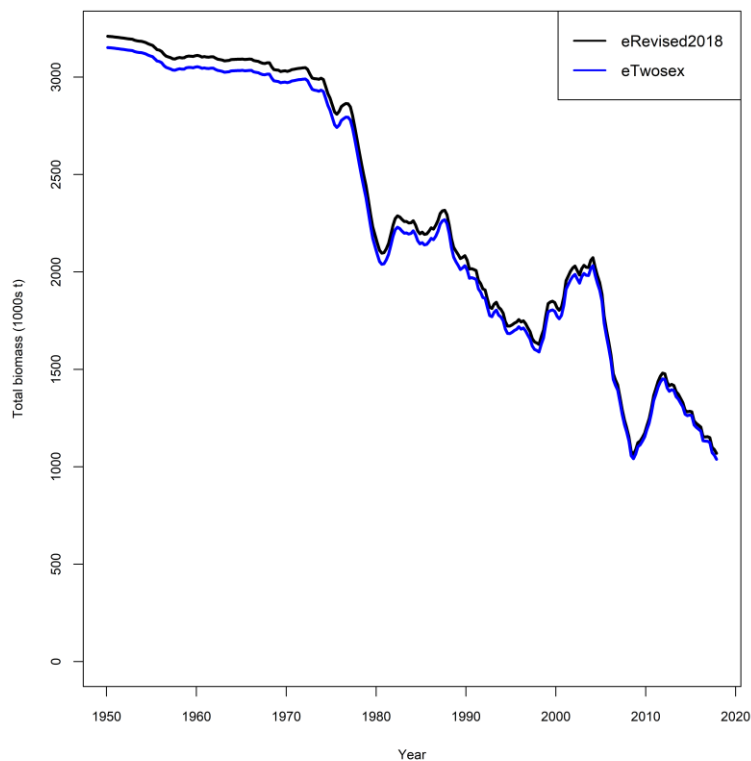


Figure C10: Total biomass trajectories from the exploratory revised model and the exploratory two-sex model (*eTwosex*).

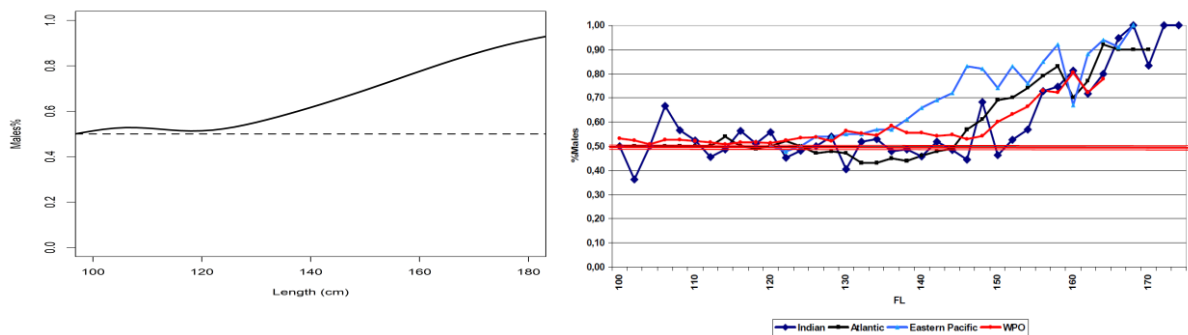


Figure C11: Estimated sex ratio (%males) at size of yellowfin from the exploratory two-sex model (left), and the average sex ratio observed on purse seiners in various oceans (Fonteneau 2005).

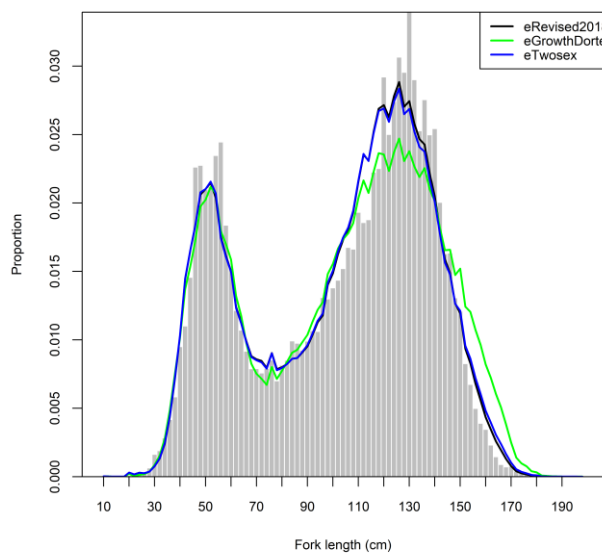


Figure C11: A comparison of the fits to the size composition data (aggregated for all fisheries and all years) between the exploratory revised model and exploratory sensitivities related to biological parameters.

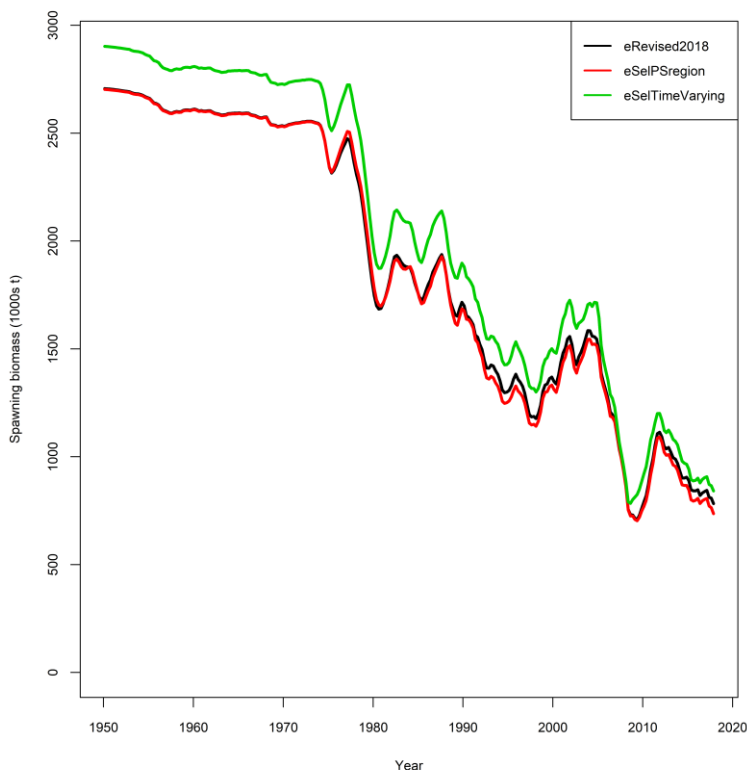


Figure C13: Spawning biomass trajectories from the exploratory revised model and exploratory model sensitivities related to fishery selectivity assumptions

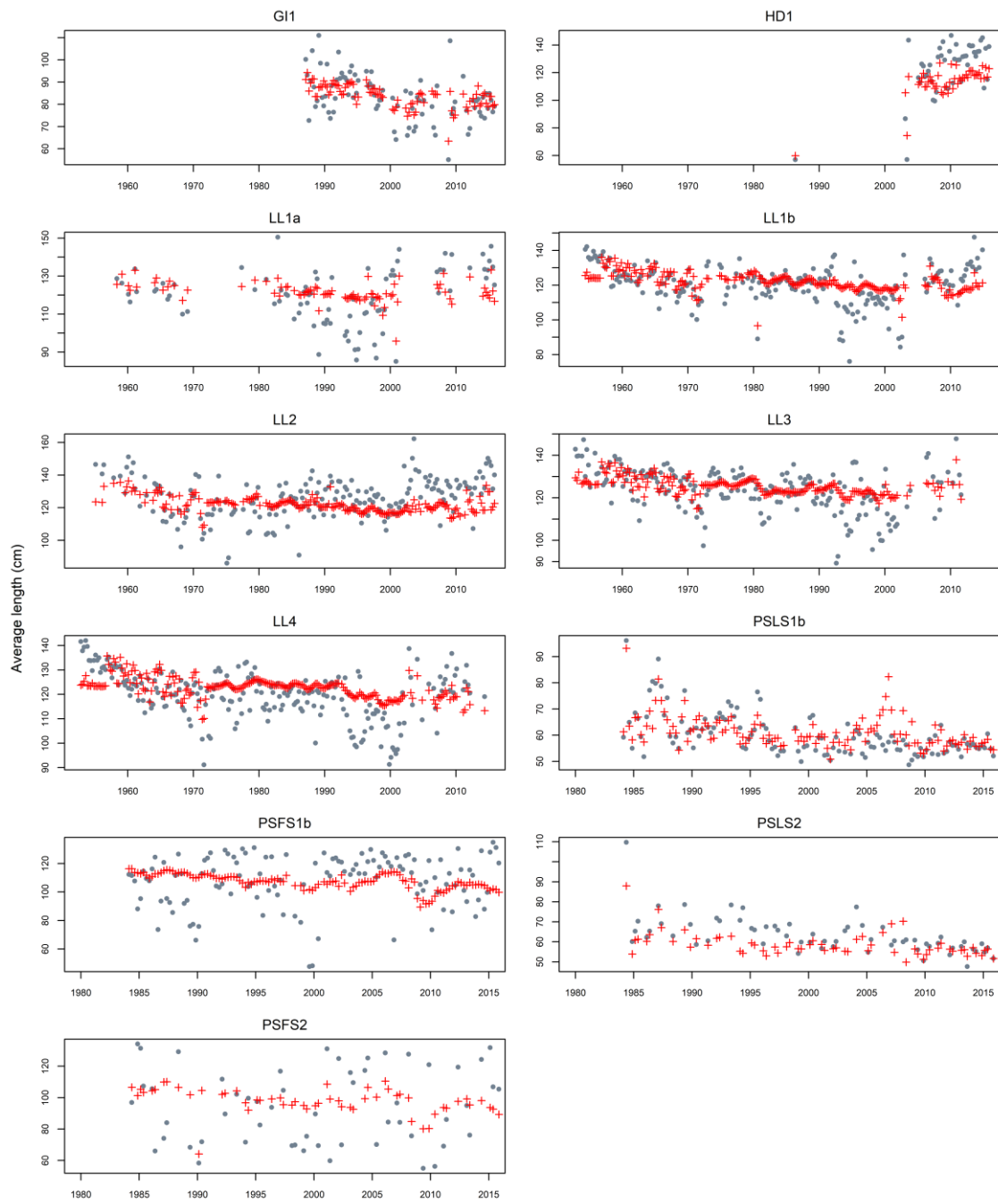


Figure C14: observed (grey points) and predicted (red points and line) average fish length (FL, cm) of yellowfin tuna by fishery for some of the main fisheries from the exploratory sensitivity model (*eSelTimeVarying*) using time-varying selectivities for these fisheries.

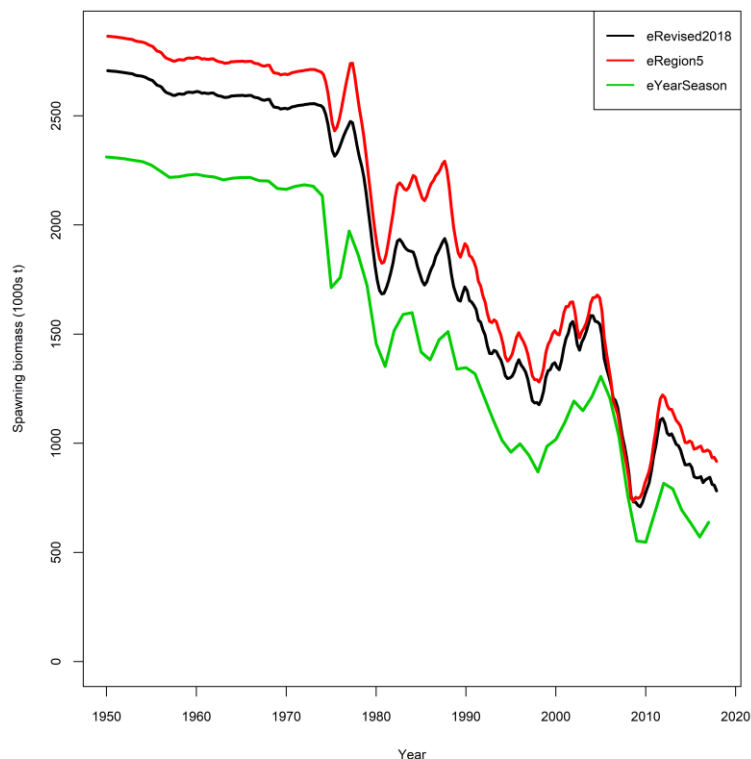


Figure C15: Spawning biomass trajectories from the exploratory revised model and exploratory model sensitivities related to spatial and temporal structure assumptions

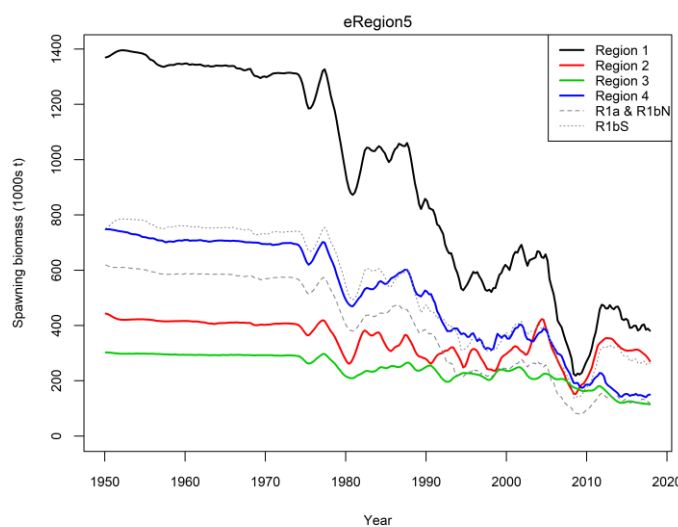


Figure C16: Regional spawning biomass trajectories from the exploratory five-region model (*eRegion5*). NOTE that the biomass was summarized for regions from the four-region structure (e.g. R1 includes R1a, R1bN, and R1bS).

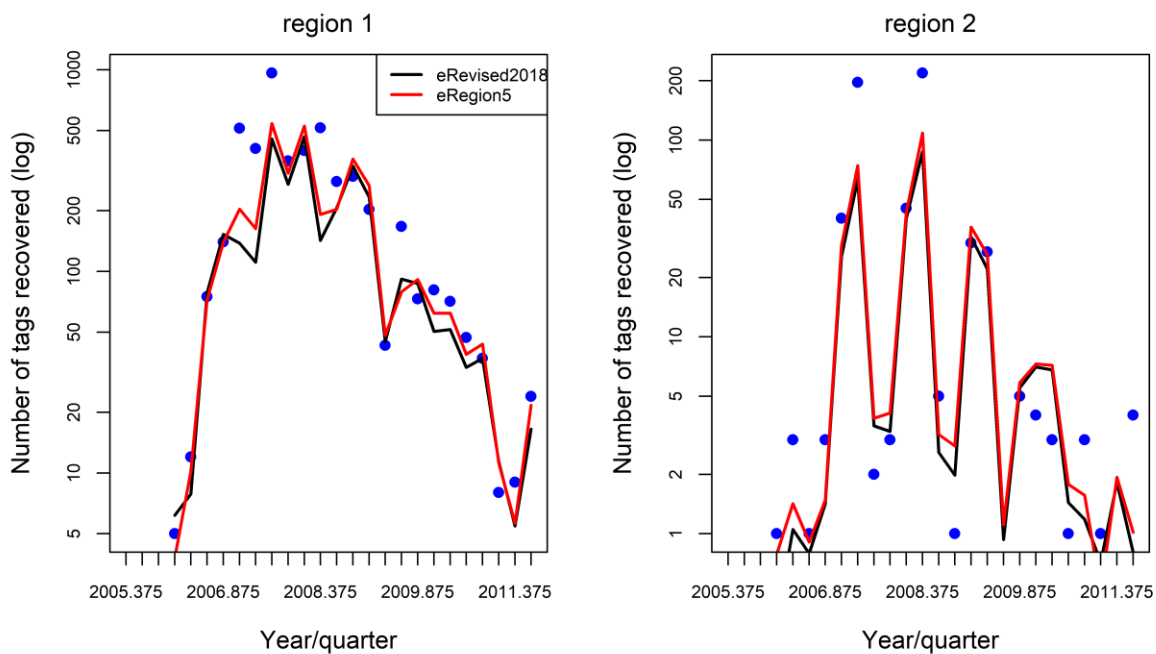


Figure C17: A comparison of the fits to the tag recoveries by region for the exploratory revised model and exploratory sensitivity using the year-season temporal structure (*eRegion5*). The dots are observed tag recoveries and the lines are model predictions (in log scale). Only tags at liberty after the three-quarter mixing period are included. Tag recoveries are aggregated for all fisheries in each region.

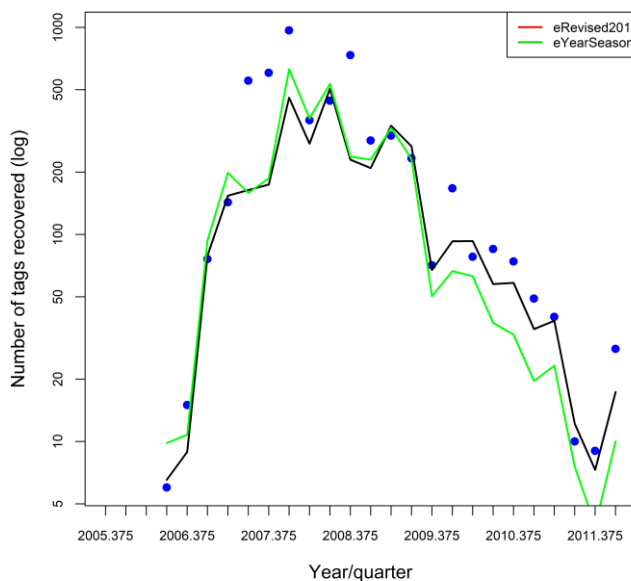


Figure C18: A comparison of the fits to the tag recoveries for the exploratory revised model and exploratory sensitivity using the year-season temporal structure (*eYearSeason*). The dots are observed tag recoveries and the lines are model predictions (in log scale). Only tags at liberty after the three-quarter mixing period are included. Tag recoveries are aggregated for all fisheries.

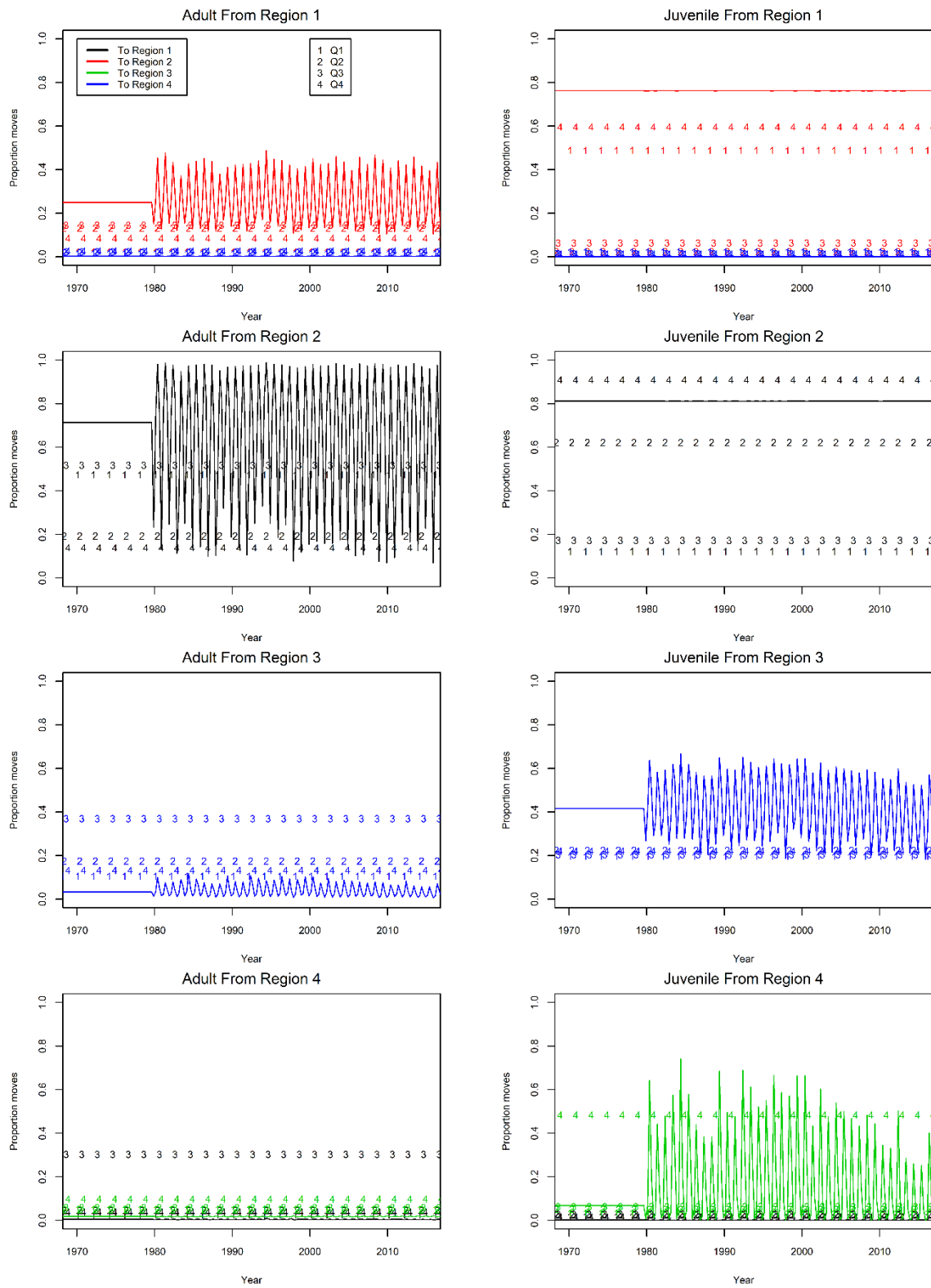


Figure C19: A comparison of quarterly movement coefficients between the exploratory revised model and the exploratory sensitivity using the year-season temporal structure (*eYearSeason*). The coefficients were estimated for each quarter separately (shown as numbers) for the latter model.

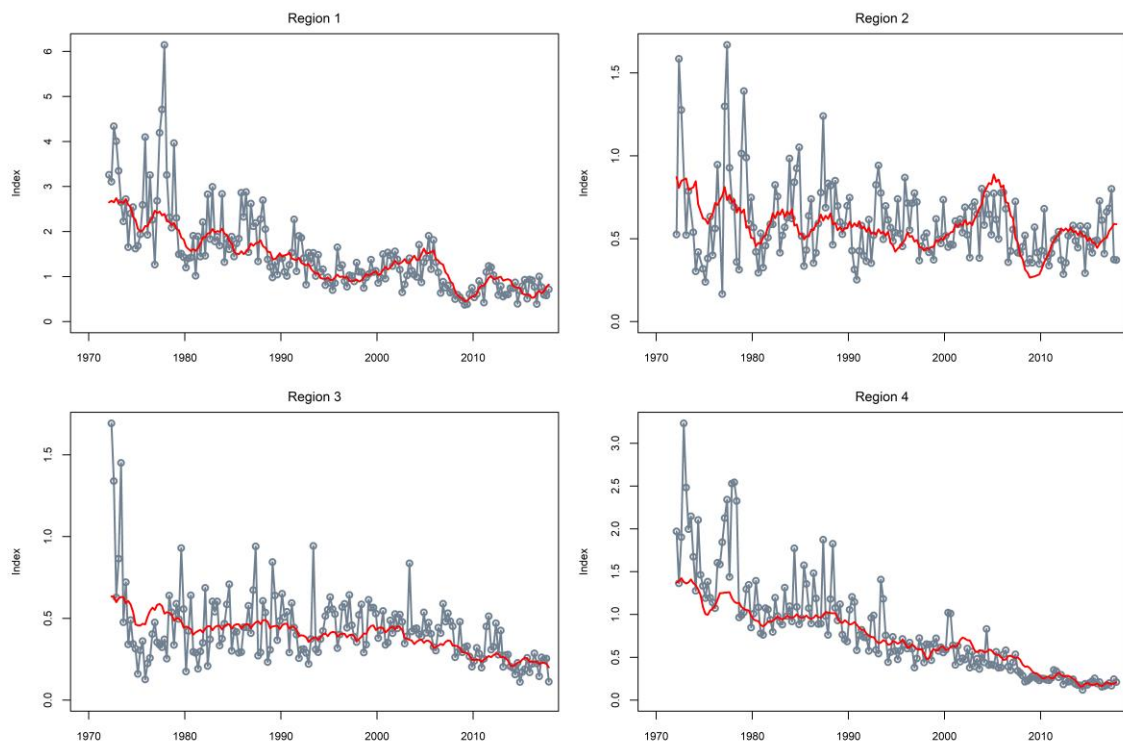


Figure C20: Fits to the regional LL CPUE indices from the exploratory sensitivity using the year-season temporal structure (*eYearSeason*).

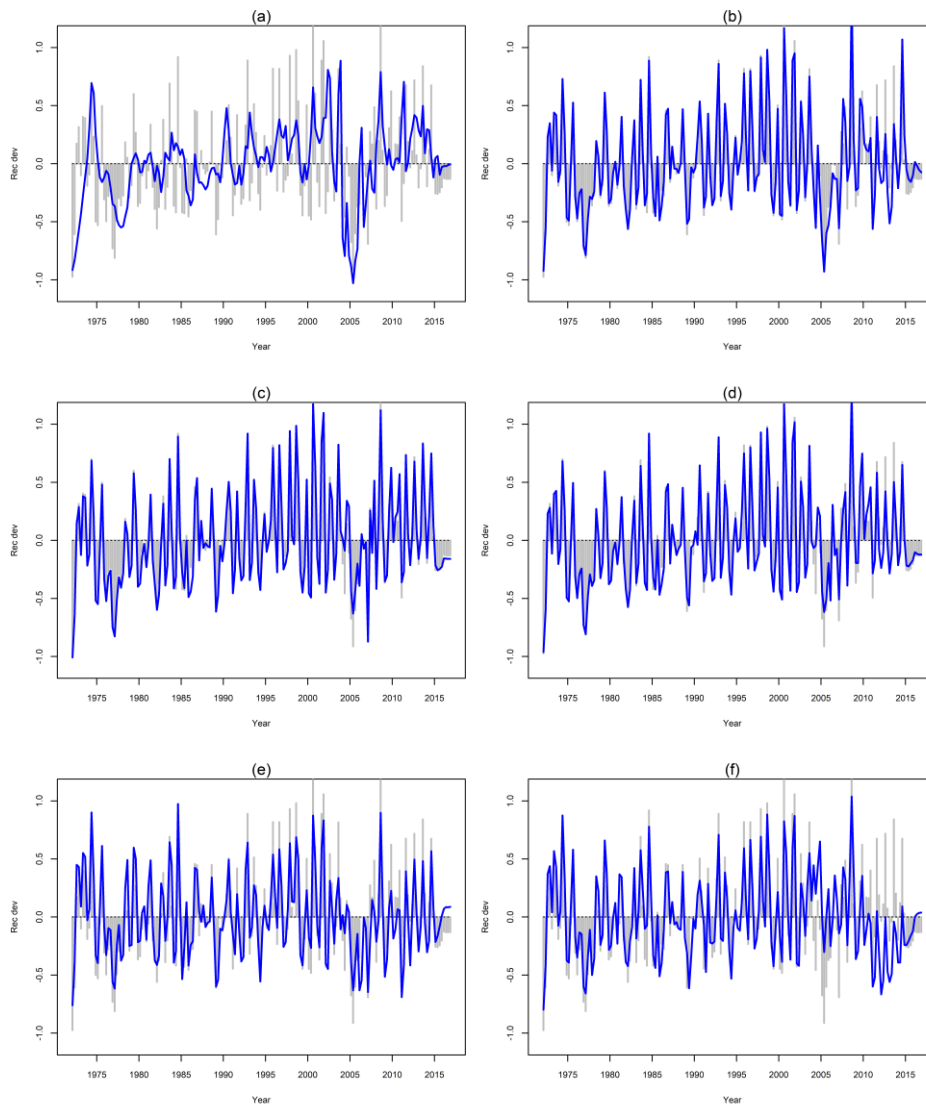


Figure C22: Recruitment deviation estimates from the exploratory revised model with some observations excluded (blue), overlaid with the original estimates (grey): (a) size composition data, (b) LL CPUE indices from the late 2000s for region 1 and 2, (c) LL CPUE indices from the late 2000s for region 3 and 4, (d) LL CPUE indices from the late 2000s for all regions, (e) tag data, (f) tag data and LL CPUE indices from the late 2000s for all regions.

APPENDIX D: RESULTS FROM SELECTED SENSITIVITY MODELS

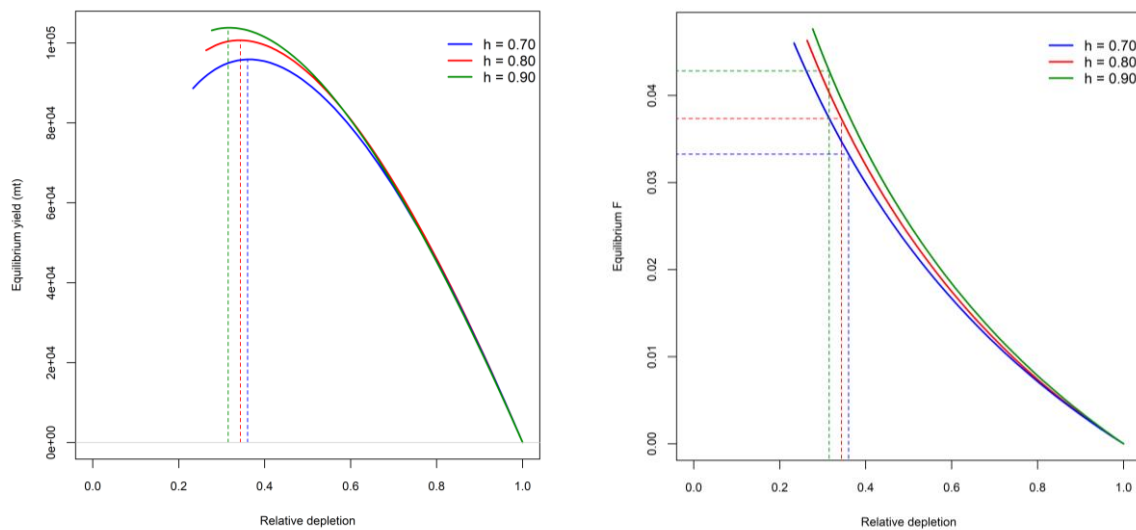


Figure D2: Equilibrium yield curves (left) and F curves (right), and for sensitivity models with different steepness h_{70} , h_{80} (base model) and h_{90} . The dashed lines in the left panel illustrating the depletion levels at SSBMSY, the dashed line in the right panel illustrate F corresponding to SSBMSY.

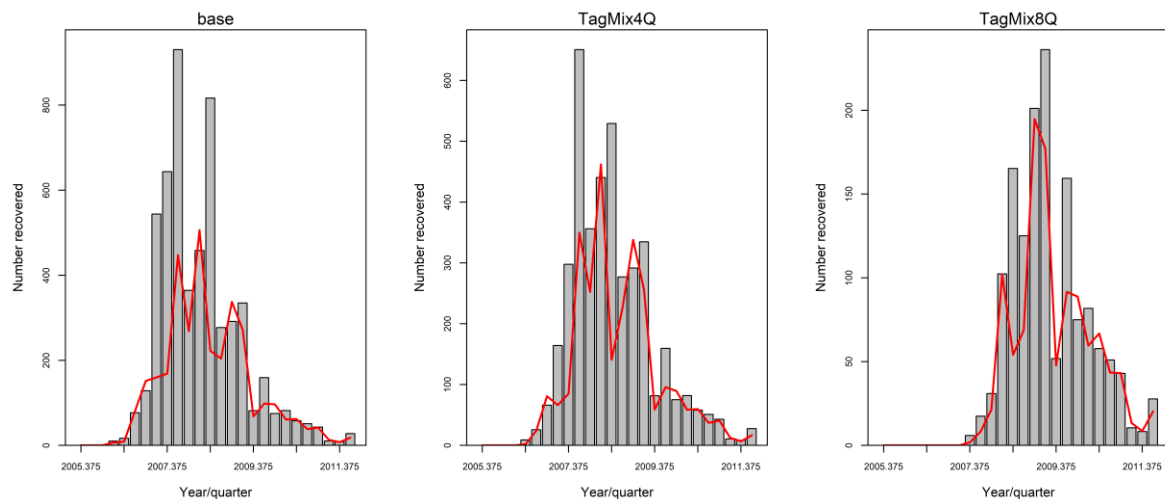


Figure D2: A comparison of the fits to the tag recoveries for the base and sensitivity models relating, mix period assumptions. The bars are observed tag recoveries and the lines are model predictions. Only tags at liberty after the assumed mixing period are included. Tag recoveries are aggregated for all fisheries.

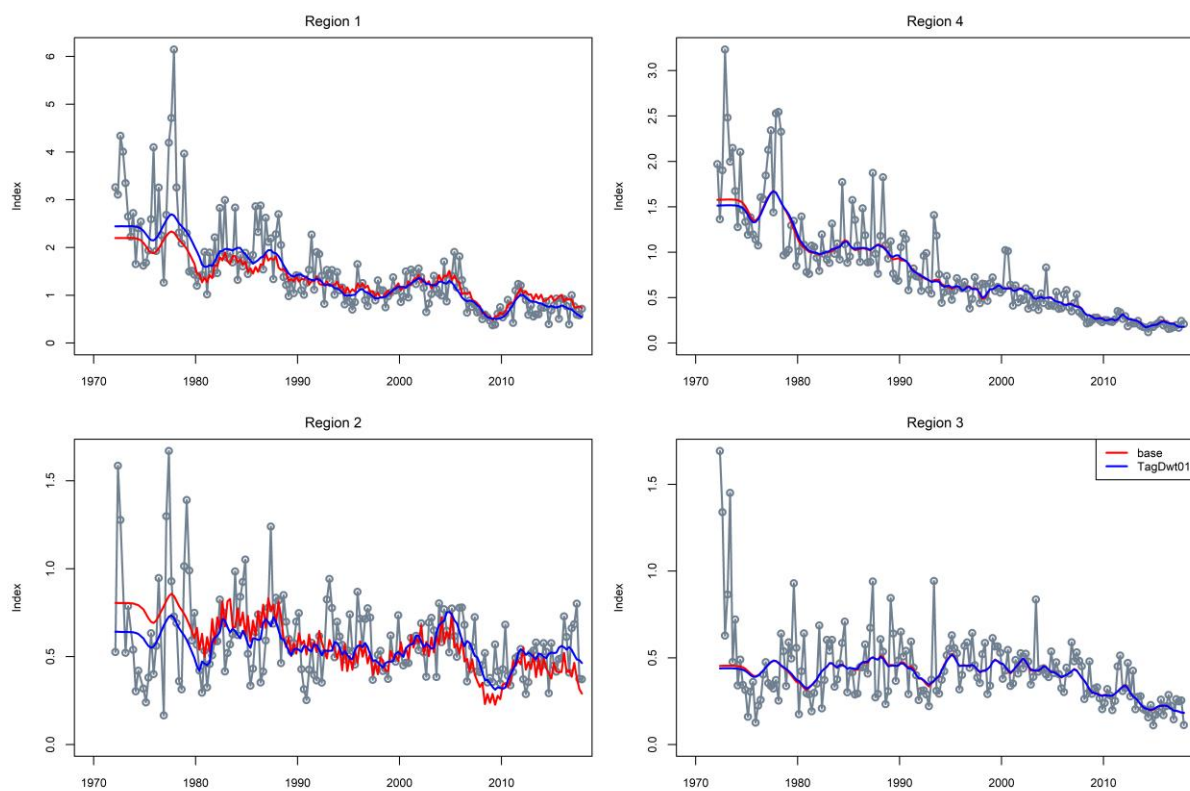


Figure D3: A comparison of Fit to the regional longline CPUE indices, 1972–2016 between the base model and the sensitivity model that assumed a tag mixing period of 4 quarters (*TagMix4Q*). The grey dotted lines indicate observed CPUE.

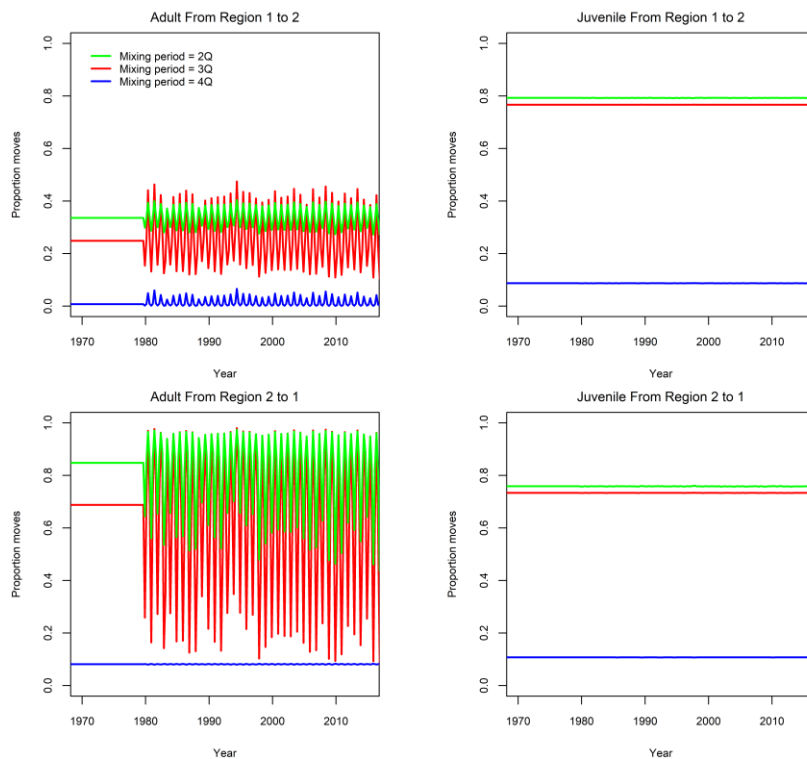


Figure D4: A comparison of quarterly movement coefficients between the models with tag mixing period assumed to be 2 quarters, 3 quarters (base), and 4 quarters (*TagMix4Q*).

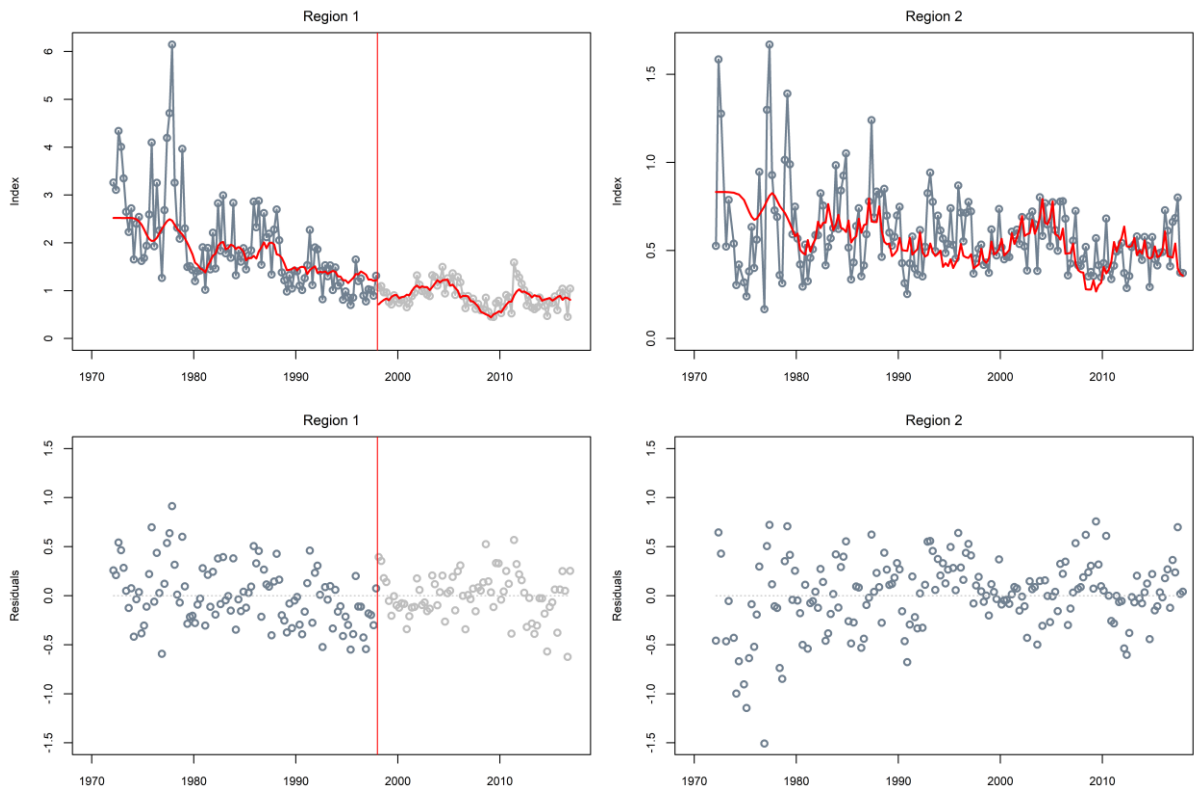


Figure D4: Fit to the longline CPUE indices (top panel) in region 1 and 2 and associated standardised residuals (bottom panel) from sensitivity model *CPUETWR1*. In region 1 the red vertical line separates the Joint indices 1972–1997 (Hoyle et al. 2018a) and the Taiwanese CPUE indices 1998–2016 (Ye et al. 2018).

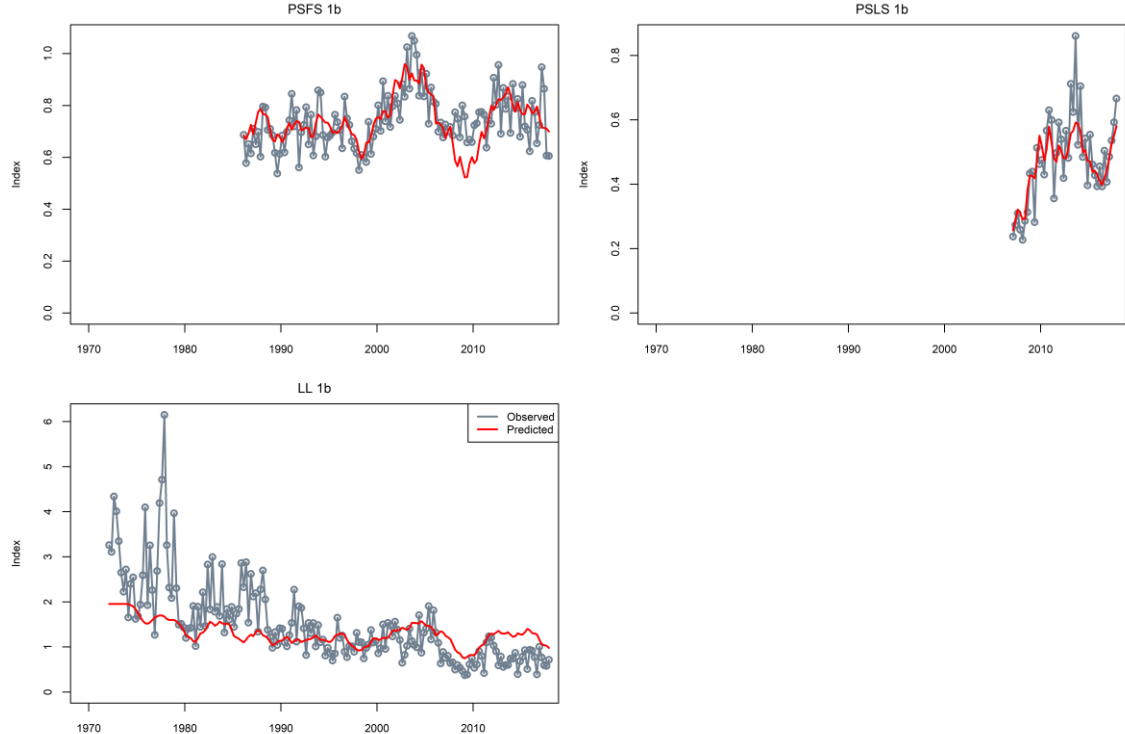


Figure D5: Fit to the PS FREE SCH CPUE 1986–2017, the PS FAD SCH CPUE 2008–2017, and the LL CPUE in region 1b from model *PS_CPURE*. The grey dotted lines indicate observed CPUE.

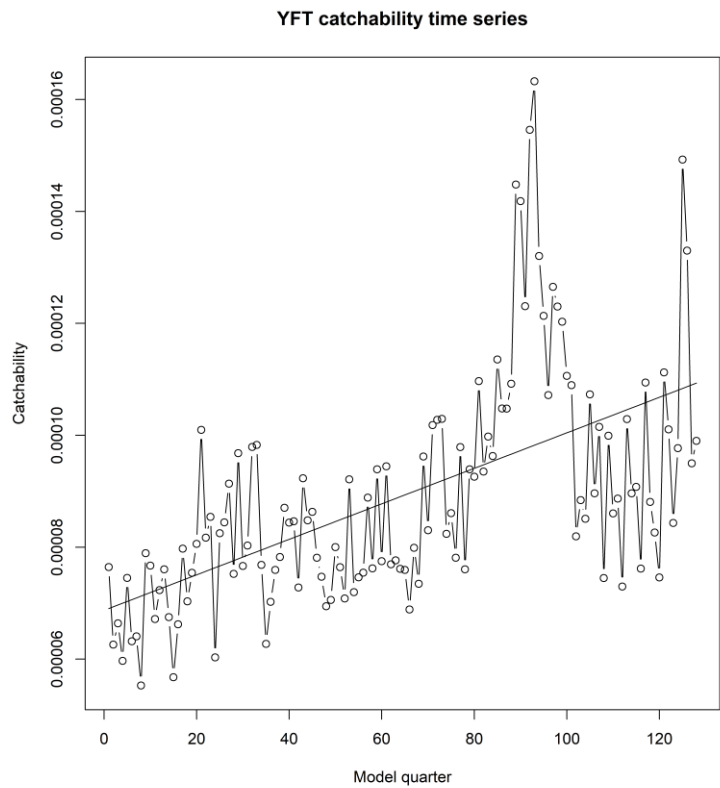


Figure D6: Time-varying catchability estimates for the yellowfin PSFS 1b fishery from model *PS_CPUE_estQ* (following the approach of Kolody (2018)). The line linear regression fit, and corresponds to a 1.5 % per year trend (compounded annually over a 32 year period)